The Institute of Paper Chemistry

Appleton, Wisconsin

Doctor's Dissertation

Ozonation of Loblolly Pine Fibers at Low Consistency

Kim Sabin Melius

June, 1984

OZONATION OF LOBLOLLY PINE FIBERS

AT LOW CONSISTENCY

A thesis submitted by

Kim Sabin Melius

B.S. 1976, University of Wisconsin - Whitewater

M.S. 1978, Lawrence University

in partial fulfillment of the requirements
of The Institute of Paper Chemistry
for the degree of Doctor of Philosophy
from Lawrence University,
Appleton, Wisconsin

June, 1984

TABLE OF CONTENTS

SUMMARY

Numerous studies have been reported in the literature describing the potential use of ozone in pulping and bleaching processes. Unfortunately, these studies have shown ozone to indiscriminately attack both lignin and carbohydrates which results in loss of pulp strength. In order to overcome this difficulty, a better understanding of the interaction of ozone with wood fibers is needed. Therefore, the objective of this thesis was to elucidate the mode and selectivity of ozone attack on wood fibers.

Mode refers to whether ozone attack occurs primarily on the external surface of the fibers or whether it can penetrate into the cell wall of the fibers. Component selectivity refers to whether ozone preferentially reacts with a specific wood component or reacts with all wood components indiscriminately. Tissue selectivity refers to the relative rate of ozonation of earlywood fibers versus latewood fibers.

The experimental approach involved ozonation of individual, intact latewood or earlywood fibers having a lignin coated surface. Ozonations of these fibers were carried out at specified times ranging from 5-180 minutes, at low consistency (0.5%) in an aqueous acetic acid/sodium acetate buffer solution (pH 3). Chemical, physical and microscopic analyses were performed on untreated and ozonated fibers. The mode of ozone attack was investigated by scanning electron, transmission electron and light microscopies to observe changes in external surface and internal cell wall structures of the fibers. Selectivity of ozone attack was monitored by analyses such as yield, carbohydrate and lignin content, carbohydrate viscosity and degree of polymerization.

Results from chemical, physical and microscopic analyses showed for both latewood and earlywood that ozone does not demonstrate a wood component

selectivity in that both lignin and carbohydrates were rapidly degraded. However, there was preferential removal of the wood components in the order of lignin >> hemicellulose >> cellulose. It was not possible to determine whether preferential removal of wood components was due to chemical reactivity or topochemical restraint.

Microscopic analyses showed ozone attack on latewood and earlywood fibers occurred not only at the external surfaces, but penetrated and degraded their cell wall material. The pattern of lignin removal was found to start at the outer fiber cell wall and proceeded toward the lumen.

The rate constants for delignification of latewood and earlywood fibers were found from the following general empirical rate expression:

$$\ln R_L = \ln k + a \ln [\text{lignin}] + b \ln [\text{ozone}]$$

where R_L is the rate of delignification and a and b are the reaction orders for lignin and ozone, respectively.

The rate constants for delignification (k) of latewood and earlywood fibers were determined to be 7.59×10^{-4} $\underline{mM}^{-0.24}$ sec^{-1} ($5.68 \times 10^{-4} \longrightarrow 10.2 \times 10^{-4}$ $\underline{mM}^{-0.24}$ sec^{-1}) and 5.30×10^{-4} $\underline{mM}^{-0.11}$ sec^{-1} ($4.17 \times 10^{-4} \longrightarrow 6.74 \times 10^{-4}$ $\underline{mM}^{-0.11}$ sec^{-1}), respectively. The rates of delignification were not statistically different.

Chemical, physical, microscopic and kinetic analyses of latewood and earlywood fibers were in agreement, demonstrating ozone does not exhibit tissue selectivity (i.e., does not react with earlywood at a different rate than latewood).

INTRODUCTION

Increased emphasis in the area of environmental control has prompted the pulp and paper industry to investigate new pulping and bleaching processes. Ozonation of wood is one such process. Ozone utilization for pulping and bleaching shows considerable potential since it would minimize or eliminate sulfur and chlorine containing components in effluents.

Unfortunately, ozone purportedly acts as an indiscriminate reagent attacking both lignin and carbohydrates which result in loss of pulp strength. Since the distribution of wood components on the surface and within the cell wall of the wood fibers influences properties important to papermaking (e.g., drainage, fiber-to-fiber bonding, fiber flexibility, brightness), it would be beneficial to gain a better insight into the pattern of ozone attack on wood components. Therefore, the objective of this thesis was to elucidate the mode and selectivity of ozone attack on wood fibers under aqueous conditions.

THE CHEMISTRY OF OZONE

GENERAL CONSIDERATIONS

Ozone is a nonlinear triatomic molecule consisting of three oxygen atoms. It is a nonparamagnetic molecule possessing two oxygen-oxygen bonds of equal length (1.278 Å) and an average bond angle of 116°49' (1,2). The ozone molecule can be described as a resonance hybrid of structures I-IV (Fig. 1).

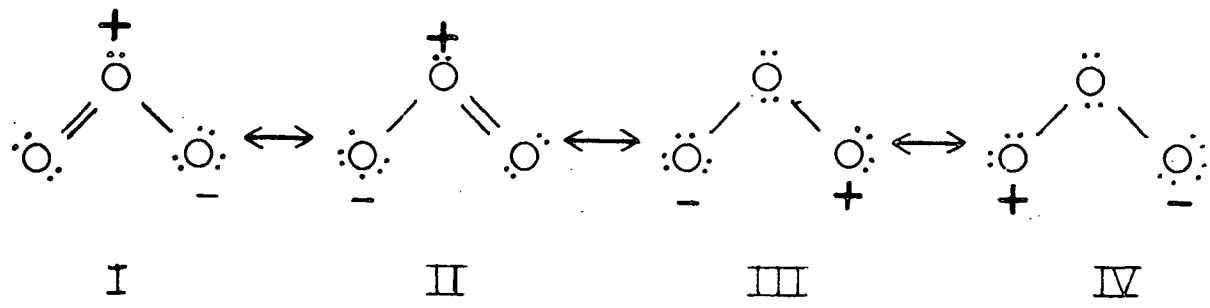

Figure 1. Resonance structures of ozone (18,19).

The oxygen atoms in resonance structures I and II possess a full octet of electrons whereas the terminal oxygen atoms in structures III and IV have only a sextet of electrons. The electron deficient terminal oxygen atom shown in structures III and IV (Fig. 1) gives ozone an electropositive nature (1,2). Thus ozone is capable of electrophilic attack on electron rich substrates (2). Structures III and IV also allow ozone to be classified as a 1,3-dipolar compound (1,2). Therefore, ozone is capable of undergoing concerted addition reactions (18). Both of these types of reactions can occur in the gaseous phase or in aqueous media. Since pulping and bleaching of fibers are primarily carried out in the presence of water, a brief review of ozone chemistry in aqueous media will be presented.

OZONE IN AQUEOUS SOLUTIONS

Many thorough investigations dealing with the chemistry of ozone in aqueous solutions have been carried out for alkaline (3-10), neutral (11-16), and acidic (17-22) conditions. Results of these investigations will be briefly discussed below.

Researchers have found ozone concentration in aqueous solutions decreases as hydroxide ion concentration increases (3-9). Ozone decomposition was

inhibited when radical scavengers such as carbonate ions (9,10) and aliphatic alcohols (10) were added to the alkaline solutions. This suggested ozone decomposition proceeds via a chain radical mechanism in which hydroxide ions are involved in the reaction. This appears to be the general consensus of the investigators; however, disagreement and uncertainty still remain about the initiation step and the type of radical intermediate species formed upon decomposition.

Weiss (3) followed the decomposition of ozone in aqueous potassium hydroxide solutions at -40°C and found ozone concentration was inversely proportional to hydroxide ion concentration. Based on this observation, Weiss (3) proposed a decomposition mechanism which involved hydroxide ion in the initiation step:

$$O_3 + {}^-OH \longrightarrow O_2^{\cdot-} + HO_2^{\cdot} \quad (1)$$

$$O_3 + HO_2^{\cdot} \longrightarrow 2O_2 + {}^{\cdot}OH \quad (2)$$

$$O_3 + {}^{\cdot}OH \longrightarrow O_2 + HO_2^{\cdot} \quad (3)$$

$$2HO_2^{\cdot} \longrightarrow O_3 + H_2O \quad (4)$$

$$HO_2^{\cdot} + {}^{\cdot}OH \longrightarrow O_2 + H_2O \quad (5)$$

Gorbenko-Germanov and Kozlova (7) investigated the decomposition of ozone in 8M potassium hydroxide solutions at -50°C using electron spin resonance and absorption spectroscopies. By comparing ozone decomposition spectra with potassium ozonide (KO_3) and potassium superoxide (KO_2) spectra, they concluded that ozonide radical anion and superoxide radical anion were intermediate species in ozone decomposition. Gorbenko-Germanov and Kozlova (7) suggested an initiation step for ozone decomposition involving a single electron transfer from hydroxide ion to ozone forming an ozonide radical anion ($O_3^{\cdot-}$):

$$O_3 + {}^-OH \longrightarrow O_3^{\cdot-} + {}^{\cdot}OH \quad (6)$$

The ozonide radical anion would then react with water to form different radical species [i.e., superoxide radical anions ($O_2^{\cdot-}$) and hydroxyl radicals ($^{\cdot}OH$)].

Staehelln and Hoigne (8) and Forni, et al. (9) studied ozone decomposition over the pH range 5-13 and suggested two possible initiation steps. The first initiation step, described in Eq. (1), was that proposed by Weiss (3). The superoxide radical anion and hydroperoxy radical ($HO_2^{\cdot}$) could then decompose through the steps shown in Eq. (7)-(9).

$$O^3 + {}^{-}OH \longrightarrow O_2^{\cdot-} + HO_2^{\cdot} \quad (1)$$

$$HO_2^{\cdot} \rightleftharpoons O_2^{\cdot-} + H^+ \quad (7)$$

$$O_3 + O_2^{\cdot-} \longrightarrow O_3^{\cdot-} + O_2 \quad (8)$$

$$O_2^{\cdot-} + H_2O \longrightarrow {}^{\cdot}OH + {}^{-}OH + O_2 \quad (9)$$

The second initiation step which may occur involves the reaction of ozone with hydroxide ions to form oxygen and hydroperoxy anions [HO_2^-, Eq. (10)]. The hydroperoxy anions react with additional ozone to form $HO_2^{\cdot}$ and $O_3^{\cdot-}$ [Eq. (11)]. These reactive intermediates can further decompose via Eq. (7)-(9).

$$O_3 + {}^{-}OH \longrightarrow HO_2^- + O_2 \quad (10)$$

$$O_3 + HO_2^- \longrightarrow HO_2^{\cdot} + O_3^{\cdot-} \quad (11)$$

Ozone decomposition studies have also been carried out in neutral or acidic media (15-22). The rate of ozone decomposition was found to decrease rapidly as pH decreased from pH 7 to 4 (16-19). Below pH 4, the rate of decomposition was found to be slow and relatively pH insensitive (17-19). The rate of ozone decomposition is influenced by the type of acid used in solution preparation. Pan, et al. (19) compared the rates of ozone decomposition in sulfuric, nitric and acetic acid solutions. They found the rate of ozone decomposition was approximately twice as fast in sulfuric and nitric acid solutions compared to

acetic acid solutions at pH values between 5.0-3.5. Decreases in rate of ozone decomposition in acetic acid solutions relative to other acidic solutions have been observed by several researchers (14,20-22). It is thought acetic acid acts as a radical scavenger inhibiting ozone decomposition (19,21,22).

The presence of trace amounts of transition metal ions has been shown to enhance ozone decomposition (19-22). Pan, et al. (19) investigated transition metal ion catalyzed decomposition of ozone in sulfuric, nitric and acetic acid solutions. For all acidic solutions studied, the rate of ozone decomposition in the presence of transition metal ions decreased in the order of

$$Co^{2+} >> Fe^{2+} > Cr^{3+} > Cu^{2+},\ Ni^{2+}$$

for metal ion concentrations in excess of 3 ppm. For metal ion concentrations less than 0.5 ppm, only the cobaltous ion enhanced ozone decomposition (19).

Pan, et al. (19) observed transition metal ion catalyzed ozone decomposition was reduced drastically in the presence of acetic acid compared to nitric and sulfuric acid solutions. Hill (21,22) also found cobaltous ion catalyzed ozone decomposition was slower in acetic acid than perchloric acid solutions. Both Pan, et al. (19) and Hill (22) rationalized this observation in terms of a mechanism proposed by Walling and El-Taliawi (23):

$$CH_3COOH + OH\cdot \longrightarrow {}^{\cdot}CH_2COOH + H_2O \qquad (12)$$

$${}^{\cdot}CH_2COOH + M^{2+} \longrightarrow {}^{-}CH_2COOH + M^{3+} \qquad (13)$$

$${}^{-}CH_2COOH + H^{+} \longrightarrow CH_3COOH \qquad (14)$$

Acetic acid inhibited ozone decomposition by acting as a hydroxyl radical scavenger. In addition, the metal ions are oxidized from the M^{2+} to the M^{3+} state which does not participate in ozone decomposition.

REACTIONS OF OZONE WITH LIGNIN

Reactions of Ozone with Olefins

Numerous investigations have been carried out on the ozonation of lignin model compounds (24-28) and isolated lignins (29-34). Results from these investigations have led researchers to believe ozonolysis of lignin occurs primarily through a cycloaddition mechanism proposed by Criegee (35) involving oxidative cleavage of carbon-carbon double bonds. This mechanism is important in pulping and bleaching since lignin contains olefinic and aromatic bonds.

The Criegee mechanism (Fig. 2) entails a 1,3-dipolar cycloaddition of ozone across a carbon-carbon double bond to form a 1,2,3-trioxolane intermediate (V). This intermediate decomposes via a 1,3-dipolar cycloreversion to yield a syn or anti isomer of carbonyl oxide (VI) and a carbonyl fragment (VII). One of three pathways may then be followed involving the carbonyl oxide as an active intermediate.

The first pathway that may be taken is the recombination of the carbonyl oxide with the carbonyl fragment through another 1,3-dipolar cycloadditon step to form a "final" ozonide (VIII). This reaction is thought to be the major pathway in nonprotic solvents (e.g., carbon tetrachloride and acetone).

The second pathway is the dimerization of carbonyl oxides to form diperoxides (IX) and polymeric peroxides (36). This usually occurs in the case of tetra-substituted olefins (36) and nonprotic solvents (36,37).

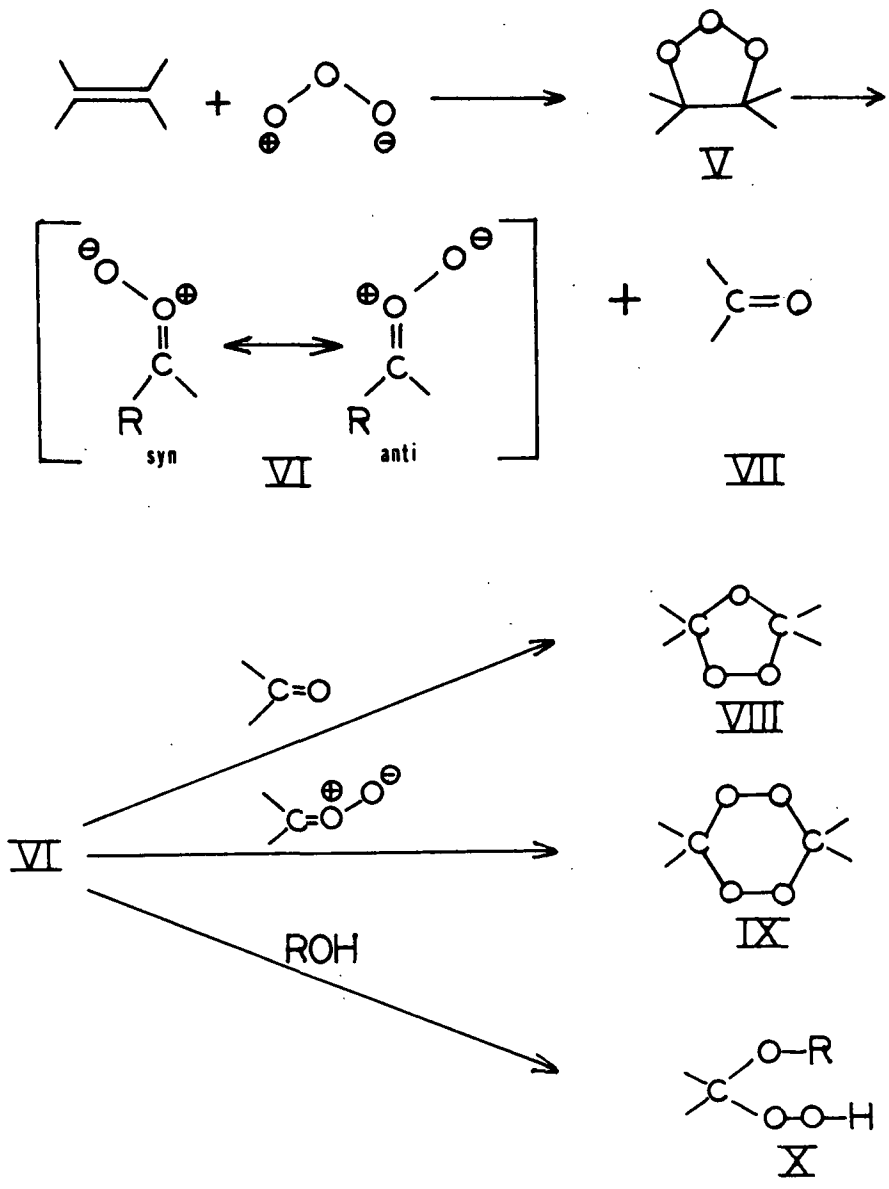

Figure 2. Modified Criegee mechanism of olefin ozonolysis.

The third pathway involves reaction of the carbonyl oxide with the "participating solvent" to form a hydroperoxide (X). This is thought to be the major pathway in protic solvents (e.g., alcohols, carboxylic acids and water).

Intermediates (VIII-X) may decompose to form stable products such as acids, aldehydes, or ketones.

Reactions of Ozone with Aromatic Compounds

Reaction of ozone with aromatic rings has not been investigated as thoroughly as the reaction of ozone with olefins (37). Many of the mechanistic concepts about ozonation of aromatic compounds are extrapolations from the knowledge about olefinic reactions (37). As in the case for olefins, ozonolysis of aromatic rings is also thought to occur by a 1,3-dipolar cycloaddition mechanism resulting in cleavage of carbon-carbon double bonds (Fig. 3). The reactive intermediates can further decompose to form stable products such as acids, aldehydes or ketones (28,36,37).

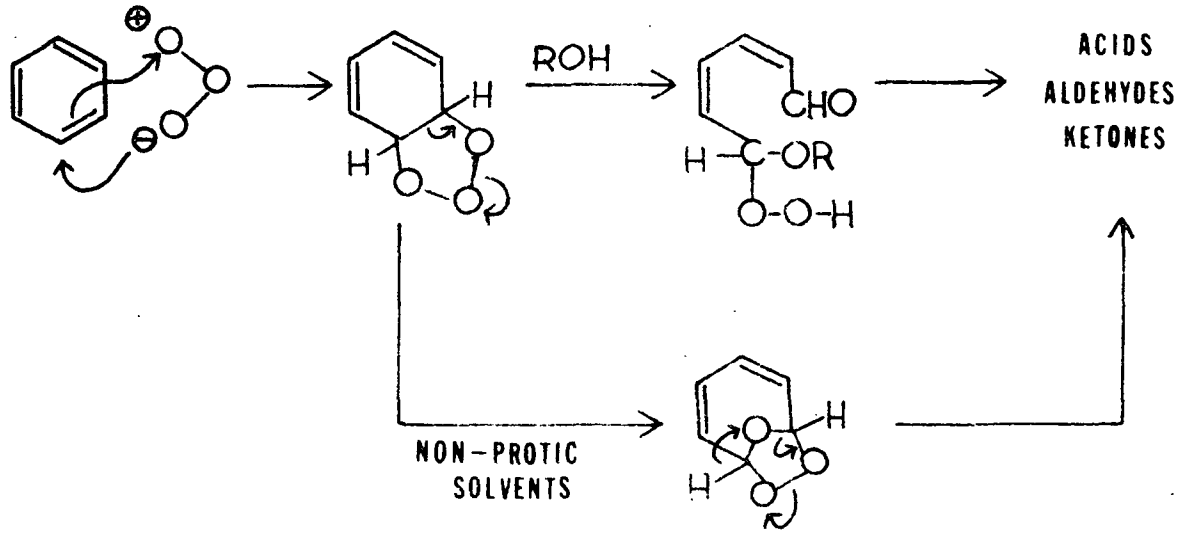

Figure 3. Probable mechanism for aromatic ozonolysis.

Ozonation of aromatic nuclei may also proceed through electrophilic substitution (37). This type of reaction results in ring hydroxylation rather than ring cleavage (Fig. 4). The hydroxylation products usually react further with ozone to form acids. Consistent with the concepts of electrophilic substitution, the reactivity of aromatic rings with ozone has been shown to be influenced by ring substituents (25-28). Electron withdrawing substituents tend to decrease aromatic ozonolysis whereas electron releasing substituents tend to increase reactivity. Ozone reactivity with aromatic compounds decreased in the order of phenolic > benzene > aromatic compounds containing α-carbonyl groups.

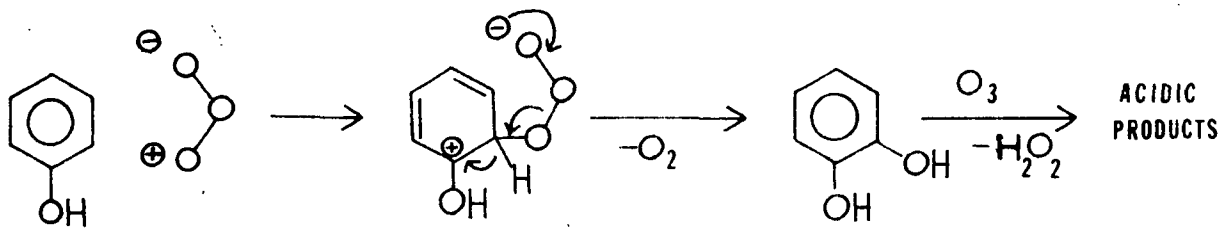

Figure 4. Electrophilic substitution of aromatic nuclei with ozone.

REACTIONS OF OZONE WITH CARBON-HYDROGEN BONDS

Ozonolysis of carbon-hydrogen bonds of aldehydes, alcohols, ethers and secondary and tertiary carbon-hydrogen bonds of hydrocarbons can occur (28,36, 37) as shown in Fig. 5. Ozone reacts with the carbon-hydrogen bond via a 1,3-dipolar insertion mechanism to form a hydrotrioxide intermediate (XI). This intermediate can then decompose to form oxidation products such as aldehydes, alcohols, esters and ketones (24,36). There is disagreement as to whether the decomposition proceeds through an ionic or free radical mechanism (37,38).

REACTIONS OF OZONE WITH CARBOHYDRATES

Katai and Schuerch (39) ozonated methyl α-D-glucoside and found the major product to be glucose and minor products to be arabinose and unidentified compounds. The reaction mixture was also found to contain relatively large amounts of "active oxygen," indicating the presence of organic peroxides or hydroperoxides.

They concluded ozonolysis of methyl α-D-glucoside proceeded by pathway A shown in Fig. 6. This pathway involves an electrophilic attack of ozone on the

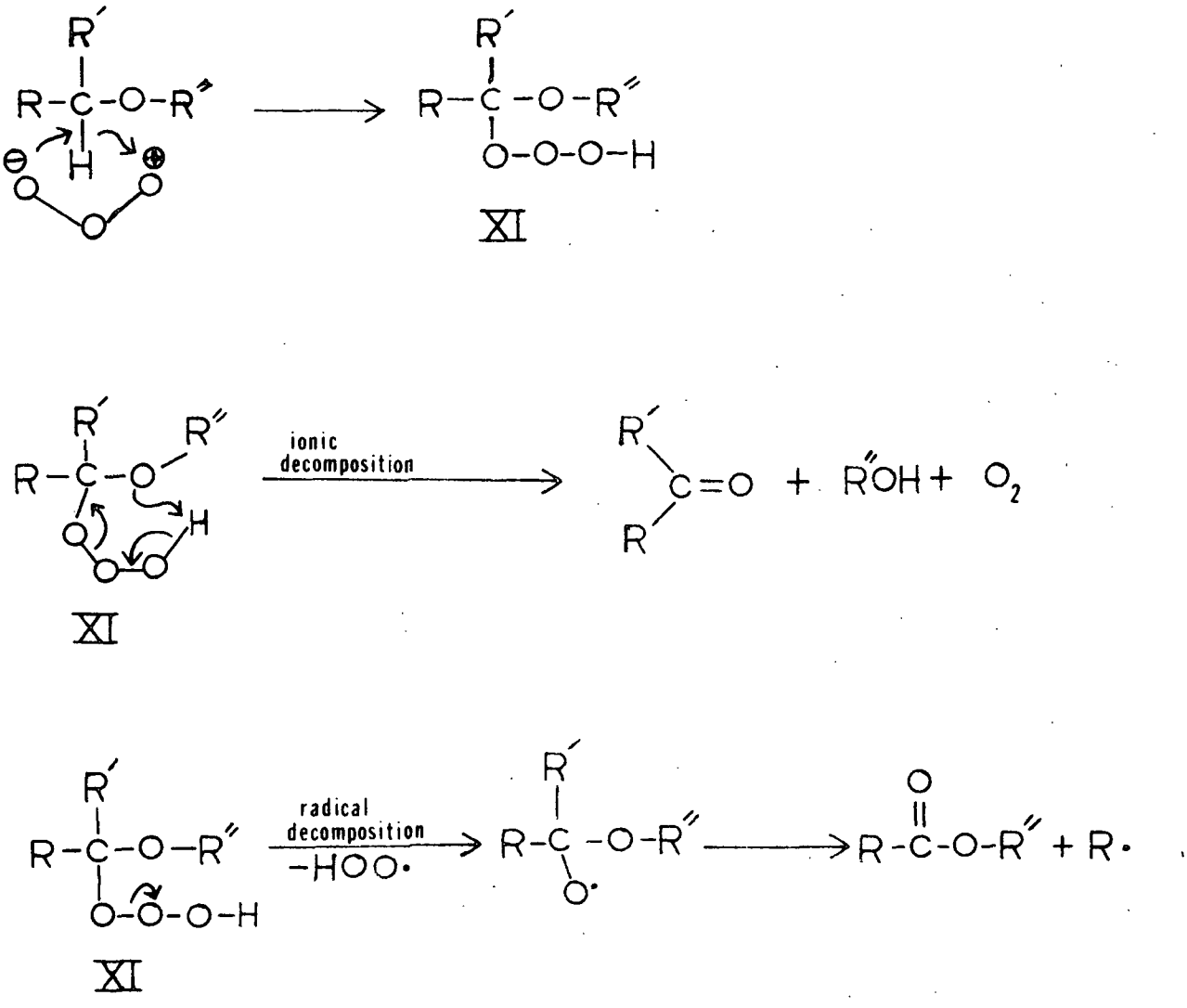

Figure 5. Ozone insertion mechanism of carbon-hydrogen bonds.

acetal oxygen of the glycosidic linkage forming a tetraoxide intermediate (XIV). The tetraoxide decomposes to a carbonium ion (XV) and a hydrotetraoxide compound (XVI). Addition of water to the carbonium ion followed by deprotonation yields glucose. Organic peroxides and hydroperoxides present in the reaction mixture can decompose generating free radicals. These radicals

can react with glucose, oxidizing it to gluconic acid (XX) which may undergo decarboxylation to give arabinose.

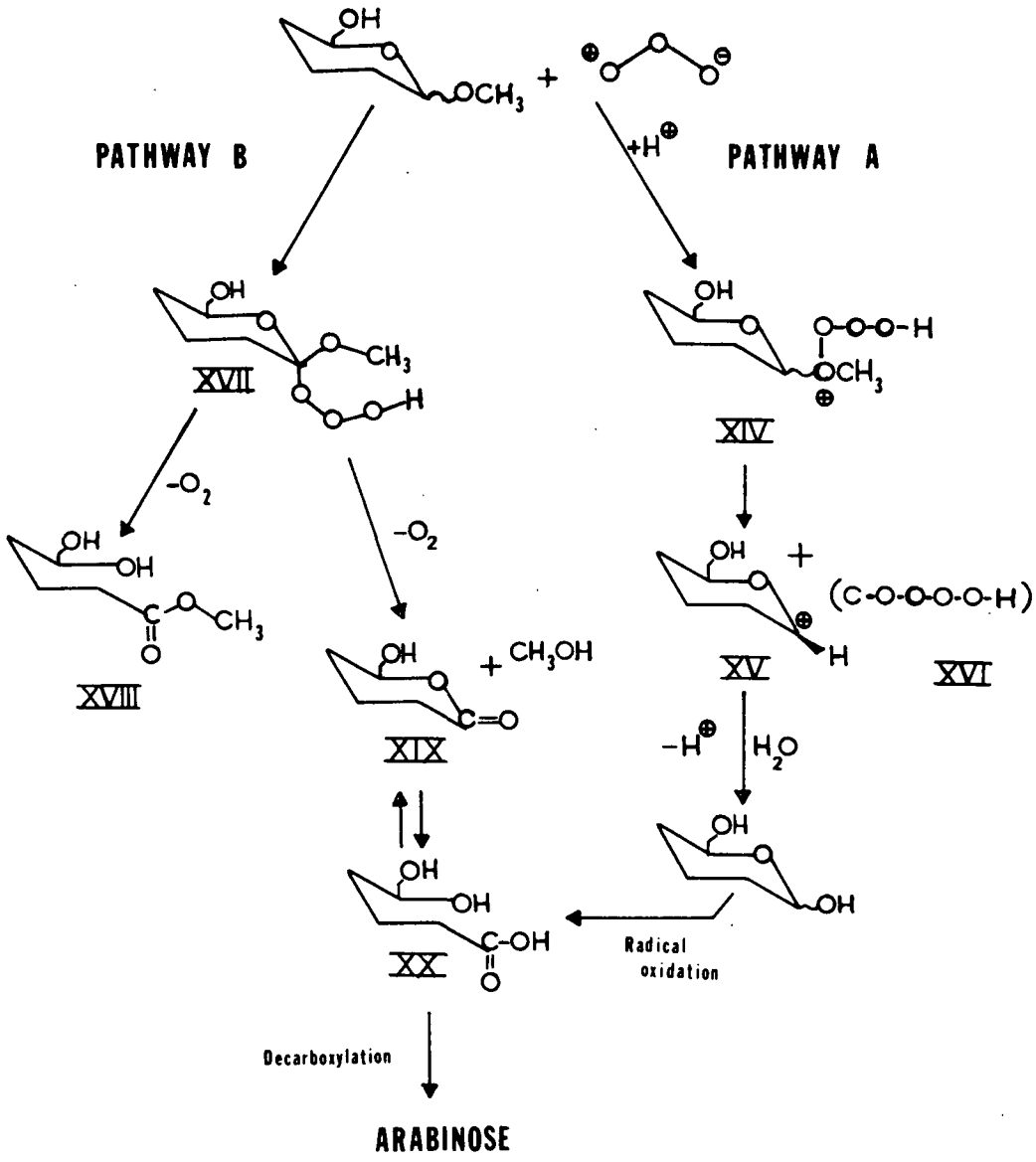

Figure 6. Ozonation of methyl α,β-D-glucosides.

Pan, et al. (19) ozonated methyl β-D-glucoside and found the reaction products to consist mainly of gluconic acid δ-lactone and gluconic acid. Minor amounts of glucose and arabinose were found in the product mixture. In addition, the mixture contained considerable amounts of "active oxygen."

Pan, et al. (19) concluded that the primary reaction route for ozonolysis of methyl β-D-glucoside was pathway B (Fig. 6) which involves the electrophilic attack of ozone at the anomeric carbon forming a hydrotrioxide intermediate (XVII). This intermediate can decompose to give a gluconic acid ester (XVIII) or a gluconic acid-δ-lactone (XIX) liberating oxygen in the process. The lactone may then hydrolyze to gluconic acid (XX) which can undergo decarboxylation to arabinose.

Since glucose was found in minor amounts, Pan et al. (19) concluded pathway A must also occur to some extent during ozonation. They suggested that ozonolysis of α-anomers follows pathway A whereas ozonolysis of β-anomers follows pathway B. This is in agreement with Deslongchamps, et al. (40-42) work on ozonation of α- and β-anomers of various acetals.

REACTION OF OZONE WITH WOOD PULPS

Previous work has concentrated on gas phase ozonation of high consistency (30-50%) pulps (44-70). Relatively little research has been directed toward ozonation of pulps at low consistencies (<3%) or in aqueous suspensions (69-80).

For gas phase ozonation of high consistency pulps, the following observations have been commonly reported (44-70):

1. Ozonation of mechanical pulps results in an increase in sheet strength properties and a decrease in brightness (58,60,75,79.)
2. Ozonation of chemical pulps results in a decrease in strength properties and an increase in brightness (43,56,58,65).
3. Ozone is a nonselective reagent, attacking both lignin and carbohydrates (58,59,61).
4. Ozone attack on wood pulp fibers occurs essentially on the external surface of the fibers (62-67).
5. Ozone reacts faster with earlywood than latewood (54,66,68).

Only the first three points have been observed for ozonation of pulps at low consistency. Researchers have suggested the last two points occur; however, they made these suggestions based on data received from ozonation of pulps at high consistency. The last three points will be discussed further in the following sections.

Selectivity of Ozone Attack

Ozone has been found to be an indiscriminate reagent attacking both lignin and carbohydrates (59,61,67). However, in a study on ozonation of spruce bisulfite pulp over a temperature range of -10 to 20°C, Soteland (59) found maximum ozone attack of lignin (based on removal) occurred from -10 to 0°C with minimal attack on carbohydrates (based on viscosity). By extrapolating his data, he suggested maximum ozone attack on carbohydrates would occur between 30 and 50°C.

Lyse (61) and Moore, et al. (67) have reported some degree of selectivity of ozone attack at ambient temperatures. Lyse (61) ozonated fiberized loblolly pine (7% o.d. wood) and found approximately 40% of the original lignin and 25% of the total carbohydrates were removed. Moore, et al. (67) ozonated wood shavings and found ozone removed wood components in the order of lignin > hemicellulose > cellulose. However, he stated this preferential removal was only marginal.

Fiber Surface Modification

Ozone attack occurs essentially at the external surface of fibers resulting in fiber surface modifications which alter strength properties of handsheets made from these pulps (54,62-67). Mechanical pulps have poor bonding properties due to the high lignin content on the external surface of fibers. Ozonation of mechanical pulps resulted in increased handsheet strength

properties. Ozonation increases the hydrophilicity of the external surface lignin by forming carboxyl and carbonyl groups from the oxidation of lignin, thereby increasing specific bond strength (62,63).

This was substantiated by Soteland (60) and Lyse (61) who observed differences between ozonated and nonozonated mechanical pulps. Lyse (61) found carboxyl and carbonyl content of alkali fiberized loblolly pine wood increased linearly with ozone consumption. Soteland (60) found carboxyl content of spruce groundwood increased upon ozonation. Tensile strength of handsheets made from this pulp increased linearly with the carboxyl content.

Secrist and Singh (65) observed that surface modifications of hardwood kraft pulps occurred after ozonation. Electron micrographs of the fibers revealed an eroded surface structure consisting of numerous ridges and valleys. Kibblewhite, et al. (64) ozonated high-temperature thermomechanical softwood pulp and examined the fibers using transmission electron microscopy. They found ozonation modified the lignin sheath surrounding the fibers allowing the underlying fibrillar surface to become visible.

Procter (62) hypothesized ozone attack was not solely limited to fiber surfaces but could attack cell wall material as well. He based his reasoning upon large drops in cellulose viscosity for ozonated chemical pulps. Other researchers have also reported viscosity decreases of 30-50% for ozonated mechanical pulps (43,59-61). Degradation of cell wall material could contribute to increased handsheet strength properties of ozonated mechanical pulps (62-67,75) by increasing fiber flexibility and therefore fiber bonding area (75).

Further indication that ozone attack may not be limited to the external fiber surfaces can be derived from Lyse's (61) work on the ozonation of alkali-fiberized loblolly pine. Lyse (61) found 39% of the original lignin was solubilized at 7% ozone consumption (on o.d. wood). However, the maximum amount of lignin (~25%) would occur on the external surfaces of the fibers if the wood fibers were split through the middle lamella region (81). Scanning electron micrographs of Lyse's fibers after ozonation showed a lignin sheath still surrounded most of the fibers (61). This information demonstrates not all the lignin removed from the fibers came from the middle lamella region. Thus, ozone may attack cell wall material in addition to external surface lignin.

Ozone Attack on Fiber Types

Ozone reacts faster with earlywood than latewood (54,66,68). Lantican, et al. (66) and Osawa, et al. (54) performed gas phase ozonation of wood blocks from several species of trees and found earlywood defibered more rapidly than latewood. They hypothesized ozone could enter the open-structured earlywood fibers (i.e., large lumen, thin cell wall) more easily and rapidly than the close-structured latewood fibers.

Krueger and John (68) ozonated unbleached softwood kraft pulp and unbleached hardwood neutral semichemical pulp from recycled corrugated containers at high consistency (~40%). They found ozone reacted with softwood (earlywood) fibers and hardwood vessel elements faster than hardwood fibers, which reacted faster than softwood (latewood) fibers. These conclusions were based on qualitative examination of Graff C-stained fibers using light microscopy.

The reactivity of earlywood versus latewood has not been investigated for low consistency ozonation.

THESIS OBJECTIVE

There have been numerous studies reported in the literature describing ozonation of wood fibers. However, the mode and selectivity of ozone attack on fibers is not fully understood, especially in aqueous solutions. Since these factors would influence pulping and bleaching processes utilizing ozone, a better understanding of the interaction of ozone with fibers would be beneficial. Therefore, the objective of this investigation was to elucidate the mode and selectivity of ozone attack on wood fibers.

Mode refers to whether ozone attack occurs primarily at the external surface of the fibers or whether it can penetrate into the cell wall of the fibers. Component selectivity refers to whether ozone preferentially reacts with a specific wood component or reacts with all wood components indiscriminately. Tissue selectivity refers to the relative rate of ozonation of earlywood fibers *versus* latewood fibers.

EXPERIMENTAL APPROACH

To achieve the thesis objective, it was necessary to obtain a defined wood pulp as the starting material and to demonstrate control of ozonation and reactor variables. After these criteria were met, experimental runs were conducted to investigate the mode and selectivity of ozone attack on wood fibers.

For the starting material, a homogeneous and uniform wood pulp was desired. In this context, homogeneous implies one cell type and tissue type; whereas uniformity refers to fiber size distribution and surface composition. Homogeneity and uniformity of the pulp can be controlled through wood selection, refining and screening.

A softwood was selected as the fiber source in this study to eliminate cell types such as vessel elements which are present in hardwoods. Tissue type was controlled by separating the wood into mature earlywood and latewood fractions. Juvenile and transition woods were discarded. The wood fractions were steamed, refined and screened to produce a pulp consisting primarily of individual, intact fibers having a lignin coated surface.

Ozonation variables such as pH, temperature and uniformity of ozone contact with the fibers were controlled by ozonating the pulp fibers at low consistency in an aqueous suspension. All experiments were carried out at 25°C. Acidic conditions were chosen since ozone decomposition was reported to decrease at lower pH values (16-19). An acetic acid/sodium acetate buffer solution was chosen to maintain a pH 3 since ozone stability was found to be greater in this solution compared to other buffer solutions (19).

A reaction apparatus was designed to allow ozonation of pulp fibers at low consistency. In order to inhibit simultaneous liquid and gas phase ozonation of fibers, gaseous ozone was first dissolved in buffer solution and then transferred to a reaction tank where it contacted the fibers. This design also eliminated the problem of mass transfer of gaseous ozone into the bulk solution before reaction with the fibers.

Reactor design variables such as mixing and solution flow rate will influence ozonation of fibers. The mixing rate used provided uniform contact between the solution and fibers without damaging the fibers. The solution flow rate through the reactor was sufficient to provide a constant solubilized ozone concentration to the fibers. Preliminary experiments were needed to optimize these conditions.

Once the preliminary experiments were completed, experimental runs were carried out to investigate the mode and selectivity of ozone attack on wood fibers. Wood fibers were ozonated for various lengths of time and recovered for microscopic, chemical and physical analyses. Mode of ozone attack was investigated by using SEM, TEM and light microscopy to observe changes in the external surface and internal cell wall structures of the fibers. Selectivity of ozone attack was monitored by analyses such as yield, carbohydrate and lignin content, viscosity and carbohydrate molecular weight distribution.

RESULTS AND DISCUSSION

STARTING MATERIAL

Loblolly pine (Pinus taeda), which was selected as the wood source for this study, was separated into mature latewood and earlywood fractions using a guillotine blade. The fractions were steamed, refined, screened and extracted (see Experimental). The resultant fibers were analyzed for chemical composition and examined by SEM, TEM and light microscopies.

Chemical composition data for latewood (LW) and earlywood (EW) fractions of the starting material are shown in Table I. Values shown in Table I are an average of values obtained from the fibers after the first and second refining (see Experimental). These values are in agreement with those found by Lyse (61) for nonfractionated alkali-fiberized loblolly pine wood.

TABLE I

CHEMICAL COMPOSITION OF LOBLOLLY PINE FIBERS[a]

	Starting Material		Fiberized Wood (61)
	Latewood	Earlywood	
Carbohydrates, %			
Araban	1.0	1.2	1.2
Xylan	6.4	6.7	6.5
Mannan	10.6	10.6	11.8
Galactan	3.2	2.6	2.3
Glucan	45.8	46.2	46.1
Lignin, %			
Acid Insoluble	27.8	29.0	27.7
Acid Soluble	0.3	0.4	0.4
Extractives	0.8	1.2	2.7

[a]Percent on o.d. pulp.

Examination of Graff C-stained fibers by light microscopy showed good separation between earlywood and latewood was accomplished. SEM examination of critical point dried fibers showed the external surfaces to be relatively smooth with most of the splits between fibers occurring through the middle lamella region. As a result of this split, individual latewood and earlywood fibers were surrounded by a lignin sheath. This was confirmed by TEM and UV microscopies. TEM showed the middle lamella surrounding the primary wall of the LW and EW fibers (Fig. 7 and 8, respectively). These results agree with those from other researchers investigating fibers produced from high temperature refining of wood chips (83-86). Thus, a homogeneous and uniform pulp consisting of LW or EW fibers was obtained as the starting material.

CONTROL FIBERS

Control fibers were extracted fibers that were mixed in oxygenated acetic acid (HAc)/sodium acetate (NaAc) buffer solution for 90 minutes. (See Experimental). Chemical differences between control fibers and starting material were insignificant (Table II), indicating mixing the fibers in oxygenated acetic acid buffer solution did not affect their chemical composition. Microscopic analyses showed control fibers to be similar to starting material fibers. SEM examination showed control fibers had smooth external surfaces as a result of a lignin sheath surrounding them. The fibers appeared rigid and a small amount of debris appeared on the surfaces. These results were also confirmed by light and TEM microscopies. In the present work, control fibers represent fibers at 0 minutes ozonation time.

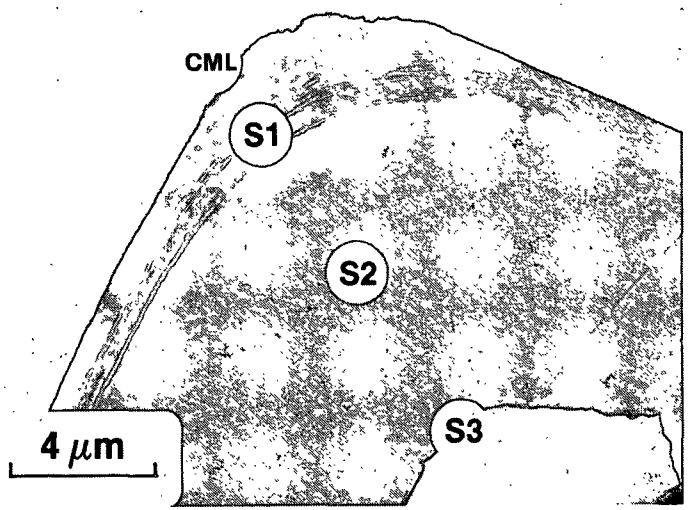

Figure 7. Starting material LW fiber showing compound middle lamella (CML) surrounding the fiber cell wall (S1, S2,S3); TEM micrograph.

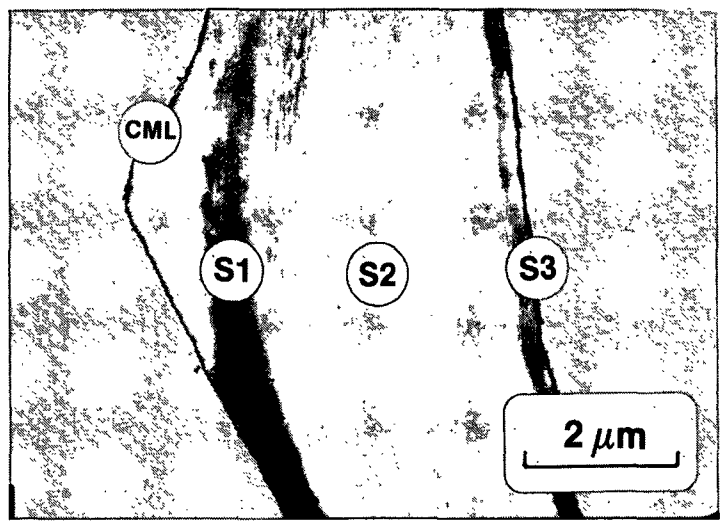

Figure 8. Starting material EW fiber showing compound middle lamella surrounding the fiber cell wall (S1,S2,S3); TEM micrograph.

TABLE II

CHEMICAL COMPOSITION OF LATEWOOD AND EARLYWOOD FRACTIONS OF LOBLOLLY PINE[a]

	Starting Material		Control Fibers	
	Latewood	Earlywood	Latewood	Earlywood
Carbohydrates, %				
Araban	1.0	1.2	1.0	1.2
Xylan	6.4	6.7	6.1	6.7
Mannan	10.6	10.6	10.7	10.8
Galactan	3.2	2.6	3.1	2.9
Glucan	45.8	46.2	44.8	46.4
Lignin, %				
Acid Insoluble	27.8	29.0	27.4	29.4
Acid Soluble	0.3	0.4	0.3	1.0
Extractives	0.8	1.2	0.0	0.0

[a]Percent on o.d. pulp.

PRELIMINARY OZONATION EXPERIMENTS

Preliminary studies were conducted using the reaction apparatus to obtain controllable and reproducible experimental conditions. Variables such as buffer solution concentration, ozone gas flow rate, mixing rate, buffer solution flow rate and fiber consistency were investigated. Results of these preliminary studies are presented in Appendices V-VI. Based on these results, the experimental conditions used during ozonation of fibers were selected as follows:

Temperature: 25°C
pH: 3
Buffer Solution Concentration: 0.4M HAc/0.0072M NaAc
Buffer Solution Flow Rate: 0.3 L-soln/min
Ozone Gas Flow Rate: 2 L-gas/min
Mixing Rate: 500 rpm
Fiber Consistency: 0.05%

OZONATION OF LATEWOOD FIBERS

Ozonation of latewood fibers was carried out at specified times ranging from 5 to 180 minutes under the conditions given above. Mean values, standard deviations and per cent coefficient of variation for ozone concentration with respect to reaction time are given in Appendix VII. Plots for ozone concentration mean values (± standard deviations) versus reaction time are also shown in Appendix VII. All the curves are similar in shape. Coefficients of variation range from 1 to 9% with the largest variation occurring for the five minute sample.

A representative plot of ozone concentration versus reaction time for 180 minutes is shown in Fig. 9. The time interval from -15 to 0 minutes was the ozone concentration measured in the reactor prior to fiber addition. An equilibrium ozone concentration was reached at 9.67 ± 0.29 mg/L-soln. Upon fiber addition (T=0 minutes), ozone concentration dropped, suggesting the rate of ozone input into the reactor was less than the rate of reaction of ozone with the fibers. As ozone concentration reached a minimum (~10 minutes), the rate at which ozone reacted with the fibers was approximately equal to the rate of ozone input. As ozone concentration increased, the rate of ozone input into the reactor became greater than the rate of ozone reaction with the fibers.

Once preliminary experiments were completed, fibers were ozonated for specified times and compared to control fibers using physical, chemical and microscopic analyses. These will be discussed further in the following sections.

PHYSICAL AND CHEMICAL ANALYSES OF LATEWOOD FIBERS

Fiber yield decreased to about 60% (by weight) after 180 minutes of ozonation, indicating ozone removed wood components from the fibers (Fig. 10).

This was confirmed by results obtained from chemical and microscopic analyses of the fibers.

A chemical composition summary as per cent oven dried wood is shown in Table III and Figure 11 for control and ozonated fiber samples. Total lignin content was determined as the sum of Klason and acid soluble lignin (Appendix X). Hemicellulose and cellulose contents were calculated from individual carbohydrate contents (Appendix XI). The sum of the total lignin and carbohydrate contents was approximately 5% less than the total yield for a given sample. This discrepancy was attributed to uronic acids which were not determined in the carbohydrate analysis. Uronic acids have been found to represent about 4-5% (by weight) of loblolly pine wood (87).

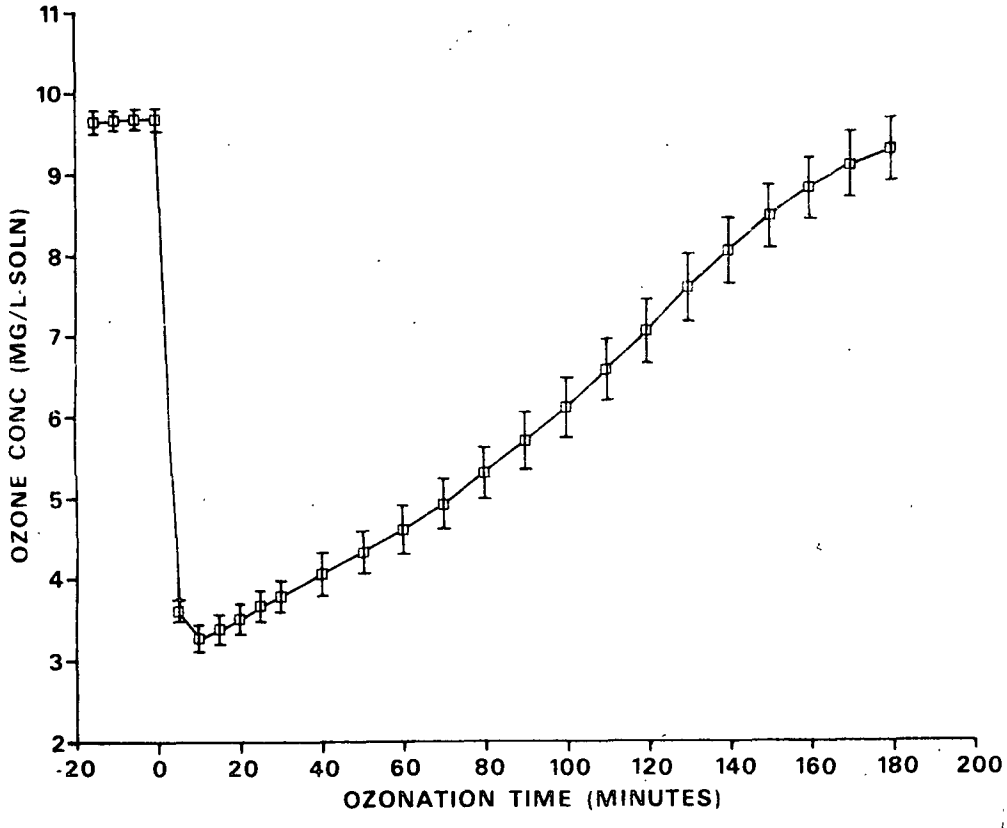

Figure 9. A representative plot of ozone concentration versus reaction time for the ozonation of LW fibers in acetic acid buffer solution.

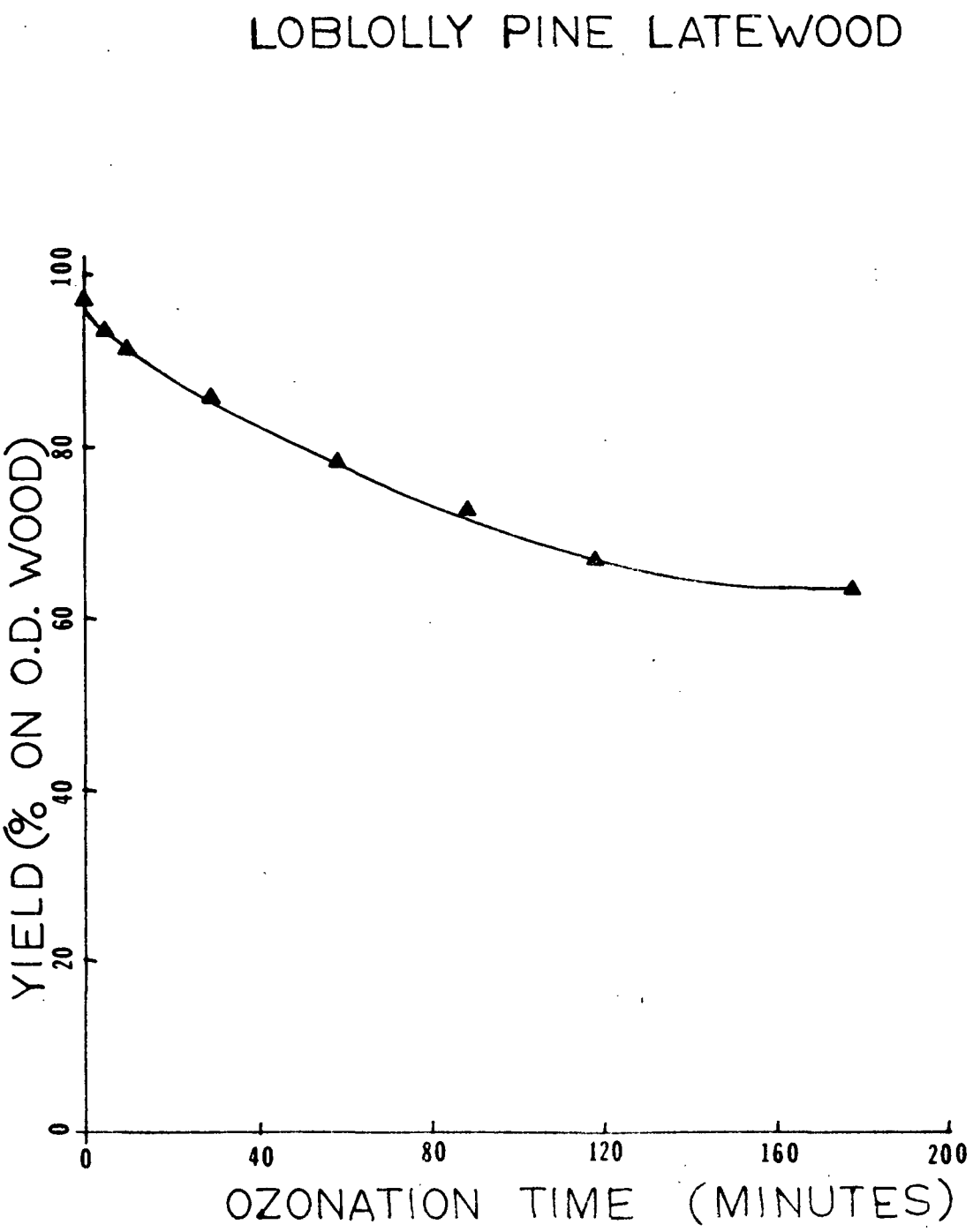

Figure 10. The relationship of LW fiber yield with respect to ozonation time.

TABLE III

CHEMICAL COMPOSITION SUMMARY OF OZONATED LATEWOOD FIBERS[a]

Ozonation Time, min	Total Yield, %	Total Lignin, %	Total Hemi-cellulose, %	Total Cellulose, %	Total Carbo-hydrates, %	Deligni-fication,[b] %	Solubilized[b] Hemicellulose, %
0	98.4	27.7	24.9	40.8	65.7	0.0	0.0
5	94.5	24.5	24.8	40.8	65.6	11.6	0.0
10	92.3	22.6	24.8	40.8	65.6	18.6	0.0
30	86.7	17.7	22.1	40.3	62.4	36.3	11.4
60	78.9	11.0	21.9	39.8	61.7	60.4	12.0
90	72.9	5.6	20.8	41.5	62.3	79.6	16.5
120	67.0	2.5	20.2	39.6	59.8	91.0	18.9
180	63.6	1.1	17.6	40.4	58.0	95.9	29.4

[a]Percent o.d. wood basis.
[b]Percent of original content.

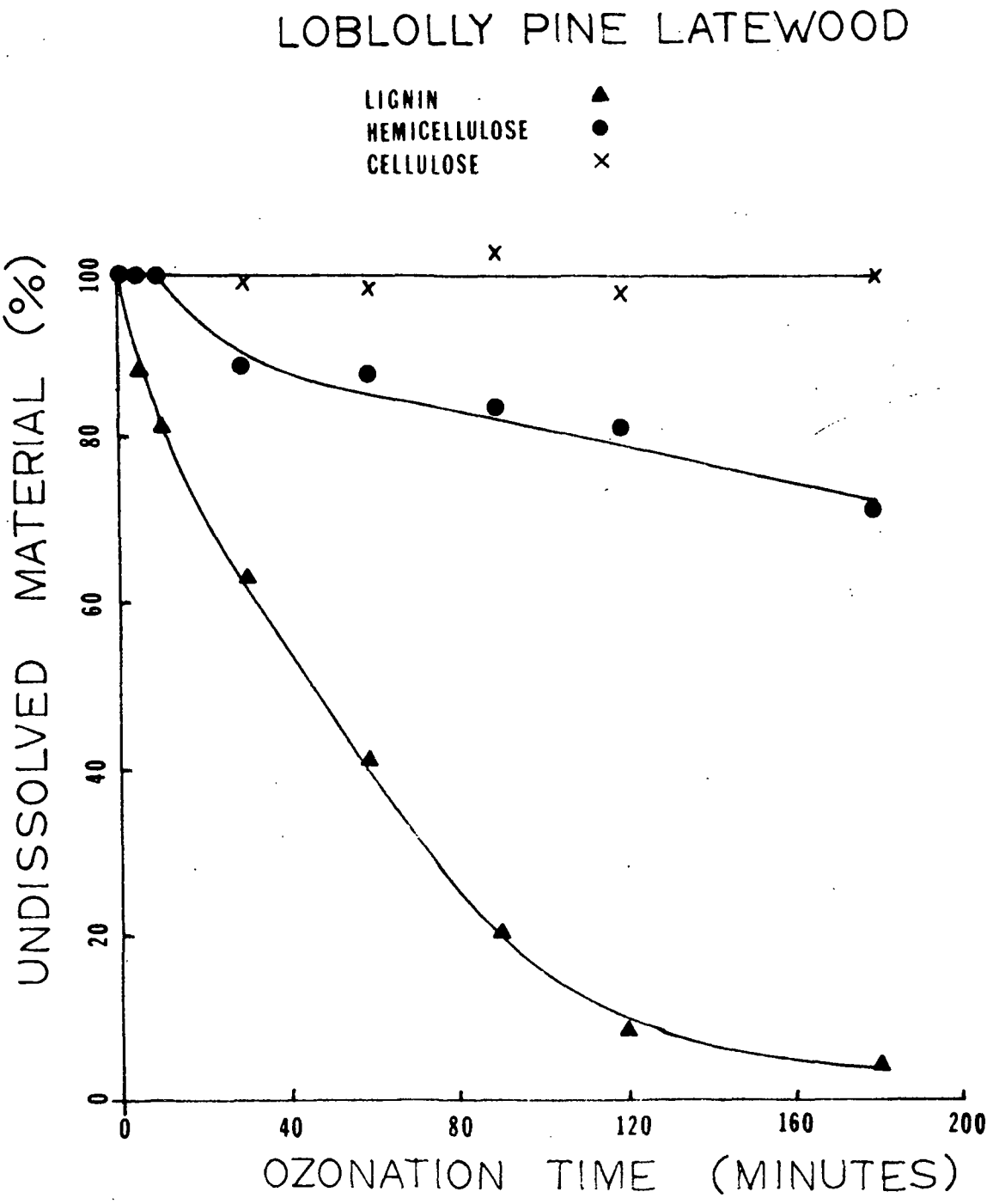

Figure 11. The relationship between undissolved wood components (% of original content) and ozonation time for LW fibers.

The relationship between undissolved LW wood components and ozonation time is shown Fig. 11. It can be seen that cellulose was not removed after 180 minutes of ozonation. Hemicellulose was not removed for the first 10 minutes of ozonation. However, longer ozonation times resulted in its removal. Approximately 30% of the hemicelluloses were removed after 180 minutes of ozonation. Lignin was removed during the entire ozonation period. Approximately 96% of the lignin was removed over 180 minutes of ozonation. This data indicated that ozone preferentially removed wood components from the fibers. The relative rates of removal were in the order of lignin > hemicellulose >> cellulose. It was not possible to determine whether preferential removal of wood components was due to chemical reactivity or topochemical restraint. This agrees with previous investigations on the ozonation of wood components (59,61,67).

Lignin and hemicellulose data shown in Fig. 11 indicate ozonation to be indiscriminate with respect to these components, since loss of both occurred. It is probable these wood components were degraded prior to to their solubilization. In contrast, cellulose was not removed during the entire reaction period. However, the lack of cellulose removal does not exclude the possibility of its partial degradation.

Viscosity and degree of polymerization measurements were determined for holocellulose samples prepared from LW fibers to investigate the extent of cellulose degradation by ozonation. Even though data from these measurements are not absolute due to hemicellulose interference, they are considered appropriate for monitoring extent of cellulose degradation. The contribution from cellulose toward holocellulose viscosity and degree of polymerization should predominate over that for hemicellulose due to its higher weight

percentage in this sample (Table III) and its higher degree of polymerization relative to hemicellulose (81).

Cupriethylenediamine (CED) viscosities and degree of polymerization viscosity averages (DPv) are presented in Table IV. For CED viscosities, the holocellulose samples did not completely dissolve in the CED solutions. Mbachu (73) also noted incomplete dissolution of holocellulose samples prepared from control and ozonated spruce wood meal in CED solutions. Even though reported CED viscosity values are not exact, they can be viewed as significant for showing trends in cellulose degradation during ozonation. A 40-50% CED viscosity drop occurred within the first 5-10 minutes of ozonation indicating significant degradation of the cellulose during the initial stages of ozonation. Values for DPv were calculated from CED viscosities (Table IV).

TABLE IV

VISCOSITIES OF OZONATED LATEWOOD FIBERS

Ozonation Time, min	0.5% CED Viscosity, cp	Degree of Polymerization,[a] viscosity average
0	19.3	1340
5	11.1	969
10	10.0	900
30	7.5	714
60	--	--
90	5.4	506
120	--	--
180	5.1	471

[a]Degree of polymerization calculated from the following Equation given by Mbachu (73):

$$[n] = 954 \log(0.5\% \text{ CED viscosity}) - 325 \qquad (15)$$
$$0.905 \log DP = \log 0.75 + \log [n]$$

Cellulose DPv was found to approach 400 during ozonation. This is comparable with Mbachu's (73) findings for ozonated spruce wood meal which

reached a DPv limit near 350 after 120 minutes ozonation. A leveling-off DP of about 200-400 has been observed by other researchers for ozonated wood shavings (67,69). They concluded this leveling-off degree of polymerization corresponded to the crystalline regions of native wood cellulose which were inaccessible and therefore resistant to ozone attack.

Degree of polymerization number averages (DPn) and weight averages (DPw) were determined for cellulose by the tricarbanilation procedure of Schroeder and Haigh (88). A drop in DPn from 340 to 220 occurred within the first 5 minutes of ozonation and remained constant over the entire ozonation period (Table V). The initial rapid drop in DPn may be in part attributed to low tricarbanilation yields for 5-30 minutes. It is thought higher DPn and DPw polysaccharide material does not undergo tricarbanilation as readily as lower DP material resulting in lower yields (89). Thus, DPn values determined for samples ozonated for 5-30 minutes may be slightly low as a result of the low tricarbanilation yields.

TABLE V

DEGREE OF POLYMERIZATION FOR OZONATED LATEWOOD FIBERS

Ozonation Time, min	Total Yield[a], %	DP Number Average	DP Weight Average
0	67.5	340	4300
5	40.9	220	1590
10	44.5	220	1580
30	48.4	240	1780
60	--	--	--
90	65.6	240	1440
120	--	--	--
180	69.0	240	1820

[a]Total carbanilate yield.

Tricarbanilation yields increased to about 70% after 120 minutes ozonation resulting in more accurate DP measurements. Degradation of cellulose was evidenced by the decrease in DPn from 340 to 240 after 180 minutes ozonation. A DPn of 4-7 is necessary for cellulose solubilization in water at 30°C (90). Thus, a loss in cellulose was not observed for ozonated samples (Table III).

In summary, results from physical and chemical analyses of LW fibers have shown ozonation of the fibers to be indiscriminate in that both lignin and polysaccharides were degraded. Therefore, ozone does not demonstrate a wood component selectivity. However, there was preferential removal of wood components in the order of lignin > hemicellulose >> cellulose. It was not possible to determine whether preferential removal of wood components was due to chemical reactivity or topochemical restraint.

Physical and chemical analyses of the LW fibers were supported by microscopic analyses which will be discussed in the following section.

MICROSCOPIC ANALYSES OF LATEWOOD FIBERS

Light, TEM and SEM microscopes were used to qualitatively monitor lignin removal from the cell walls of fibers and to examine the external surface structure of fiber cell walls before and after ozonation.

Never-dried LW fibers were Graff C-stained and examined using polarized light microscopy. Under polarized light, areas of the fiber containing lignin appear yellow to orange whereas areas containing mainly carbohydrates appear white. Control LW fibers (Fig. 12) appeared orange indicating the presence of lignin throughout their cell walls.

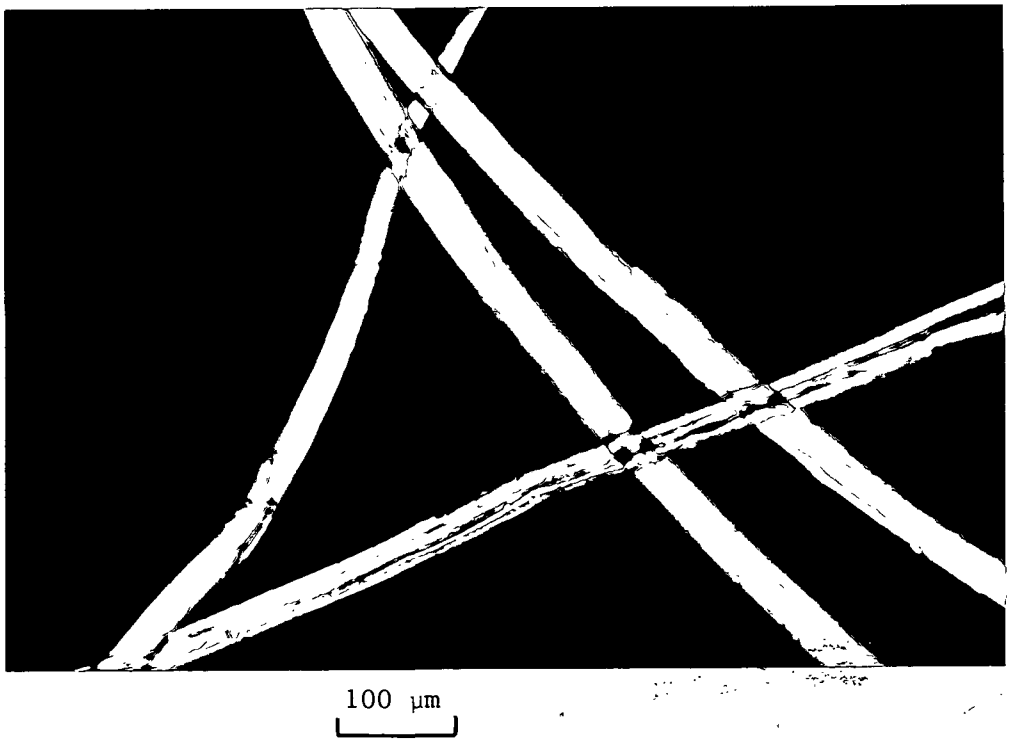

Figure 12. Graff C-stained control LW fibers under polarized light; orange appearance indicates presence of lignin.

TEM micrographs (Fig. 13-14) of cross-sectioned, embedded control LW fibers show the various cell wall layers. Middle lamella and corner middle lamella can be seen on the outer cell wall of the fibers (Fig. 13). Most of the splits between the fibers were found to occur through the middle lamella region resulting in a lignin sheath surrounding the outer cell wall of the fibers. The S1, S2, and S3 layers of the secondary cell wall appear intact and microfibrillar structure of these cell wall layers are faintly visible.

SEM micrographs (Fig. 15-16) of critical point dried control fibers show these fibers to be rigid and have smooth, nonfibrillar surfaces. The smooth appearance of the fibers is consistent with a lignin sheath surrounding the outer fiber cell wall.

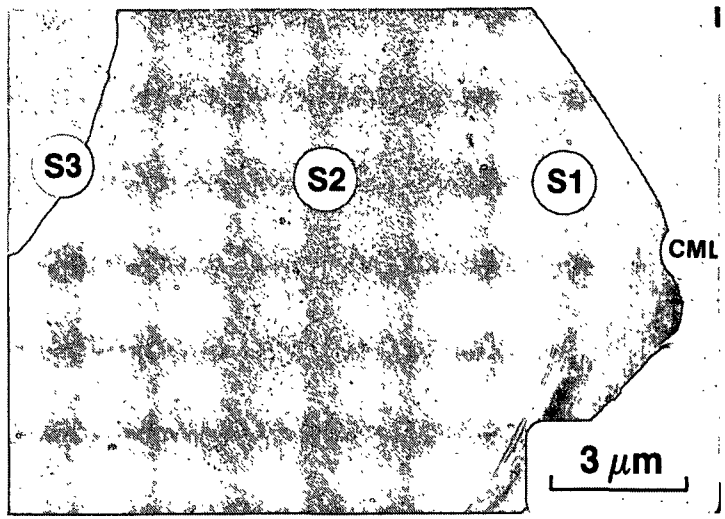

Figure 13. Cross sectional view of a portion of a LW fiber showing compound middle lamella (CML), S1, S2, and S3 layers; TEM micrograph.

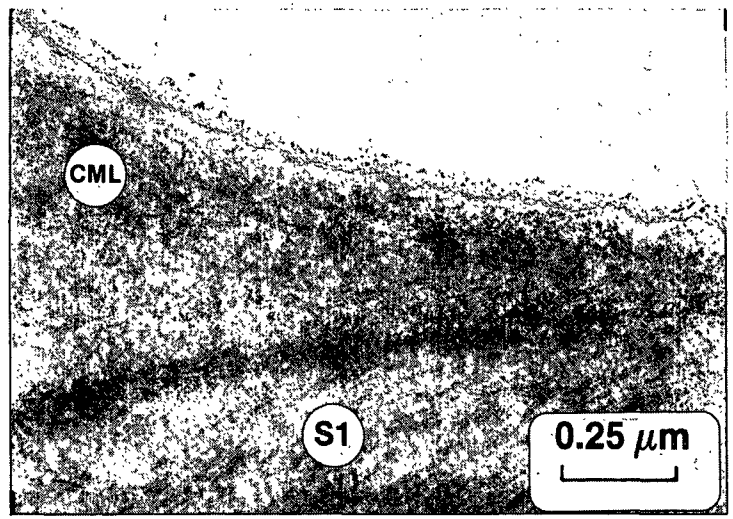

Figure 14. Cross sectional view of a portion of a LW control fiber showing CML and S1 layers; TEM micrograph.

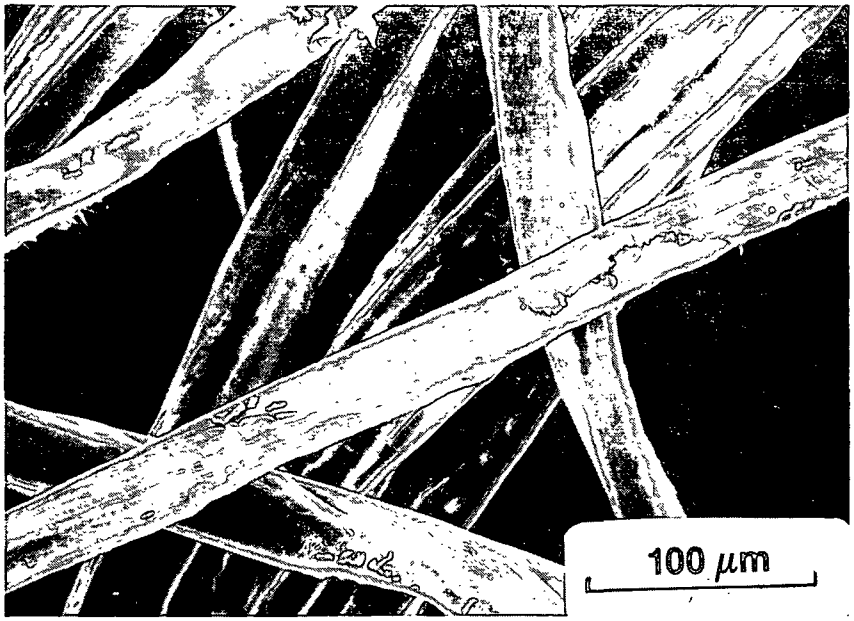

Figure 15. Control LW fibers appear rigid with smooth surfaces; SEM micrograph.

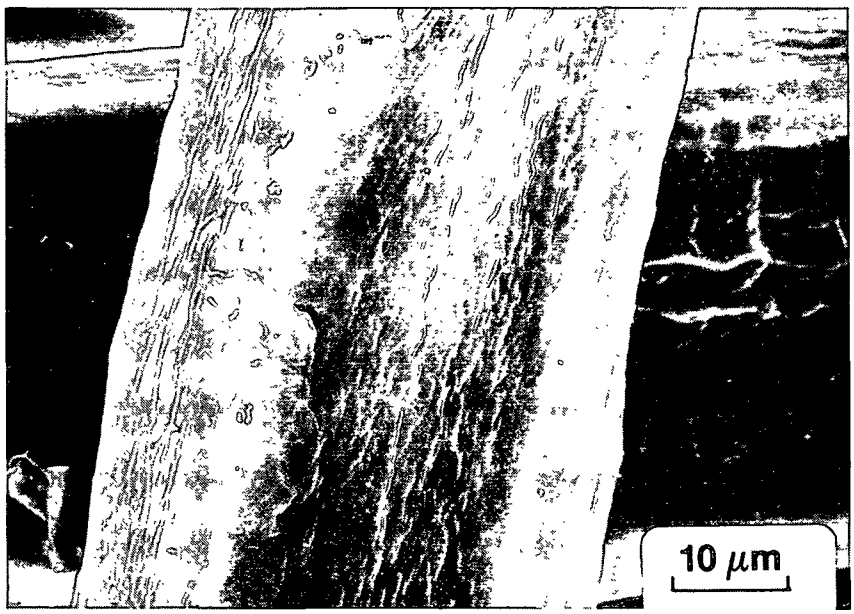

Figure 16. Control LW fiber surfaces appear smooth and almost free of fibrillar debris; SEM micrograph.

Light micrographs of LW fibers ozonated for 5-10 minutes (Fig. 17-18) show these fibers to be primarily orange indicating the presence of lignin in these areas. The tips of the fibers are white indicating lignin removal from these areas. This parallels lignin removal (~20%) determined by chemical analyses (Table III and Fig. 11) for these ozonation times.

TEM micrographs of LW fibers ozonated for 5-10 minutes are shown in Fig. 19-21. Slight degradation of the compound middle lamella (middle lamella and primary wall) can be observed for fibers ozonated 5 minutes (Fig. 19). Increased degradation of the compound middle lamella (CML) occurred after 10 minutes of ozonation. Fragmentation of the CML can be seen at both low and high magnifications (Fig. 20 and 21, respectively). Some fragments are pulling away from the external surface of the fiber cell walls which would account for lignin losses determined by chemical analyses (Table III). Degradation of polysaccharides occurred at these ozonation times as indicated by the 50% CED viscosity drop (Table IV).

SEM micrographs of fibers ozonated for 5-10 minutes show these fibers to be rigid and have relatively smooth surfaces (Fig. 22-25). Cell wall debris can be seen on the external fiber surfaces. Localized pitting was observed on the fiber surfaces at higher magnification (Fig. 23 and 25) demonstrating degradation of external fiber surfaces.

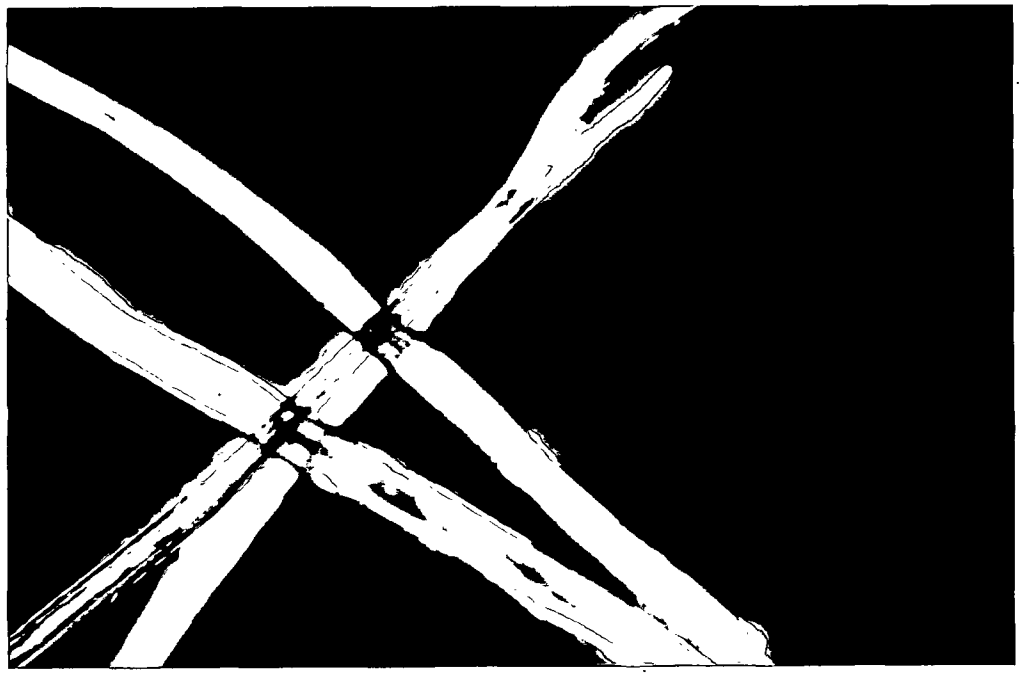

100 µm

Figure 17. LW fibers ozonated 5 minutes showing lignin removal (white area); Graff C-stained, polarized light micrograph.

100 µm

Figure 18. LW fibers ozonated 10 minutes showing lignin removal at tips of fibers (white areas); Graff C-stained, polarized light micrograph.

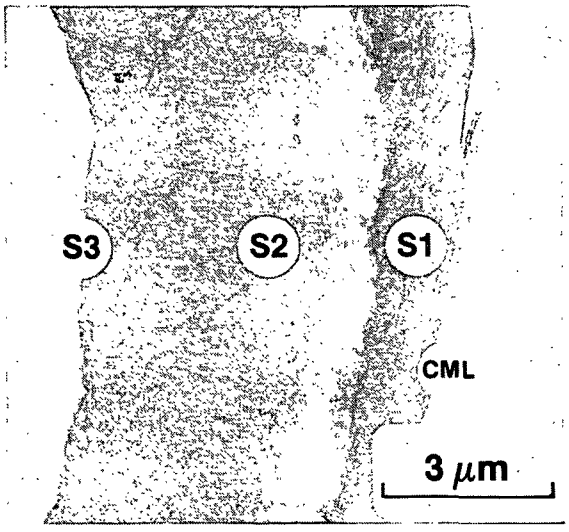

Figure 19. LW fiber ozonated 5 minutes showing slight degradation of the CML; TEM micrograph.

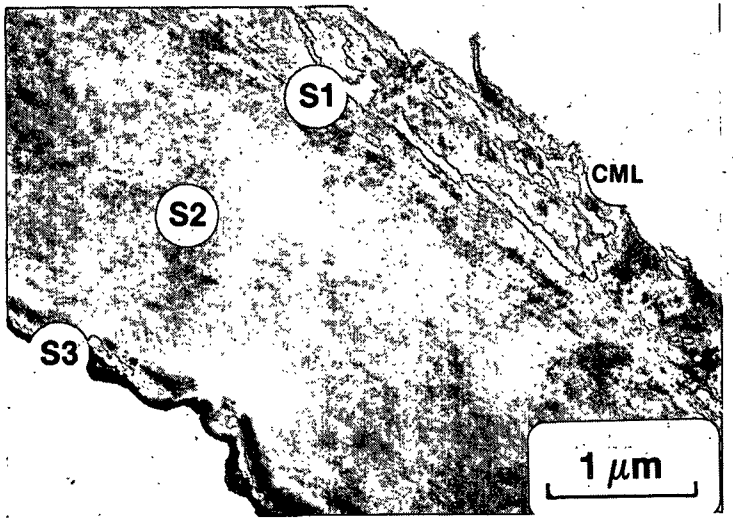

Figure 20. LW fiber ozonated 10 minutes showing fragmentation of the compound middle lamella (CML); TEM micrograph.

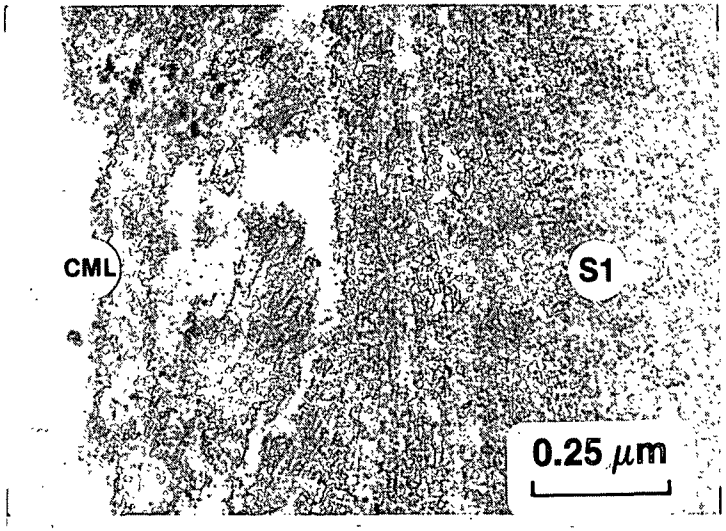

Figure 21. LW fiber ozonated 10 minutes showing fragmentation of the compound middle lamella (CML) at higher magnification; TEM micrograph.

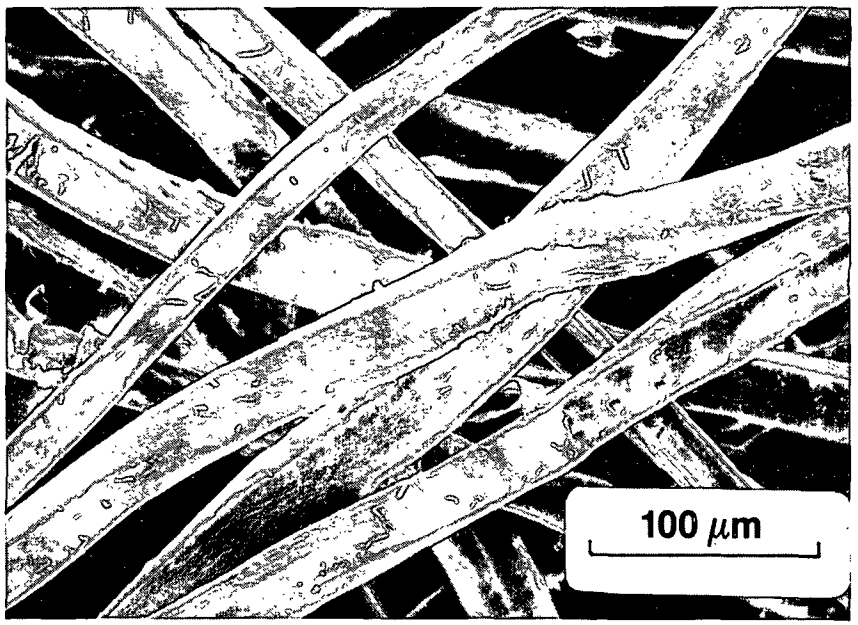

Figure 22. LW fibers ozonated 5 minutes appear rigid with relatively smooth surfaces; SEM micrograph.

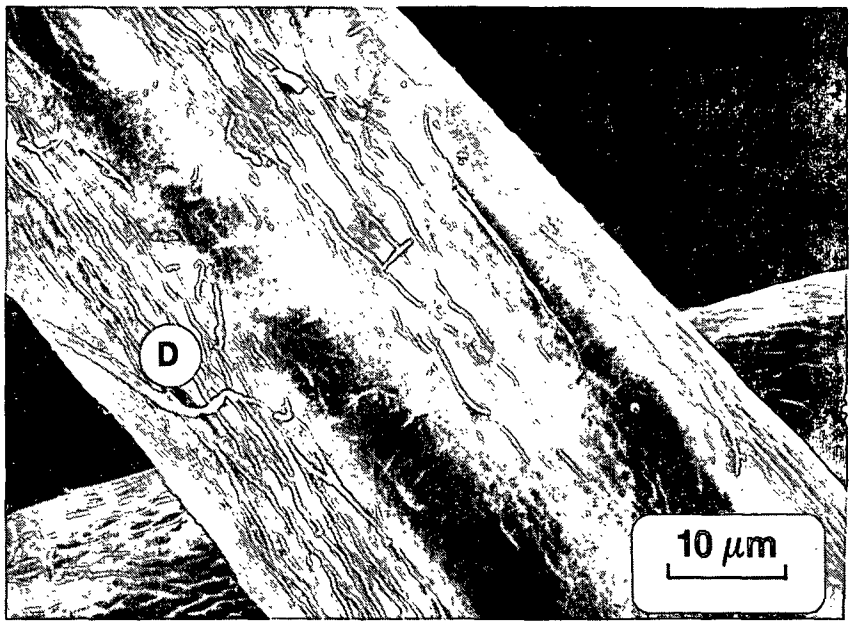

Figure 23. Small amounts of cell wall debris (D) is visible on faces of fibers ozonated 5 minutes; SEM micrograph.

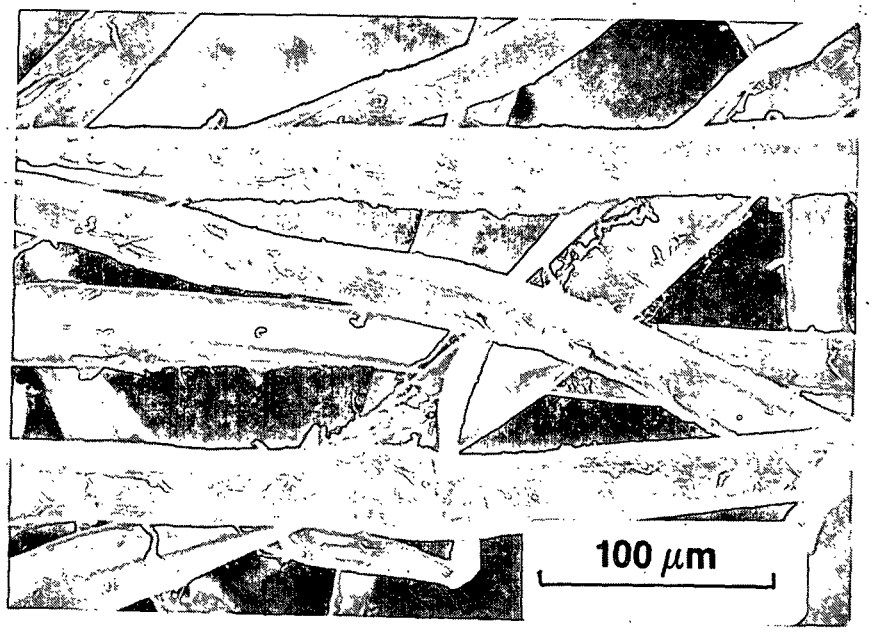

Figure 24. LW fibers ozonated 10 minutes appear rigid with increased cell wall debris; SEM micrograph.

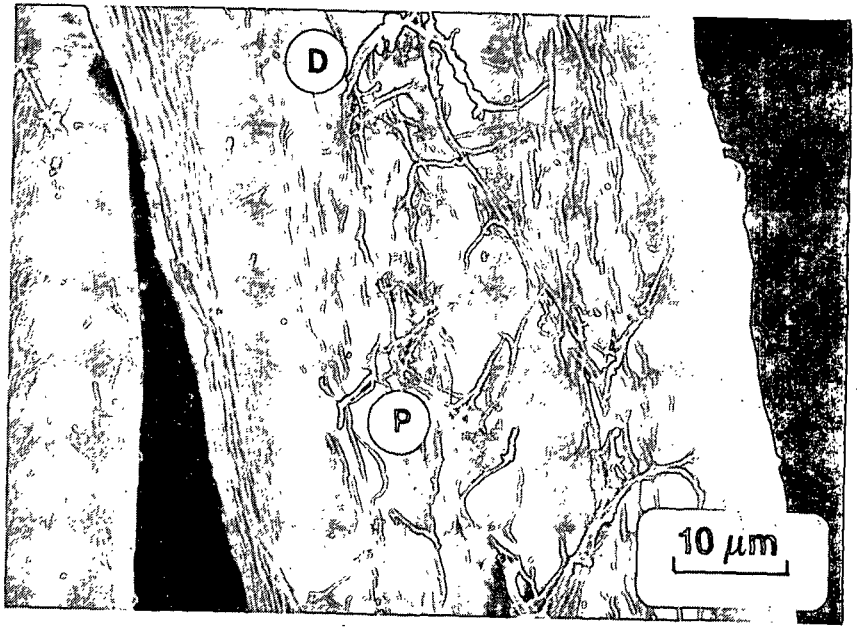

Figure 25. Localized pitting (P) and cell wall debris (D) is visible on surfaces of fibers ozonated 10 minutes SEM micrograph.

Light micrographs (Fig. 26-27) of LW fibers ozonated for 30 minutes show orange areas of fiber cell walls indicating the presence of lignin. Relatively large areas of white appear along the cell wall of the fibers indicating lignin removal. Approximately 40% lignin removal as determined by chemical analysis (Table III) occurred at this ozonation time. A higher magnification light micrograph (Fig. 27) shows these fibers are white along their outer surfaces turning orange toward the center of the fibers. This suggests lignin removal started at the outer cell wall of the fibers and proceeded through the cell wall toward the cell lumen.

Examination of TEM micrographs shows the CML was removed thereby exposing the underlying cellulosic layers (Fig. 28-29). Removal of the CML would account for a loss of about 25% of the original lignin (81). However, approximately 40% of the original lignin was removed at this ozonation time (Table III) indicating lignin removal from within the cell wall occurred. Thus, results from microscopic and chemical analyses are in agreement.

Degradation of the secondary wall by ozone is visible by TEM as indicated by separation of the fiber cell wall between the S1 and S2 layers and by modification of microfibrillar structure. Increased resolution of the microfibrillar structure can be observed for 30 minutes ozonation time (Fig. 28-29) compared to lesser ozonation times (Fig. 13-14), 20-21). Increased resolution was thought to be due to some loss of amorphous lignin and hemicelluloses within the fiber cell wall exposing the underlying microfibrillar structure. As a result of increased resolution fragmentation and change in apparent microfibrillar orientation in the cell wall structure can be observed.

Figure 26. LW fibers ozonated 30 minutes showing areas of lignin removal (white); Graff C-stained, polarized light micrograph.

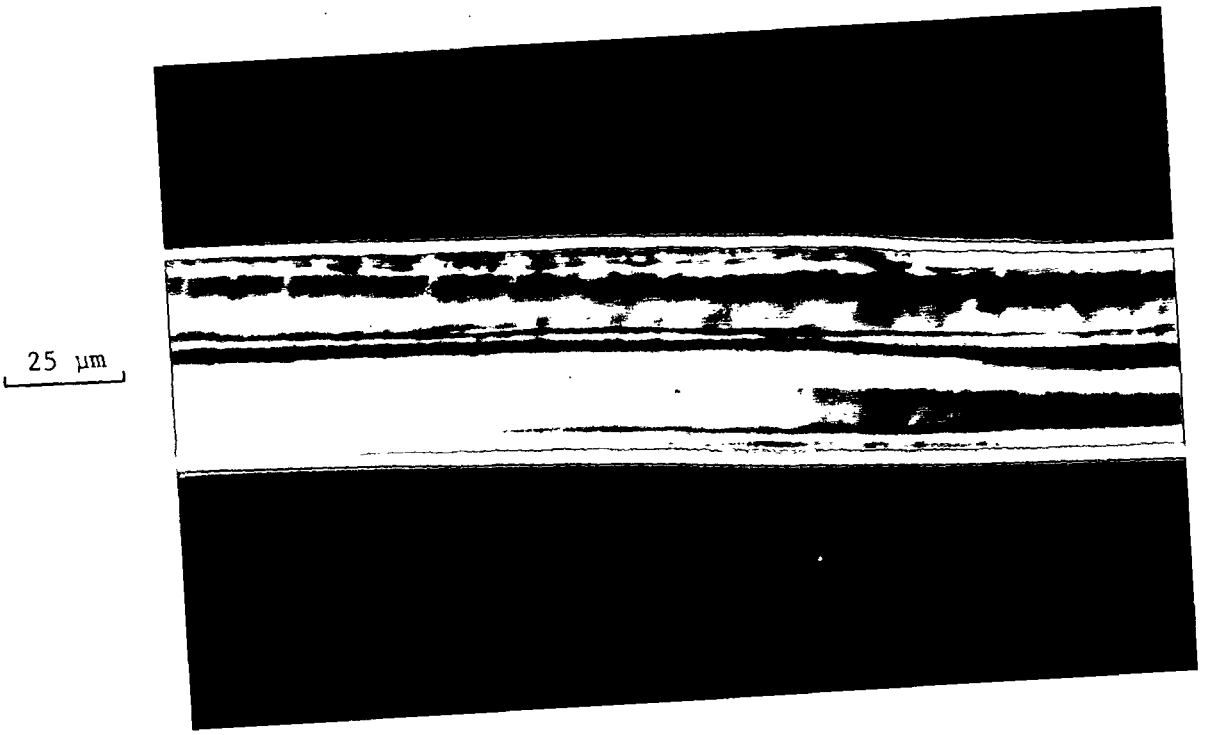

Figure 27. LW fibers ozonated 30 minutes showing lignin removal along outer cell wall, Graff C-stained, polarized light micrograph.

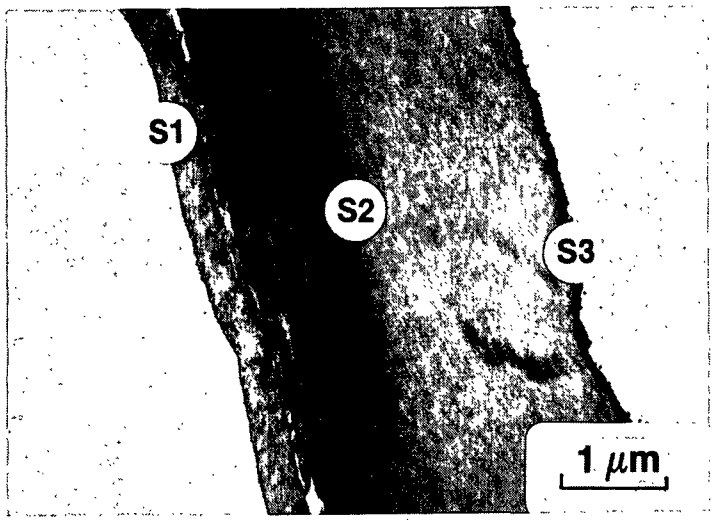

Figure 28. LW fiber ozonated 30 minutes showing S1, S2 and S3 layers; separation between S1 and S2 layers is visible; TEM micrograph.

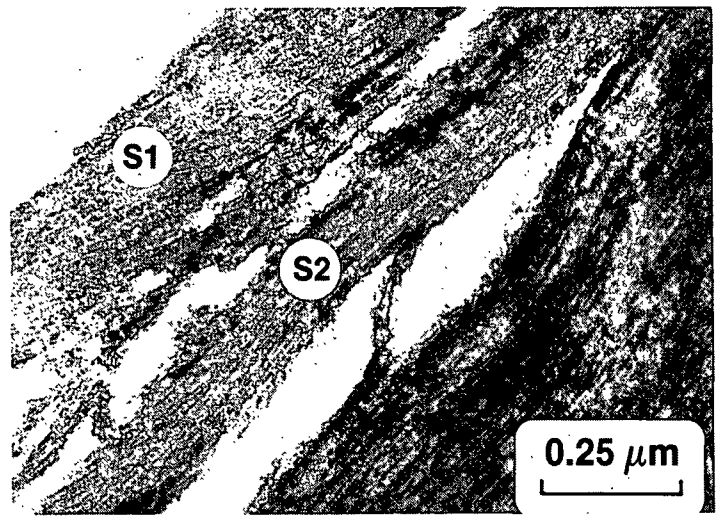

Figure 29. LW fiber ozonated 30 minutes showing separation of cell wall at S1 and S2 layers; microfibrillar orientation can be seen; TEM micrograph.

Fibers ozonated for 30 minutes still appear rigid as shown by SEM micrographs (Fig. 30-31). Increased cell wall debris is observed on the external surfaces of these fibers relative to fibers ozonated for lesser times. A higher magnification SEM micrograph (Fig. 31) shows pronounced pitting and erosion of the fiber surfaces occurred which allowed cellulosic strands to become visible. Peeling of the upper layers of the fiber wall began to occur resulting in increased surface debris.

Light micrographs (Fig. 32) show fibers ozonated for 90 minutes have a few patches of pale orange indicating the presence of lignin. Most of the fibers appear white indicating a high amount of lignin removal. This corresponds to approximately 80% lignin removal determined by chemical analysis (Table III).

TEM micrographs (Fig. 33-35) of fibers ozonated for 90 minutes show the S1 layer, buckling and pulling away from the S2 layer. Continued microfibrillar fragmentation may be seen in higher magnification TEM micrographs (Figs. 34-35) of these fibers.

Fibers ozonated for 90 minutes started to lose their rigidity and began to collapse, twist and wrinkle as shown in SEM micrographs (Fig. 36-37). This indicates ozone degradation of the internal cell wall structure of the fibers occurred. Increased cell wall debris can be seen on the external surfaces of the fibers and appears to be pulling away from the fiber walls. Pit membranes were also observed to be pulling away from the fiber walls.

Light micrographs (Fig. 38) of LW fibers ozonated for 180 minutes show these fibers are white indicating almost complete lignin removal which corresponded to 96% lignin removal determined by chemical analysis (Table III).

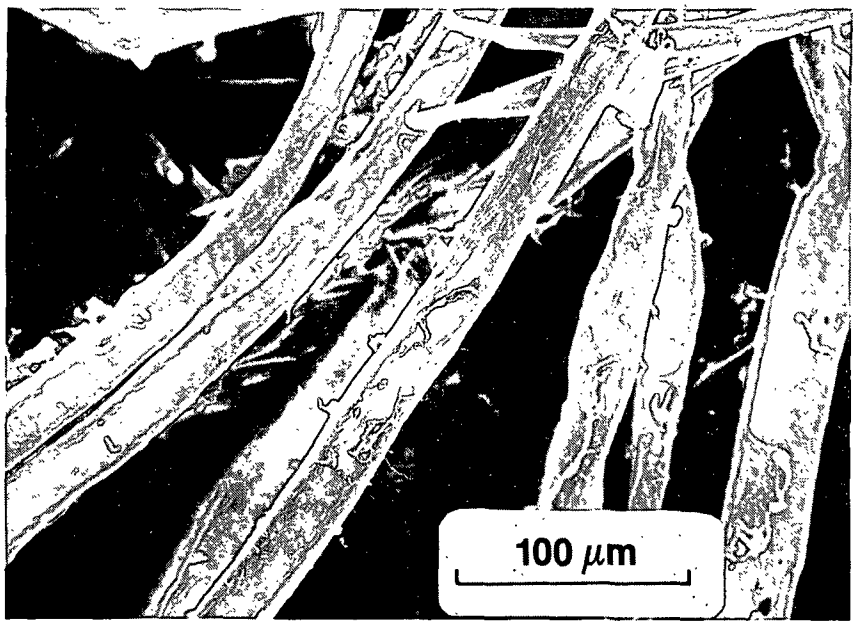

Figure 30. LW fibers ozonated 30 minutes appear rigid; notice cell wall debris on fiber surfaces; SEM micrograph.

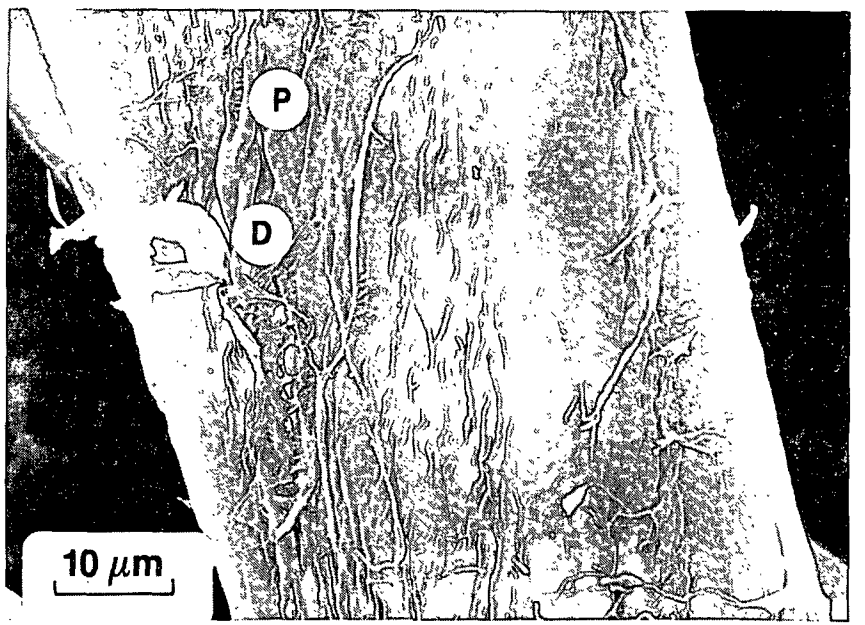

Figure 31. Pronounced pitting (P) and cell wall debris (D) appear on surfaces of LW fibers ozonated 30 minutes; SEM micrograph.

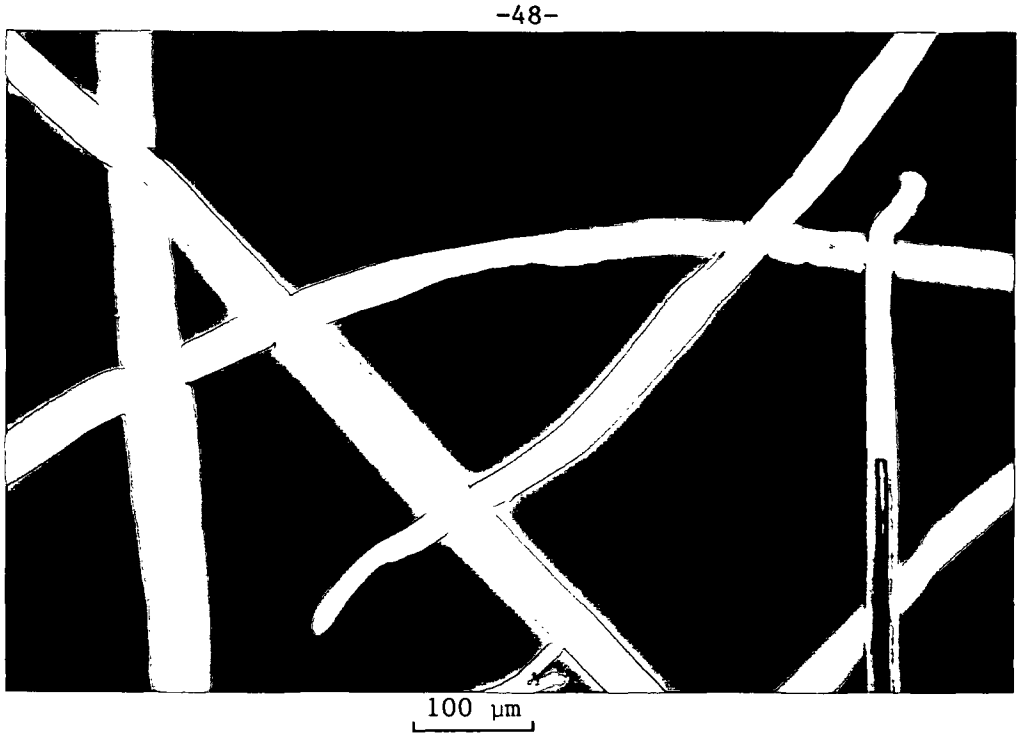

Figure 32. LW fibers ozonated 90 minutes appear almost entirely white indicating areas of lignin removal; Graff C-stained, polarized light micrograph.

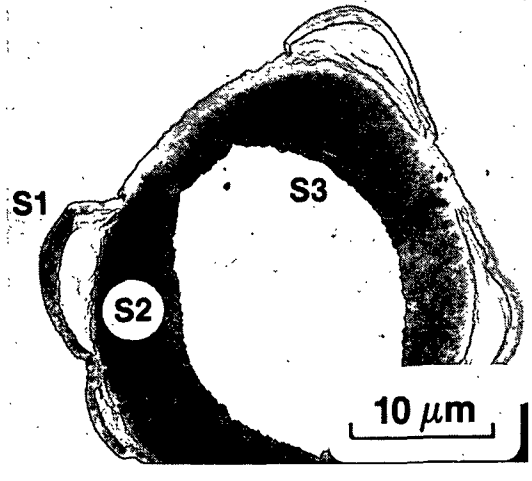

Figure 33. LW fiber ozonated 90 minutes showing increased separation between S1 and S2 layers; TEM micrograph.

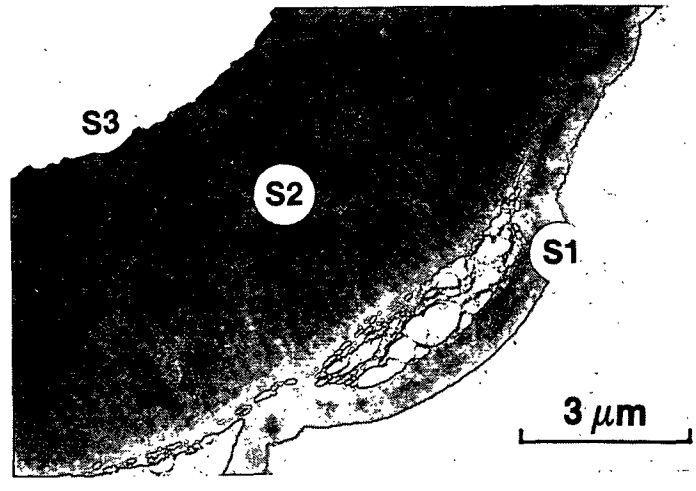

Figure 34. LW fiber ozonated 90 minutes showing buckling of S1 layer; TEM micrograph.

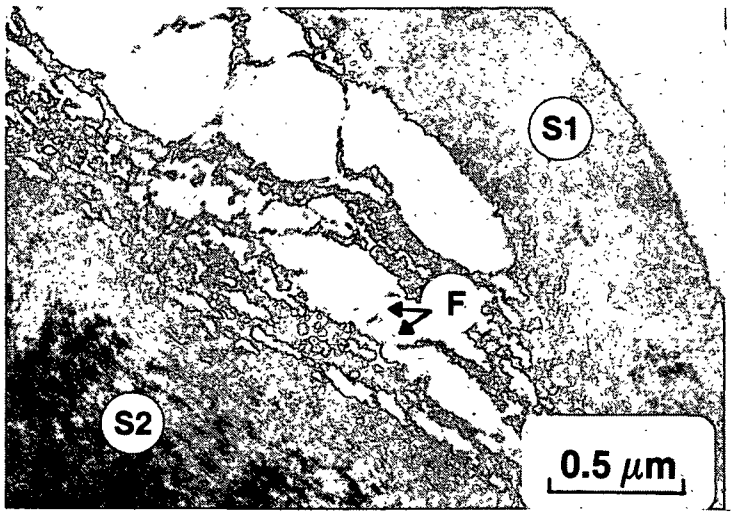

Figure 35. LW fiber ozonated 90 minutes showing change in apparent microfibrillar orientation and fragmentation (F); TEM micrograph.

TEM micrographs (Fig. 39-41) show continued separation of the S1 and S2 layers. Fragmentation and change in apparent microfibrillar orientation can be observed. Separation at the S2 and S3 interface can also be seen at this ozonation time.

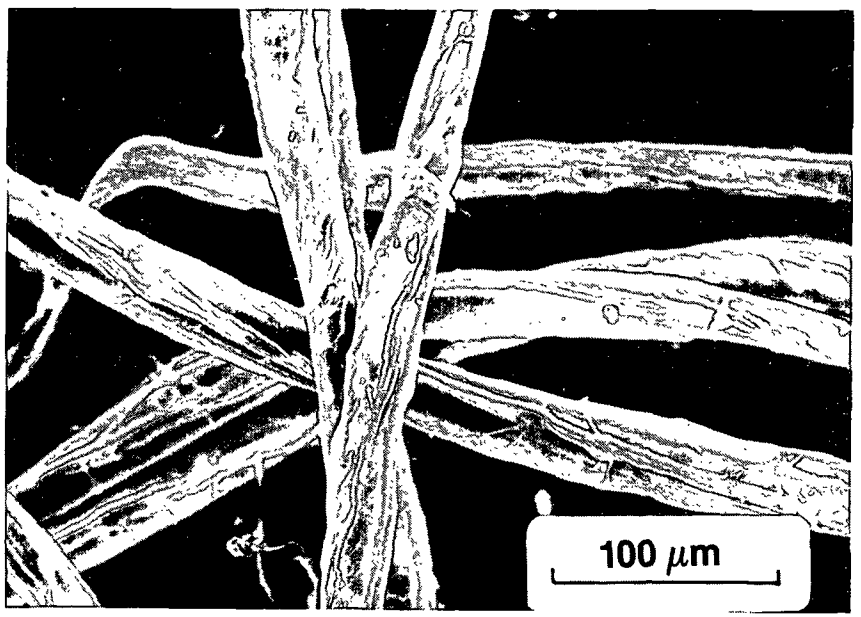

Figure 36. LW fibers ozonated 90 minutes appear twisted and wrinkled; SEM micrograph.

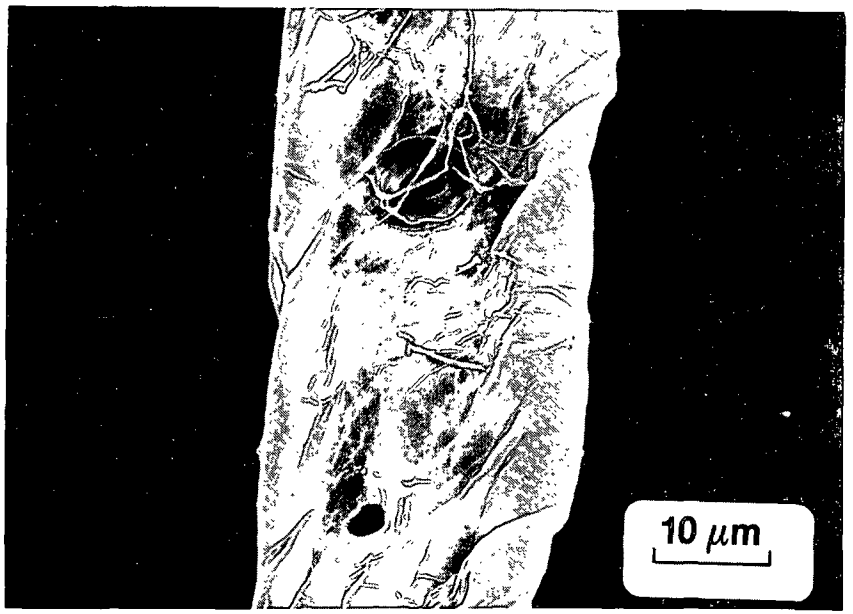

Figure 37. LW fibers ozonated 90 minutes appear collapsed and twisted; a pit membrane and cell wall debris can be seen pulling away from fiber wall; SEM micrograph.

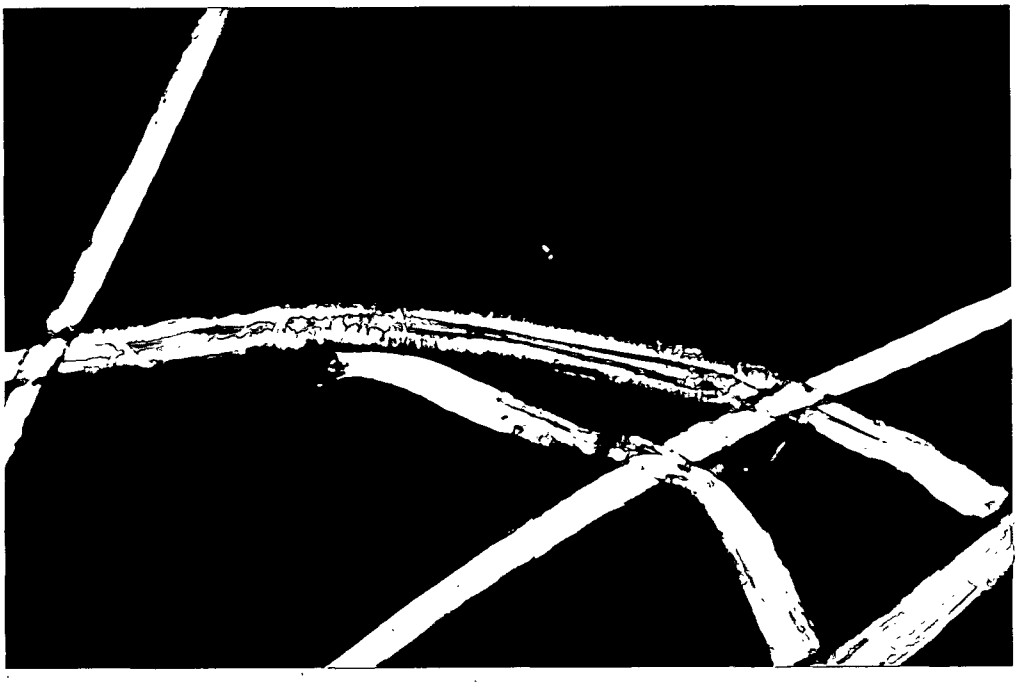

100 µm

Figure 38. LW fibers ozonated 180 minutes appear white indicating almost complete lignin removal; Graff C-stained, polarized light micrograph.

As shown in SEM micrographs (Fig. 42-43), these fibers have lost their rigidity and appear collapsed, twisted and wrinkled, indicating degradation of the internal cell wall structure. Cell wall debris and pitting can be seen on external fiber surfaces. Cracks in fiber cell walls may also be seen at this ozonation time.

In summary, results from light and TEM microscopic analyses indicated ozone penetrated and degraded cell wall material. Light microscopy showed lignin

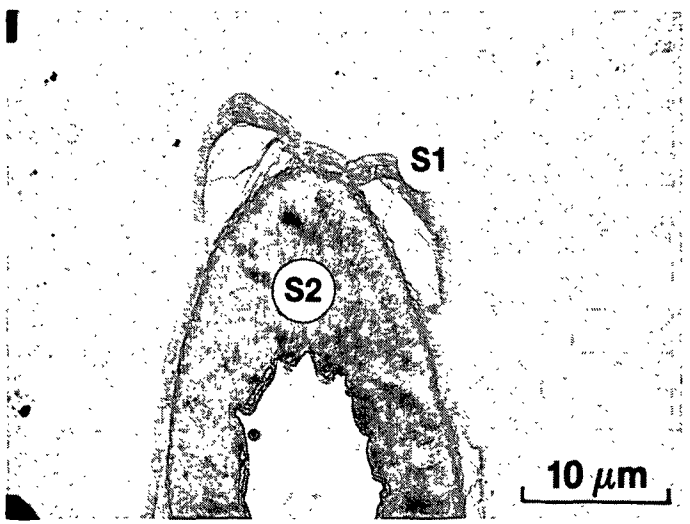

Figure 39. LW fibers ozonated 180 minutes showing continued separation between S1 and S2 layers; TEM micrograph.

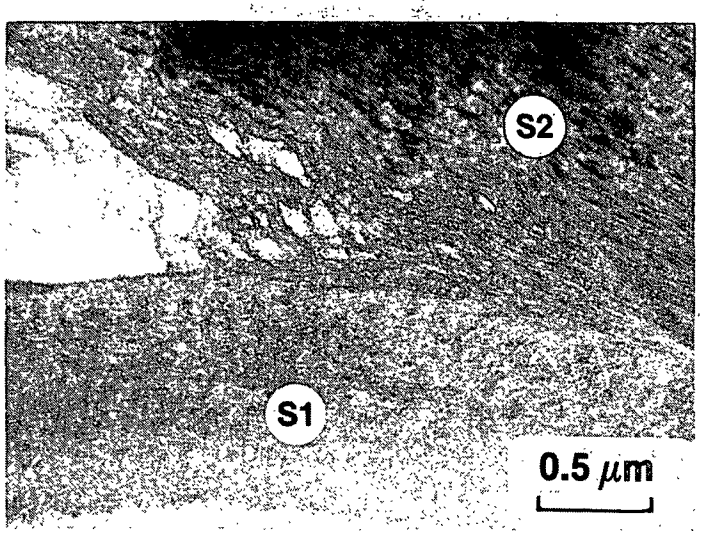

Figure 40. LW fiber ozonated 180 minutes showing change in apparent microfibrillar orientation and fragmentation; TEM micrograph.

removal started at the outer surfaces of the fibers and proceeded through the cell wall toward the lumen. TEM micrographs supported the results of light microscopy for the pattern of lignin removal and showed loss of the CML region thereby exposing the secondary cell wall. TEM micrographs also showed cell wall degradation as evidenced by an alteration in apparent microfibrillar orientation, fragmentation and separation in the S1, S2, and S3 layers. Pitting, erosion and cell wall debris were observed on external surfaces of LW fibers after ozonation as shown by SEM micrographs. Thus, ozonation was shown to result in degradation of the components of the internal cell wall structure and external surface of the fibers.

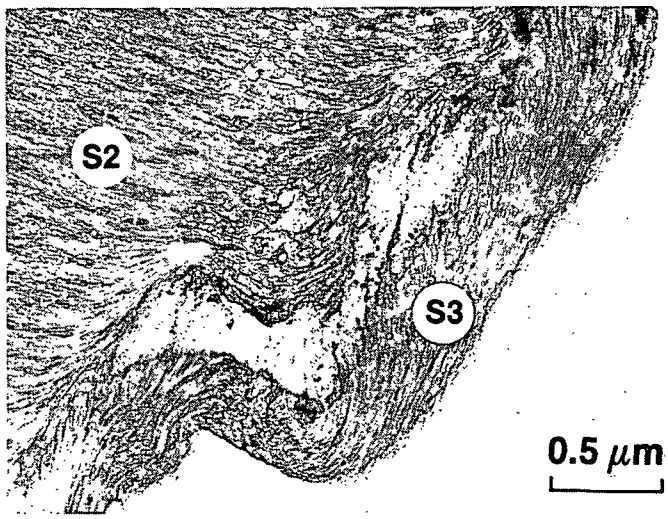

Figure 41. LW fiber ozonated 180 minutes showing separation between S2 and S3 layers; TEM micrograph.

REMOVAL OF WOOD COMPONENTS BY OZONE

As shown in Fig. 11, lignin, hemicellulose and cellulose were preferentially removed from LW fibers during ozonation. This observation can be explained with results from chemical, physical and microscopic analyses of the fibers.

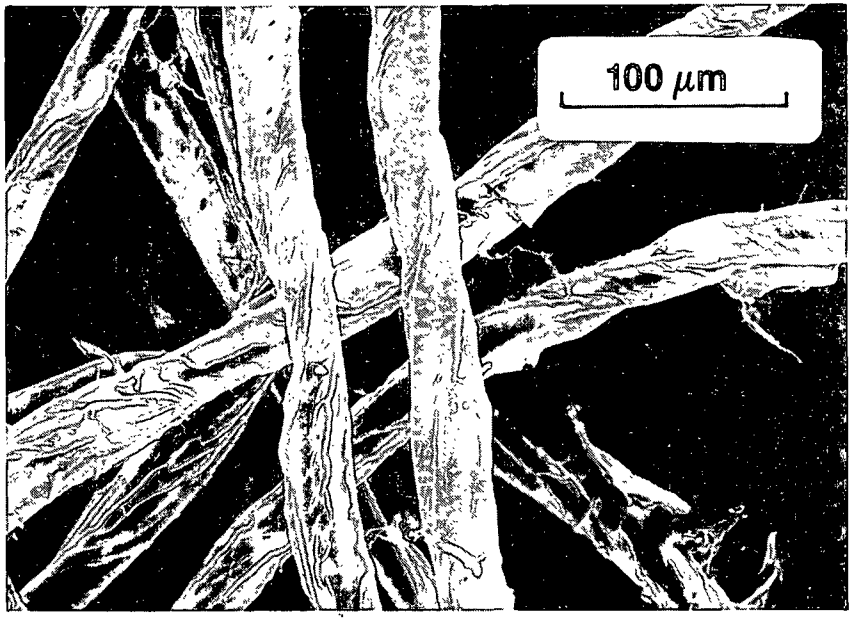

Figure 42. LW fibers ozonated 180 minutes appear collapsed, twisted and wrinkled; SEM micrograph.

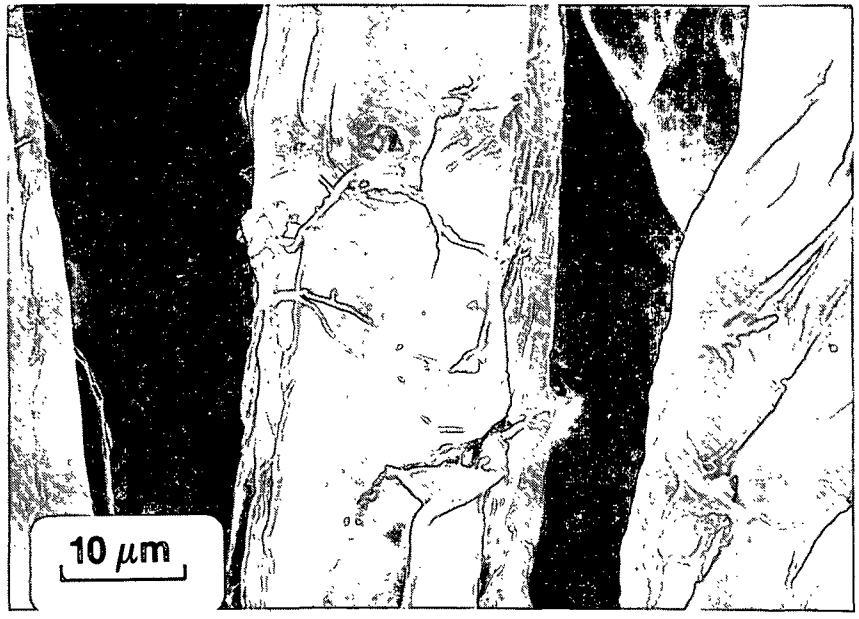

Figure 43. LW fibers ozonated 180 minutes appear collapsed; pitting of fiber surfaces and cracks in cell walls can be seen; SEM micrograph.

Prior to ozonation, microscopy showed the fibers had a lignin sheath surrounding their cell walls. Indiscriminate degradation of lignin and polysaccharides occurred in the initial stages of ozonation (5-10 minutes) as demonstrated by lignin removal and viscosity data, respectively. Therefore lignin could easily break away from the outer cell wall and be removed. The lignin sheath surrounding the cell wall was removed after about 30 minutes ozonation as shown by light and TEM microscopies. Removal of the lignin sheath exposed the cell wall structure and allowed fragmented hemicellulose to diffuse out. This would explain the onset of hemicellulose removal at this ozonation time. It was thought that cellulose removal did not occur because the cellulose fragments formed upon ozonation were not small enough to permit their solubilization. After 180 minutes ozonation, a DPn of 200-300 was determined for cellulose. A DPn of 4-7 is necessary for cellulose solubilization in water at about 30°C (90).

Thus ozonation of wood fibers resulted in indiscriminate and simultaneous degradation of lignin, hemicellulose and cellulose. However, preferential removal of wood components occurred in the order of lignin >> hemicellulose >> cellulose.

KINETICS OF OZONE-LIGNIN REACTION FOR LATEWOOD FIBERS

A general rate expression for delignification of fibers is given by:

$$R_L = d[L]/dt = k[L]^a[O_3]^b \qquad (16)$$

where

R_L = rate of delignification
t = reaction time, sec
L] = lignin content, mol/L
$_3$] = ozone concentration, mol/L
k = rate constant, $mol/L^{1-(a+b)}\ sec^{-1}$
a = reaction order with respect to lignin
b = reaction order with respect to ozone

Taking the logarithms of both sides of Eq. (35) gives:

$$\ln R_L = \ln k + a\ln[L] + b\ln[O_3] \qquad (17)$$

Delignification rate (R_L), lignin content ([L]), and ozone concentration ($[O_3]$) were determined from experimental data (Appendix XII) and fitted to Eq. (17) by multiple linear regression analysis to determine values for the reaction orders (a and b) and rate constant (k). Reaction orders and the rate constant with their respective 95% confidence interval limits are presented in Table VI for ozonation of LW fibers.

TABLE VI

REACTION ORDERS AND RATE CONSTANT FOR OZONATION OF LATEWOOD FIBERS

Component	Reaction Order	95% Confidence Interval
Lignin	0.80	0.76-0.84
Ozone	0.44	0.33-0.56
Rate Constant (10^{-4} $mM^{-0.24}$ sec^{-1})	7.59	5.68-10.2

The reaction order for lignin (0.80) was approximately twice that of ozone (0.44) indicating the rate of delignificaton was more dependent on lignin content than ozone concentration. The rate constant determined for delignification of LW fibers was 7.59 x 10^{-4} $mM^{-0.24}$ sec^{-1} (5.68 x 10^{-4} ⟶ 10.2 x 10^{-4} $mM^{-0.24}$ sec^{-1}). The values in parentheses represent the lower and upper limits for a 95% confidence interval. This agrees with the rate constant of 5.09 x 10^{-4} sec^{-1} Mbachu (71) found for ozonation of spruce wood meal.

STOICHIOMETRY OF OZONE-LIGNIN REACTION FOR LATEWOOD FIBERS

Stoichiometry of the ozone-lignin reaction was determined from the ratio of total millimoles ozone consumed during the reaction to total millimoles lignin removed (based on guaiacyl propane unit; Table VII). Calculations for the amount of ozone consumed during the reactions are described in Appendix IX. Ozone consumption due to solubilized byproducts (i.e., carbohydrate and lignin fragments) and ozone self-decomposition was taken into consideration during the calculations.

TABLE VII

STOICHIOMETRY OF OZONE-LIGNIN REACTION FOR LATEWOOD

Ozonation Time, min	Total Ozone Consumed, mM	Total Lignin Removed,[a] mM	Ozone Consumed/ Lignin Removed
0	0	0	0
5	0.34	0.15	2.27
10	0.54	0.24	2.26
30	1.12	0.48	2.33
60	1.95	0.78	2.50
90	2.62	1.06	2.47
120	3.03	1.23	2.46
180	3.24	1.27	2.55

[a]Assuming 188 mg/mmole guaicyl propane lignin unit.

Stoichiometric ratios for the ozone-lignin reaction were approximately the same for all ozonation times, 2.2-2.6 mM ozone consumed/mM lignin removed. This agrees with the stoichiometric ratio of 2.3-2.6 which Lyse (61) found for gas phase ozonation of fiberized loblolly pine wood. Values obtained for both studies were probably slightly high since ozone consumption due to *in situ* carbohydrate and lignin modification was not taken into account. The ratios

were fairly constant at all ozonation times suggesting lignin degradation was governed by the same type of reaction mechanism throughout the ozonation period.

OZONATION OF EARLYWOOD FIBERS

Ozonation of EW fibers was carried out under the same conditions (Appendices V-VI) as for LW fibers. Mean values, standard deviations and per cent coefficient of variation for ozone concentration with respect to reaction time are given in Appendix VII. Plots of ozone concentration mean values (± standard deviations) versus reaction time are also presented in Appendix VII. EW curves were similar in shape to the LW curves (Appendix VII). A representative EW fiber plot of ozone concentration versus reaction time for 180 minutes is shown in Fig. 44.

PHYSICAL AND CHEMICAL ANALYSES OF EARLYWOOD FIBERS

Results from physical and chemical analyses of EW fibers followed the same trends as for LW fibers. Fiber yield was found to decrease as ozonation time increased (Fig. 45). EW fiber yields agree with corresponding LW fiber yields over the entire ozonation period indicating a similar amount of wood component removal for both EW and LW fractions.

A chemical composition summary as per cent oven dried wood is shown in Table VIII and Fig. 46 for control and ozonated EW fiber samples. Data for lignin and carbohydrate content of EW samples are given in Appendices X and XI, respectively.

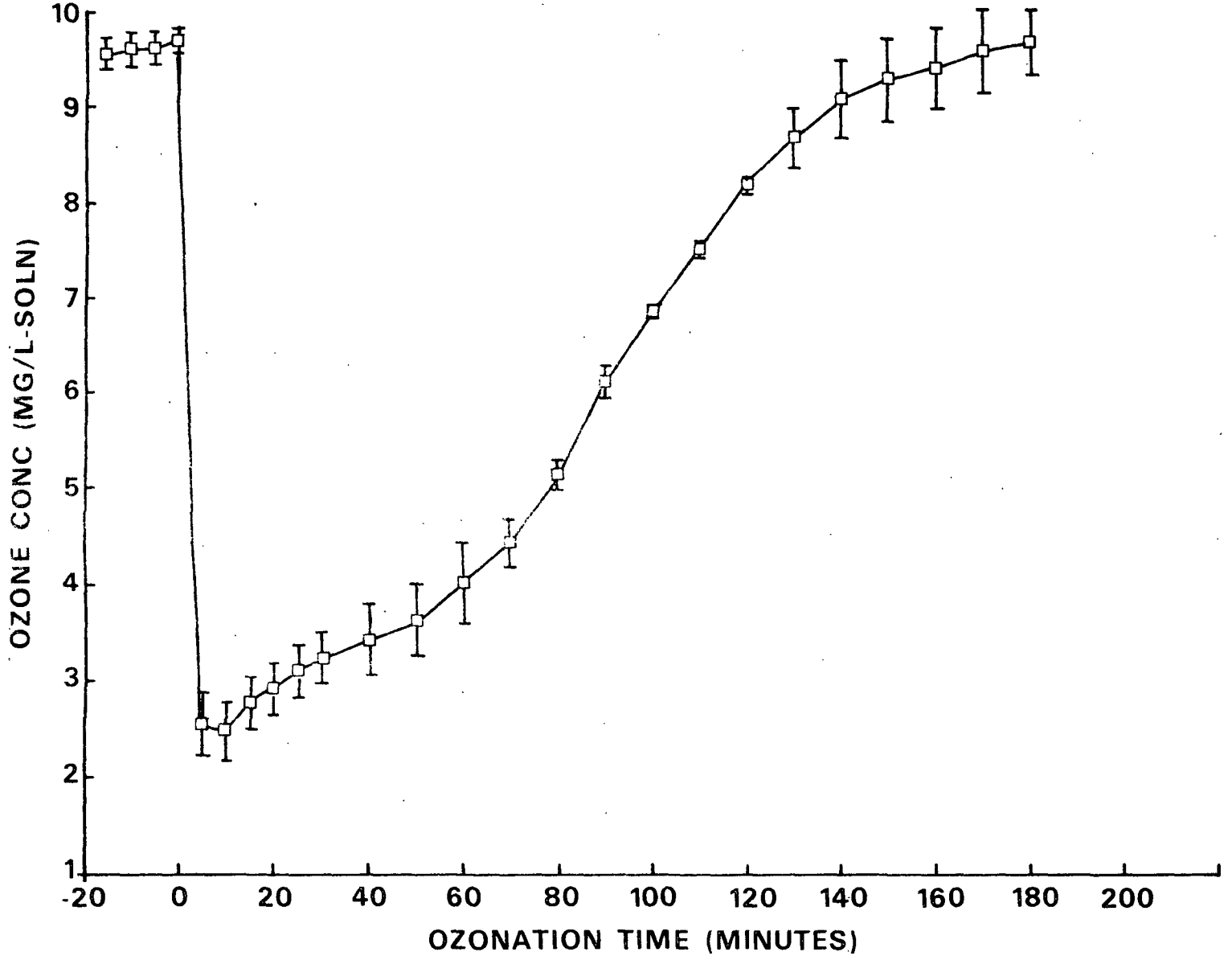

Figure 44. A representative plot of ozone concentration versus reaction time for ozonation of EW fibers in acetic acid buffer solution.

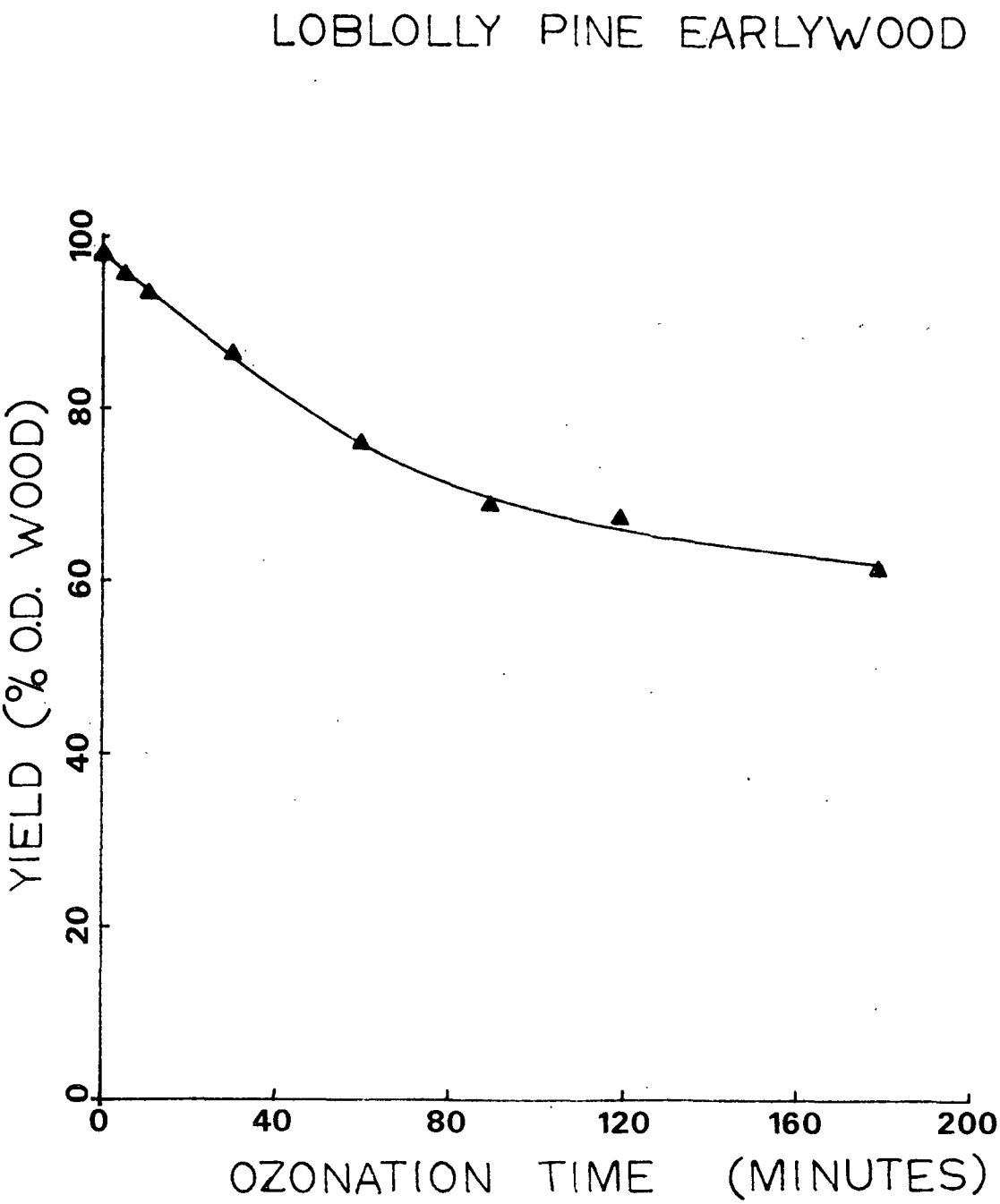

Figure 45. The relationship of EW fiber yield with respect to ozonation time.

TABLE VIII

CHEMICAL COMPOSITION SUMMARY OF OZONATED EARLYWOOD FIBERS[a]

Ozonation Time, min	Total Yield, %	Total Lignin, %	Total Hemi-cellulose, %	Total Cellulose, %	Total Carbo-hydrates, %	Delignification,[b] %	Solubilized[b] Hemi-cellulose, %
0	98.3	30.4	25.5	42.4	67.9	0.0	0.0
5	96.0	26.3	24.7	41.7	66.4	13.6	3.2
10	93.8	24.6	24.7	42.0	66.7	19.0	3.2
30	86.8	16.3	23.2	42.3	65.5	46.4	9.0
60	76.2	7.8	22.9	42.8	65.7	74.4	10.2
90	69.1	4.4	21.6	42.9	64.5	85.5	15.3
120	67.7	1.8	19.6	39.8	59.4	94.0	23.2
180	61.8	0.9	18.5	39.9	58.4	96.7	27.5

[a]percent o.d. wood basis.
[b]percent of original content.

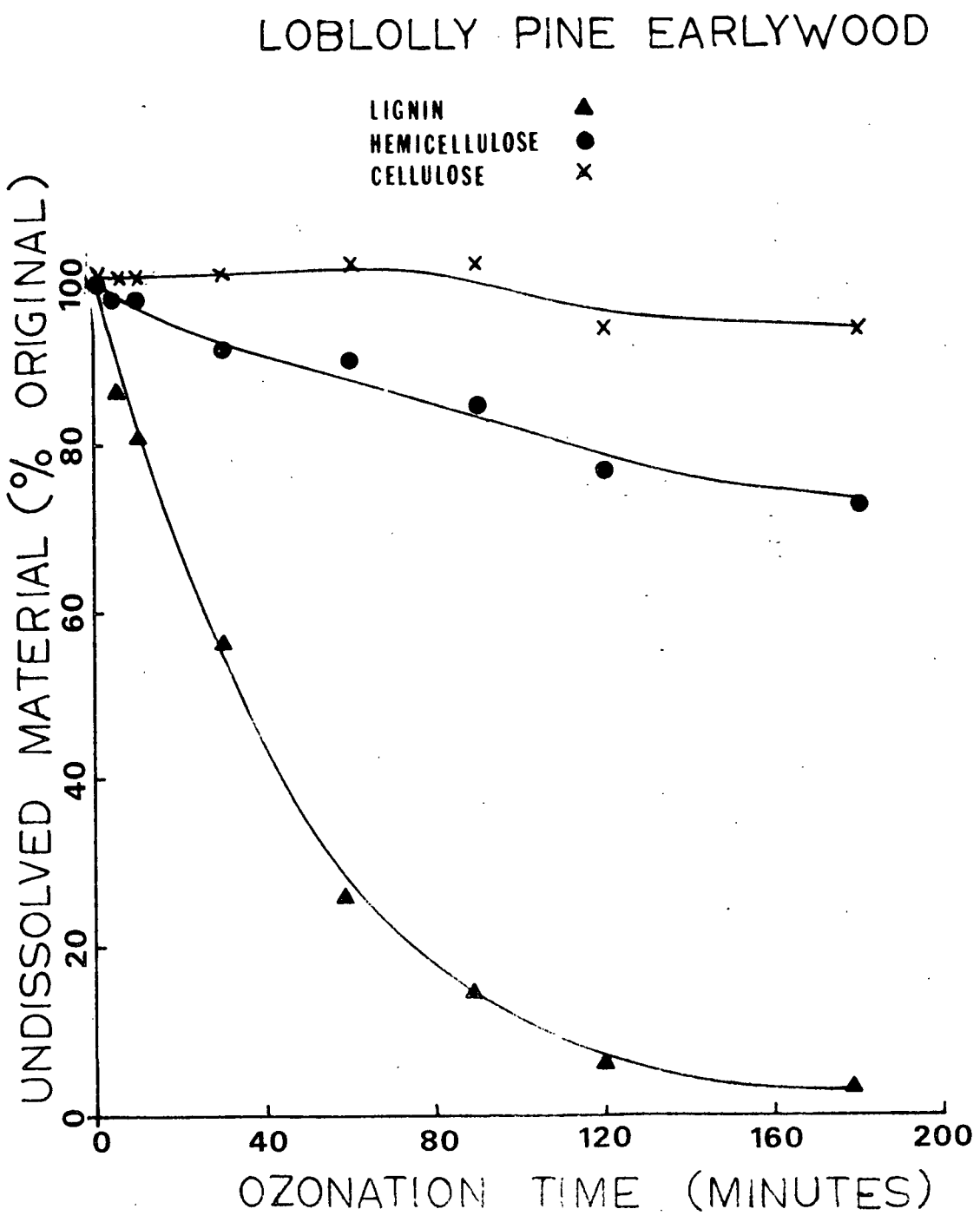

Figure 46. The relationship between undissolved wood components (% of original content) and ozonation time for EW fibers.

The relationship between undissolved wood components and ozonation time for EW samples is shown in Fig. 46. About 5% cellulose removal occurred over a period of 180 minutes ozonation. Approximately 30% hemicellulose was removed after 180 minutes ozonation, although appreciable hemicellulose removal did not occur until after 30 minutes. Approximately 97% lignin removal occurred after 180 minutes ozonation. These losses are comparable to those previously discussed for LW fibers (Table III). These data showed ozonation of EW fiber was indiscriminate since loss of both lignin and polysaccharides occurred. Thus, ozone does not demonstrate a wood component selectivity for EW fibers. However, ozone preferentially removed wood components in the relative order of lignin > hemicellulose >> cellulose. It was not possible to determine whether preferential removal of wood components was due to chemical reactivity or physical restraint. These trends are in agreement with those for ozonation of LW fibers (Fig. 11).

In summary, the amounts of individual wood components removed from EW fibers were similar to those for LW fibers at comparable ozonation times. Removal of EW components was only slightly faster than LW components suggesting reactivity of ozone with EW and LW fibers was essentially the same. Therefore, ozone does not exhibit tissue selectivity.

MICROSCOPIC ANALYSES OF EARLYWOOD FIBERS

Light, TEM and SEM microscopies were used to qualitatively examine cell wall and external surface structures of EW fibers. The procedures used to prepare the fibers for analyses were the same as for LW fibers.

Under polarized light microscopy, Graff C-stained control EW fibers appeared orange (Fig. 47) indicating the presence of lignin. Upon ozonation,

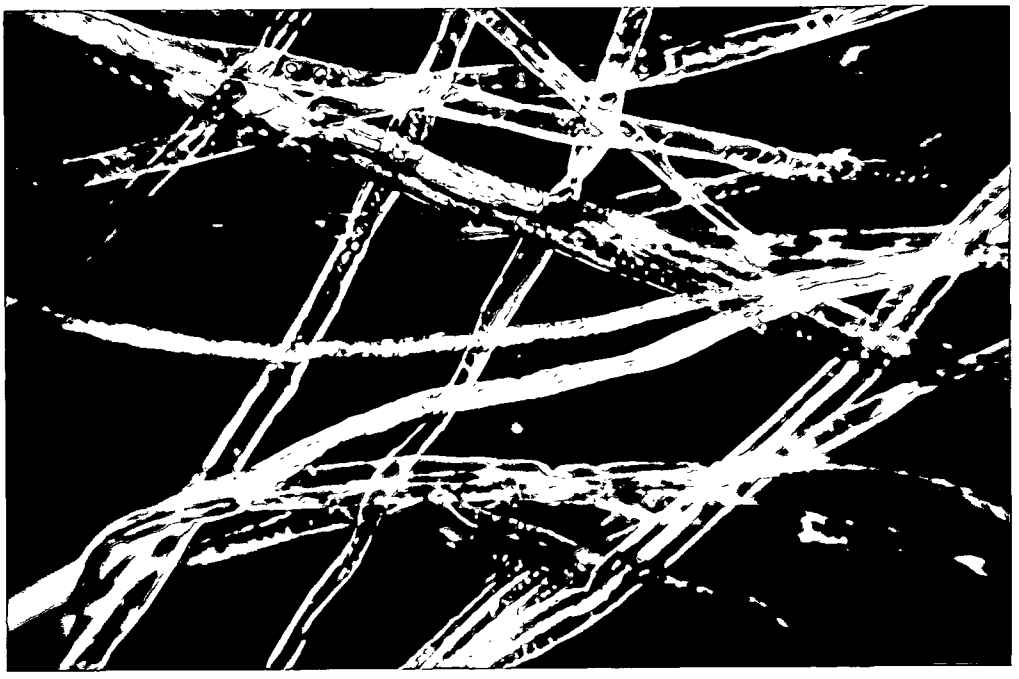

250 µm

Figure 47. Graff C-stained control EW fibers under polarized light; orange appearance indicates presence of lignin.

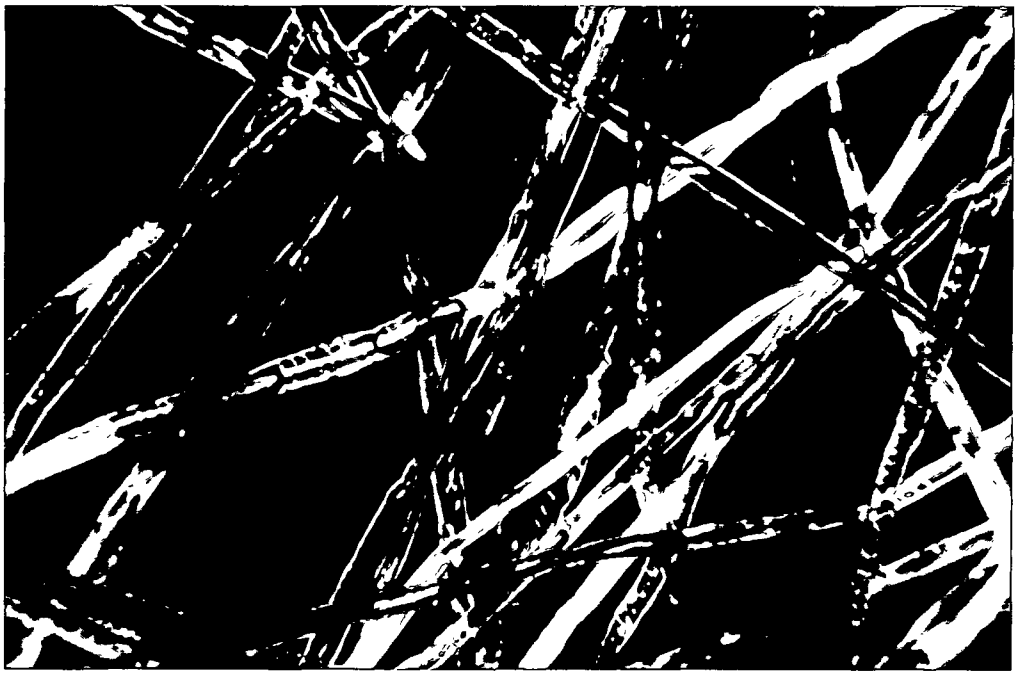

250 µm

Figure 48. EW fibers ozonated 10 minutes show removal at tips of fibers (white areas); Graff C-stained, polarized light micrograph.

Figure 49. EW fibers ozonated 30 minutes showing areas of lignin removal (white); Graff C-stained, polarized light micrograph.

Figure 50. EW fibers ozonated 90 minutes appear almost entirely white indicating lignin removal Graff C-stained, polarized light micrograph.

EW fibers gradually turned white, progressing from the outer fiber surfaces toward the lumen (Fig. 48-50). After 180 minutes ozonation, EW fibers were white indicating almost complete lignin removal (Fig. 51). This corresponds to ~ 97% lignin removal determined by chemical analyses (Table VIII). These results are in agreement with those found for LW fibers.

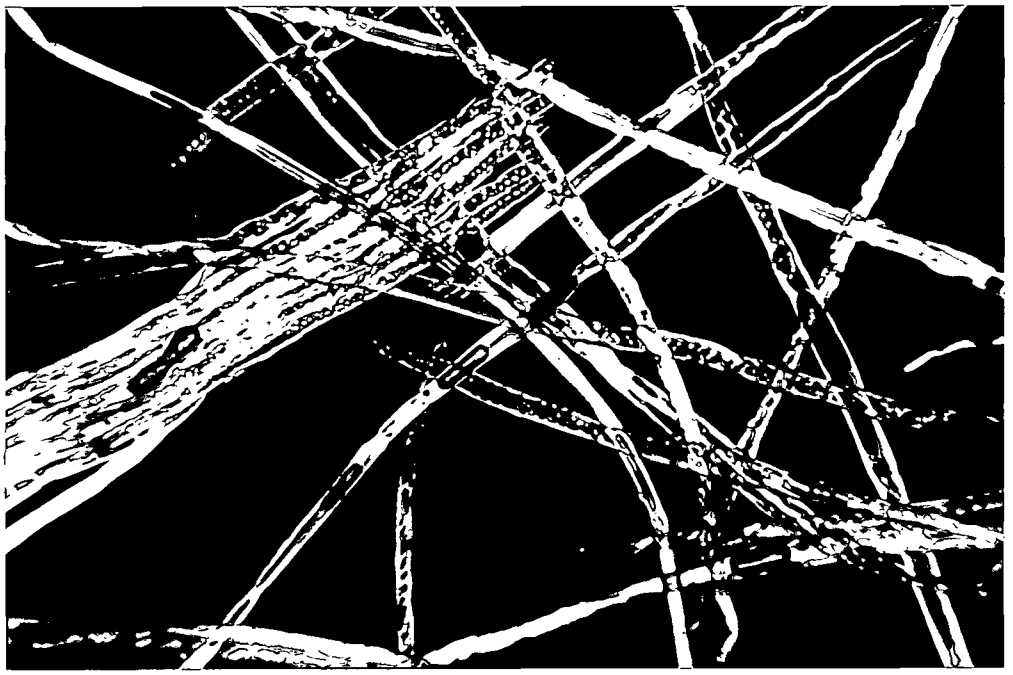

Figure 51. EW fibers ozonated 180 minutes appear white indicating almost complete lignin removal; Graff C-stained, polarized light micrograph.

TEM micrographs of cross-sectioned, control EW fibers shows the middle lamella surrounding the outer cell wall of the fibers giving the fibers a lignin coated surface (Fig. 52). Degradation of the CML occurred upon ozonation (Fig. 53). After 30 minutes ozonation, the CML was removed exposing the underlying secondary wall of the fibers (Fig. 54-56). Increased resolution of the micro-fibrillar structure can be observed at this time as a result lignin and

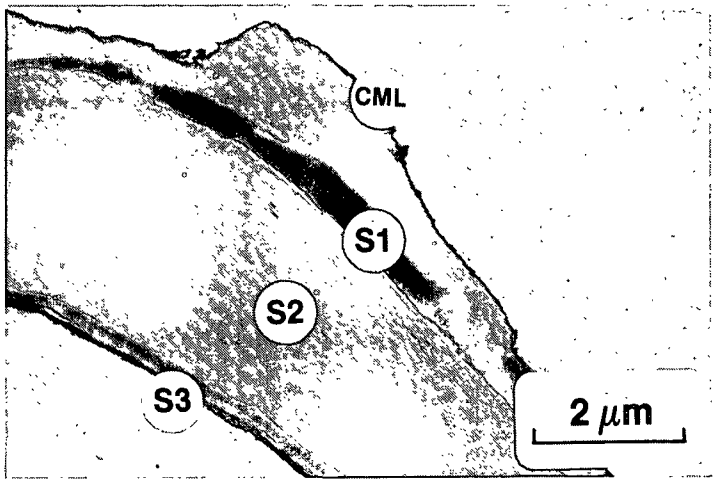

Figure 52. EW control fiber showing compound middle lamella (CML), S1, S2, and S3 layers; cross section, TEM micrograph.

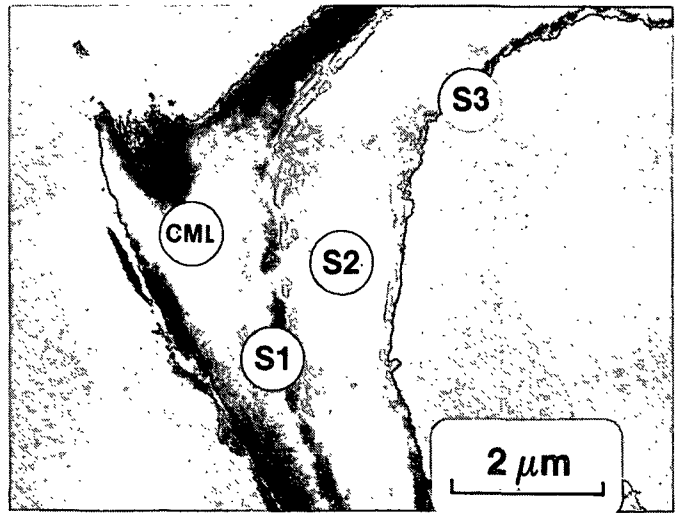

Figure 53. EW fiber ozonated 10 minutes showing degradation of compound middle lamella (CML); cross section, TEM micrograph.

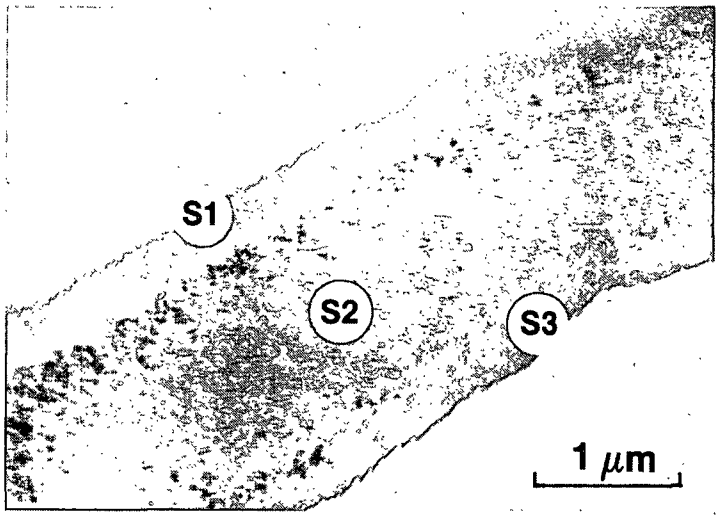

Figure 54. EW fiber ozonated 30 minutes showing S1, S2, and S3 layers; microfibrillar orientation is visible; cross section, TEM micrograph.

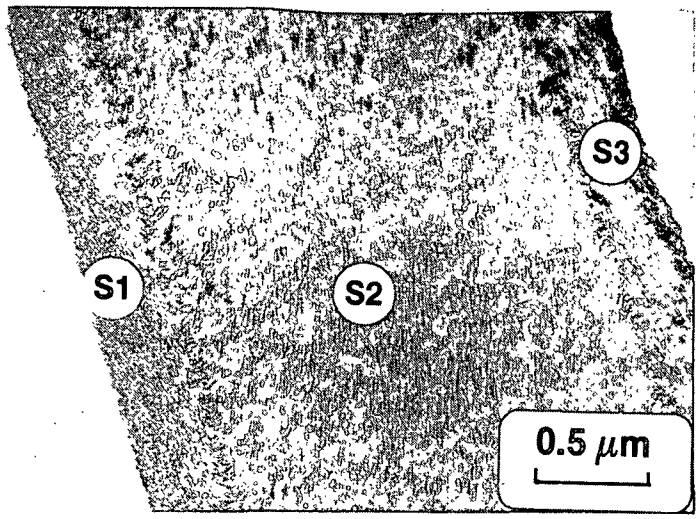

Figure 55. EW fiber ozonated 90 minutes showing cell wall layers; change in apparent fibrillar orientation is visible; cross section, TEM micrograph.

hemicellulose removal. As ozonation continued, degradation of the secondary wall was observed as evidenced by alteration in apparent microfibrillar orientation (Fig. 55-56). These observations show ozone penetrated and degraded the internal cell wall structure of EW fibers. These results are in agreement with those found for TEM analyses of LW fibers.

SEM micrographs of critical point dried control fibers shows these fibers to be rigid and have relatively smooth surfaces (Fig. 57-58). The EW fiber external surfaces became pitted, eroded and cluttered with debris (Fig. 59-66) upon ozonation. Some of the fibers had cell walls which were cracked and peeled. Loss of fiber rigidity was evident as EW fibers appeared collapsed, twisted and wrinkled (Fig. 63-66). These results indicate ozone degraded the components of the cell wall structure at both the external and internal surfaces of EW fibers. This agrees with SEM data for LW fibers.

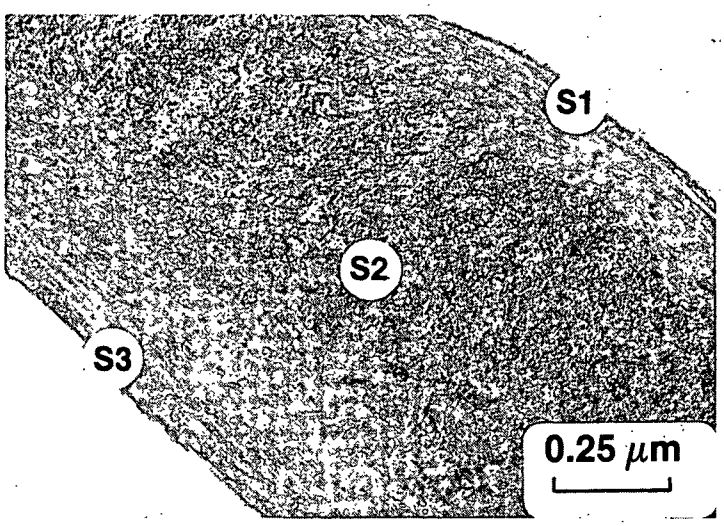

Figure 56. EW fiber ozonated 180 minutes showing change in apparent microfibrillar orientation in secondary wall; cross section, TEM micrograph.

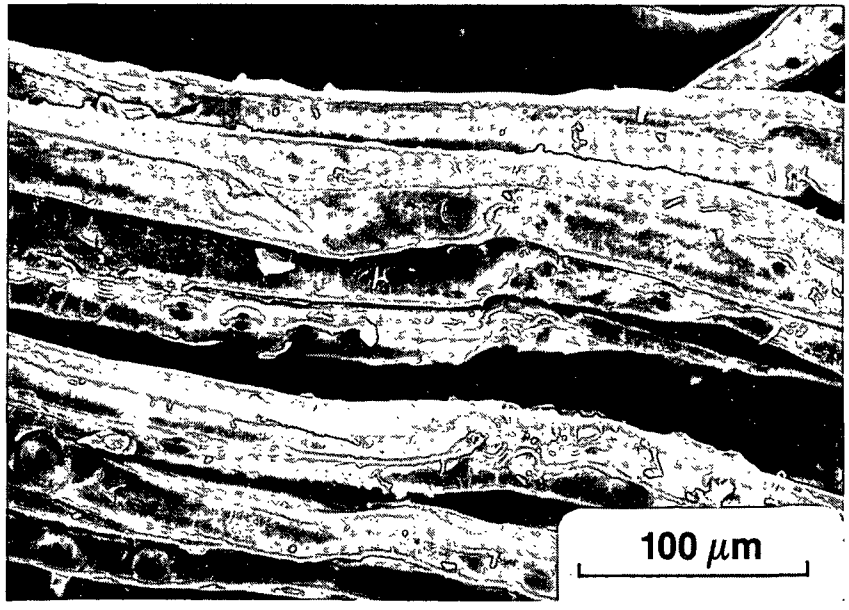

Figure 57. EW control fibers appear rigid with relatively smooth surfaces; some fibrillar debris appears on surfaces; SEM micrograph.

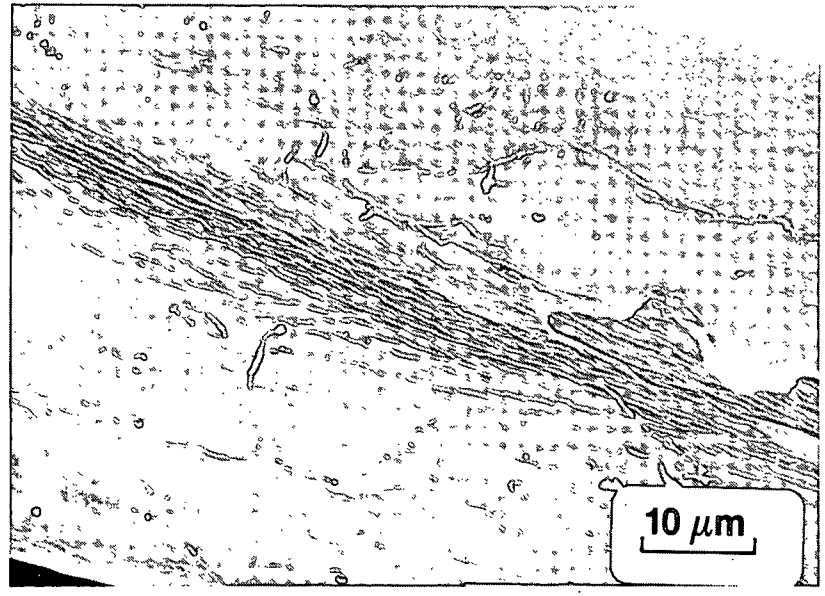

Figure 58. EW control fibers appear rigid with relatively smooth surfaces; SEM micrograph.

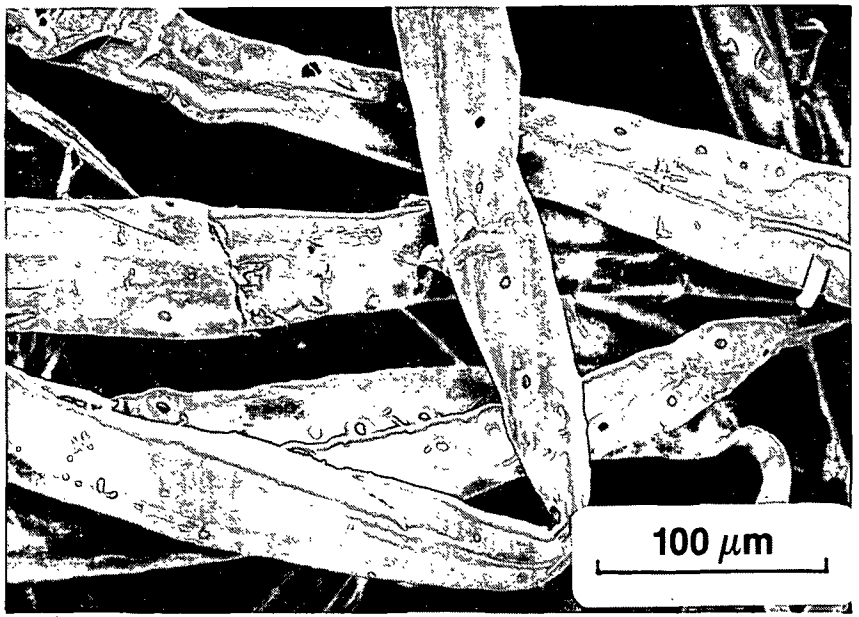

Figure 59. EW fibers ozonated 10 minutes appear rigid with relatively smooth surfaces; SEM micrograph.

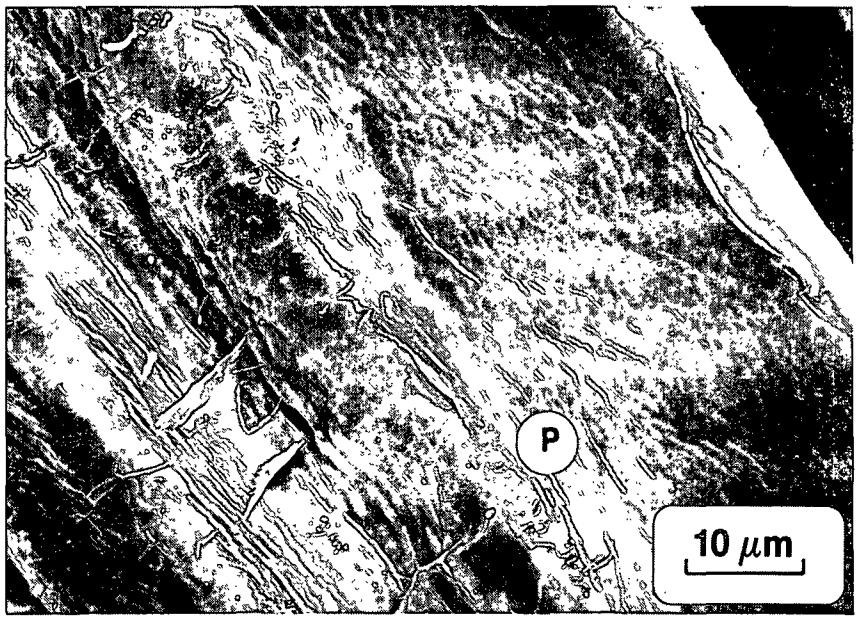

Figure 60. Localized pitting (P) is visible on surfaces of fibers ozonated 10 minutes; SEM micrograph.

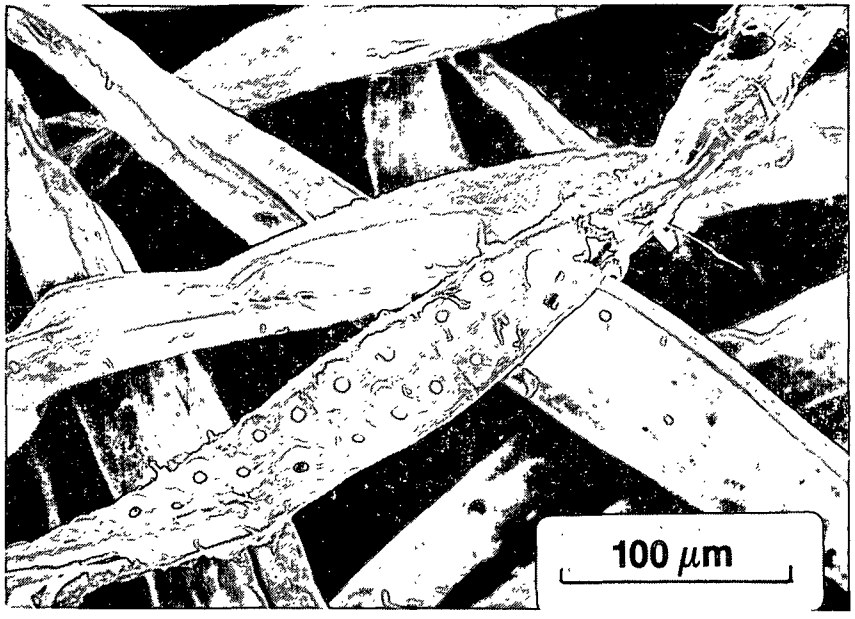

Figure 61. EW fibers ozonated 30 minutes appear rigid; SEM micrograph.

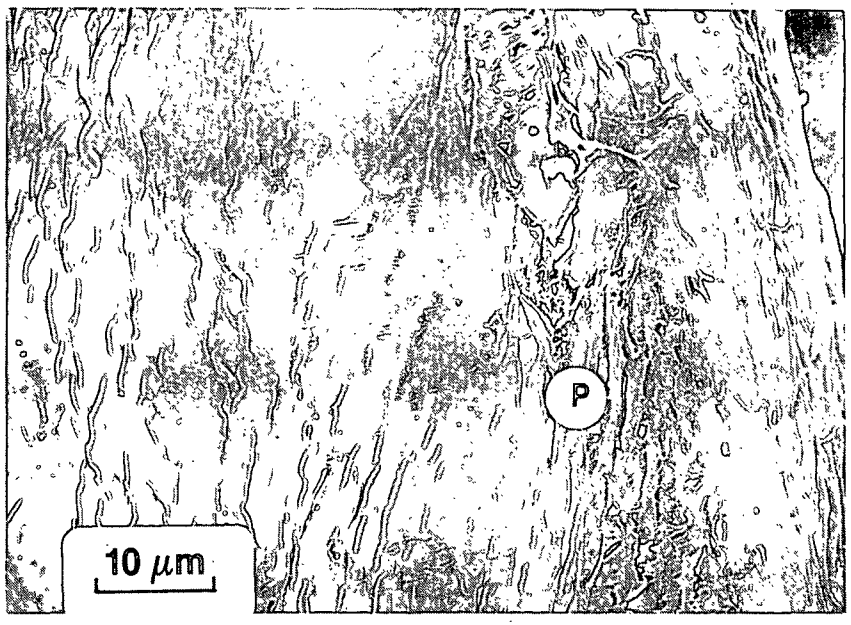

Figure 62. Pronounced pitting (P) is visible on surfaces of EW fibers ozonated 30 minutes; SEM micrograph.

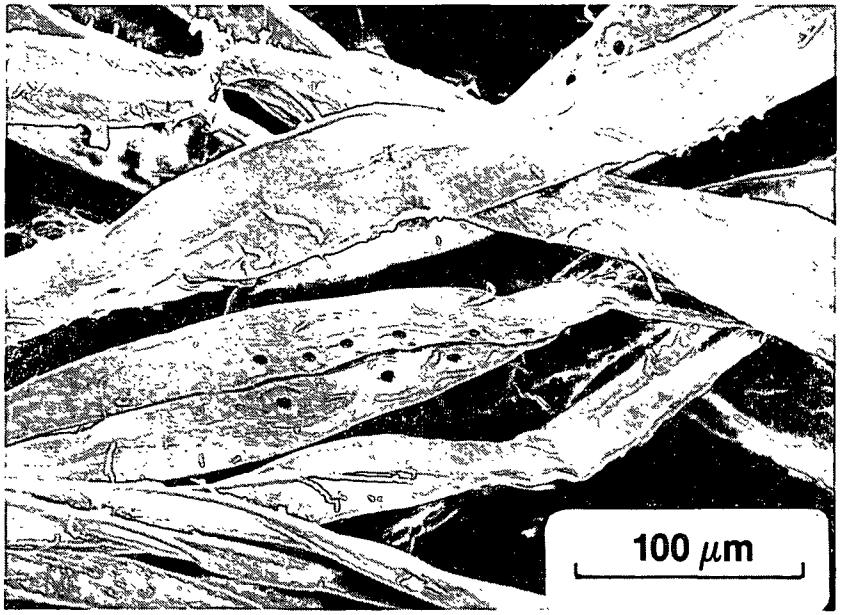

Figure 63. EW fibers ozonated 90 minutes appear collapsed and twisted; increased cell wall debris is noticeable on fiber surfaces; SEM micrograph.

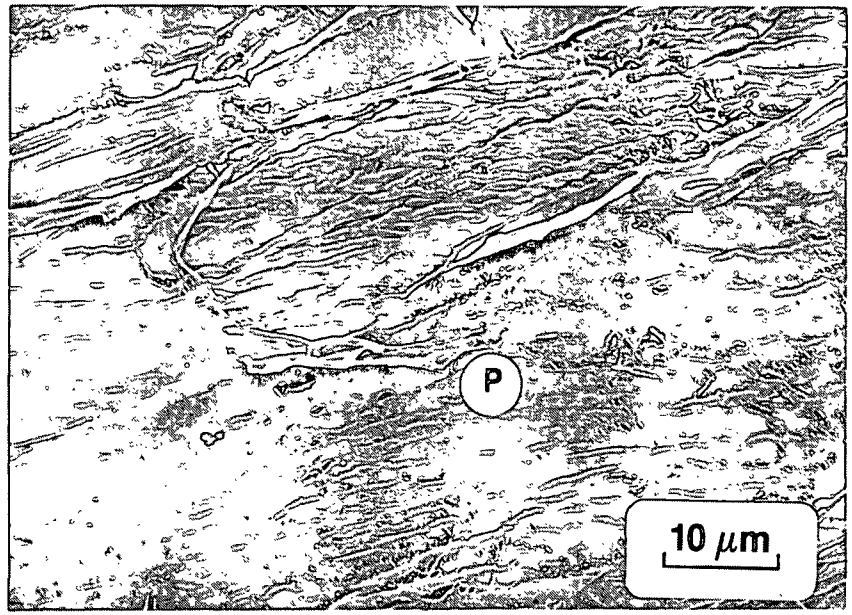

Figure 64. Pronounced pitting (P) appears on surfaces on EW fibers ozonated 90 minutes; SEM micrograph.

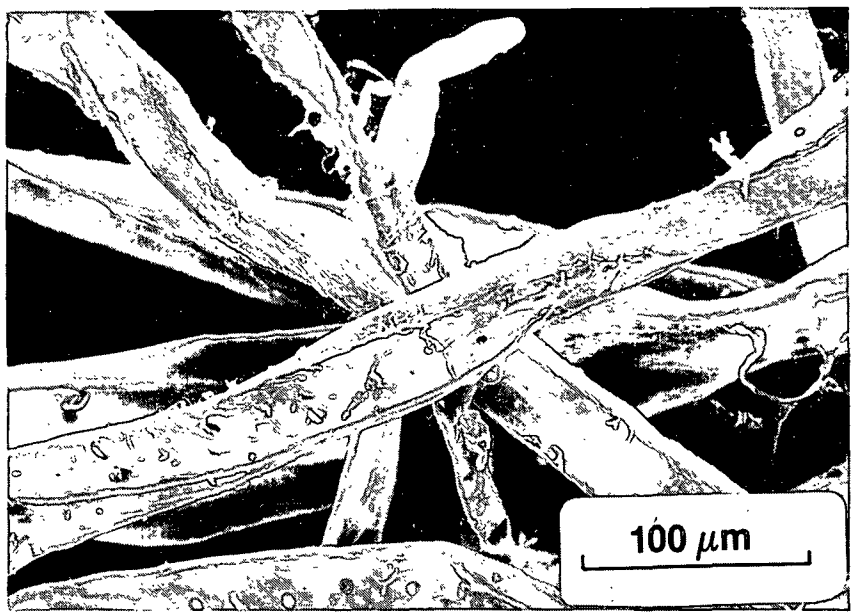

Figure 65. EW fibers ozonated 180 minutes appear collapsed and twisted; increased cell wall debris appear on fiber surfaces; SEM micrograph.

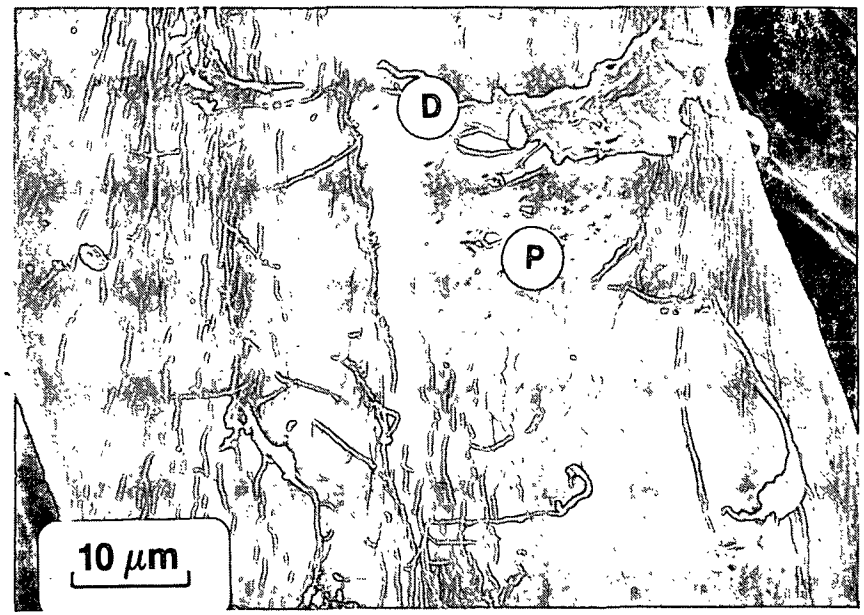

Figure 66. Pitting (P) and cell wall debris (D) appear on surfaces of EW fibers ozonated 180 minutes; SEM micrograph.

KINETICS OF OZONE-EARLYWOOD FIBER REACTION

EW fibers were ozonated separately from LW fibers to serve as an additional test for determining the mode of ozone attack on fibers (i.e., an external surface attack versus cell wall penetration and solubilization of wood components). If ozone solubilization of lignin was dependent only upon the external surface area exposed to ozone, EW fibers should have greater rate of delignification than LW fibers for the following reason. An equal weight of EW and LW fibers would have approximately the same total lignin content. In addition, the external surface lignin content for an individual EW or LW fiber would be approximately the same. However, there would be approximately twice as many EW fibers compared to LW fibers at a given weight due to differences in cell wall thickness (81). Thus, there would be about twice as much external surface lignin exposed for the EW fiber sample as compared to the LW fiber sample. If ozonation is controlled only through external surface attack and solubilization of lignin then the rate of delignification of EW fibers should be approximately twice that of LW fibers.

Rate of delignification of EW fibers by ozone was determined using the procedure described for LW fibers. The reaction orders and rate constant with their 95% confidence limits for ozonation of EW fibers are presented in Table IX. The reaction order for lignin (0.96) was larger than for ozone (0.15) indicating the rate of delignification was more dependent on lignin content than ozone concentration. The rate constant determined for delignification of EW fibers was 5.30×10^{-4} $\underline{mM}^{-0.11}$ sec^{-1} ($4.17 \times 10^{-4} \longrightarrow 6.74 \times 10^{-4}$ $\underline{mM}^{-0.11}$ sec^{-1}). The rate constant for delignification of LW fibers was 7.59×10^{-4} $\underline{mM}^{-0.24}$ sec^{-1} ($5.68 \times 10^{-4} \longrightarrow 10.2 \times 10^{-4}$ $\underline{mM}^{-0.24}$ sec^{-1}). The difference in rates of delignification for EW and LW fibers is statistically insignificant.

Therefore, lignin removal by ozone was not controlled by external surface attack but was dependent on total lignin content available for reaction.

TABLE IX

REACTION ORDERS AND RATE CONSTANT FOR OZONATION OF EARLYWOOD FIBERS

Component	Reaction Order	95% Confidence Interval
Lignin	0.96	0.92-1.00
Ozone	0.15	0.06-0.24
Rate Constant (10^{-4} $mM^{-0.11}$ sec^{-1})	5.30	4.17-6.74

STOICHIOMETRY OF OZONE-LIGNIN REACTION FOR EARLYWOOD FIBERS

Stoichiometry of the ozone-lignin reaction for EW fibers was determined as the ratio of total millimoles ozone consumed by EW fibers to the total millimoles lignin removed (based on guaiacyl propane units; Table X). Calculations for the amount of ozone consumed during the reactions are given in Appendix IX. The amount of ozone consumed by self-decomposition and byproduct degradation was subtracted from the amount of ozone consumed during the reactions (Appendix IX). Ozone consumption due to byproduct degradation was calculated using the rate of consumption data for the LW fibers (i.e., 0.14 mg/L-sec).

Stoichiometric ratios for the ozone-lignin reaction were about the same for all ozonation times (Table X). The stoichiometric ratios were about the same for both EW (1.9-2.2) and LW (2.2-2.6) fibers suggesting delignification of both tissue types may be governed by similar reaction mechanisms.

TABLE X

STOICHIOMETRY OF OZONE-LIGNIN REACTION FOR EARLYWOOD

Ozonation Time, min	Total Ozone Consumed, mM	Total Lignin Removed,[a] mM	Ozone Consumed/ Lignin Removed
0	0	0	0
5	0.41	0.20	2.05
10	0.61	0.28	2.18
30	1.25	0.63	1.98
60	2.13	1.08	1.97
90	2.75	1.25	2.20
120	3.05	1.37	2.23
180	2.99	1.41	2.12

[a]Assuming 188 mg/mmole guaiacyl propane lignin unit.

EXPERIMENTAL

PREPARATION OF STARTING MATERIAL

A loblolly pine peeler log was obtained from International Paper Company, Virgina. The log was approximately 20 inches in diameter and contained 53 annual rings. A chain saw was used to cut the log into 2-inch disks which were, in turn, cut into 2-inch wedges using a band saw. Utilizing only mature wood from the 23rd to 37th growth ring, earlywood and latewood chips (~1/8-inch x 1-inch) were hand cut from the wedges using a guillotine blade. A total of 1400 g o.d. of mature earlywood and mature latewood was collected.

The chips were impregnated with a sodium bicarbonate solution (15% o.d. wood basis) for 24 hours under vacuum. After the sodium bicarbonate was drained, the chips were presteamed in batches (120 g.o.d.) for 5 minutes at 80 g o.d. psig to a temperature of 160°C. The heated chips were then passed through an Asplund mill into a Sprout-Waldren disk refiner for 2 minutes at atmospheric pressure. The fiberized wood was washed several times with deionized distilled water. The pH of the fiberized earlywood and latewood was found to be 7.5 and 7.3, respectively (Table XI). The total yield for fiberized earlywood was 91.3%. The fiberized latewood yield could not be determined as a result of wood losses due to the steam line plugging.

The fiberized wood was screened in a Bauer-McNett classifier (91). Fibers between 10 and 150 mesh were kept for ozonation experiments. Fiberized earlywood and latewood yields were 72.9% and 52.0%, respectively. These yields were based on total material screened of a given fiber type (Table XI).

TABLE XI

CHARACTERIZATION OF FIBERIZED LOBLOLLY PINE EARLYWOOD AND LATEWOOD

	Earlywood	Latewood
Prerefining		
Total chips (oven-dried)	382.4 g	608.4 g
pH	7.8	7.9
First Refining		
Total Yield	353.7 g (91.3%)	--
pH	7.5	7.3
Screened Yields[a]:		
Fibers <150	3.3 g (1.0%)	15.5 g (4.6%)
150 <Fibers <10	92.5 g (72.9%)	174.8 g (52.0%)
Fibers >10	257.9 g (26.1%)	146.1 g (43.4%)
Second Refining[b]		
Total Yield	186.6 g (72.4%)	113.8 g (77.9%)
pH	7.4	7.5
Screened Yields[a]:		
Fibers < 150	1.5 g (0.8%)	6.3 g (5.5%)
150 < Fibers < 10	50.7 g (72.0%)	53.9 g (47.4%)
Fibers > 10	134.4 g (27.2%)	53.6 g (47.1%)

[a]Yield based on total screened material.
[b]Yield based on rejected fibers (> 10 mesh).

Fibers greater than 10 mesh were buffered, refined and screened again according to the above procedure. The screened yield and pH for earlywood after the second refining are shown in Table XI.

An extraction procedure involving several steps was used to remove resins from the fiberized wood. The fibers (50 g o.d.) were placed in a Soxhlet apparatus and extracted with the following sequence: ethanol (95%, 1500 mL, 12 hr), ethanol/benzene (1/2, 1500 mL, 24 hr), ethanol [95%, 2X (1500 mL, 4 hr)].

The extractives content and chemical composition for both the first and second refined fibers are shown in Table XII. Since chemical compositions were not significantly different, the first and second refined fibers were thoroughly mixed in a 0.3% EDTA solution (3L) for 24 hours, filtered and washed several times with triply distilled water (3 x 500 mL). The fibers were then extracted in the Soxhlet apparatus with triply distilled water (2 x 1500 mL) for 6 hours. Fiber samples (0.9 g o.d.) were sealed in polyethylene bags and stored in the dark at 4°C.

TABLE XII

CHEMICAL COMPOSITION OF LOBLOLLY PINE AFTER FIRST AND SECOND REFININGS[a]

	Latewood		Earlywood	
	First Refining	Second Refining	First Refining	Second Refining
Carbohydrates, %				
Araban	0.9	1.0	1.2	1.2
Xylan	6.5	6.4	6.8	6.6
Mannan	10.7	10.6	10.7	10.4
Galactan	3.2	3.2	2.7	2.5
Glucan	45.7	45.9	46.6	45.7
Lignin, %				
Acid Insoluble	27.8	27.7	29.4	28.7
Acid Soluble	0.3	0.3	0.3	0.4
Extractives	0.4	0.4	0.8	0.4

[a]Percent on o.d. pulp.

PROCEDURE FOR OZONATION OF FIBERS

FLOW DIAGRAM OF REACTION APPARATUS

Construction of the ozone saturation tank and reaction tank is described in Appendix IV. A flow diagram of the reaction apparatus is illustrated in

Fig. 67. Gaseous ozone from the generator is split into a sample line and a reactor line. The ozone stream from the sample line was directed into two ozone traps connected in series. The reactor line stream was fed into the ozone saturation tank. Buffer solution was also fed into the saturation tank from two 25 L carboys. The buffer solution flow rate was measured using a rotameter and could be controlled with a polyvinyl chloride (PVC) needle valve located between the carboys and ozonation saturation tank. Ozonated buffer solution was directed into the reaction tank. The solution flow rate between the saturation and reaction tanks was controlled by a PVC needle valve. The spent solution then flows from the reaction tank to a 50 L waste tank. Sample aliquots of solution were withdrawn via a three way stopcock located between the reaction tank and waste tank. UV absorption measurements of the aliquots were recorded from which ozone concentrations were calculated.

OPERATION OF REACTION APPARATUS

The ozone generator was allowed to come to equilibrium as described in Appendix I. Prior to the run, the saturation tank was filled with 0.4M acetic acid/0.0072M sodium acetate buffer solution (1800 mL) and mixed at 500 rpm. The gaseous ozone stream was diverted to the saturation tank. After 15 minutes, the reaction tank was filled with ozonated buffer solution (1800 mL) at a flow rate of 5 cc/sec and mixed at 500 rpm. The three-way stopcock was opened to allow solution flow to the waste tank. The ozonated buffer solution was allowed to flow through the reaction tank until an equilibrium ozone concentration was reached. When the ozone concentration in the reaction tank reached equilibrium, fibers (0.9 g.o.d.) dispersed in buffer solution (50 mL)

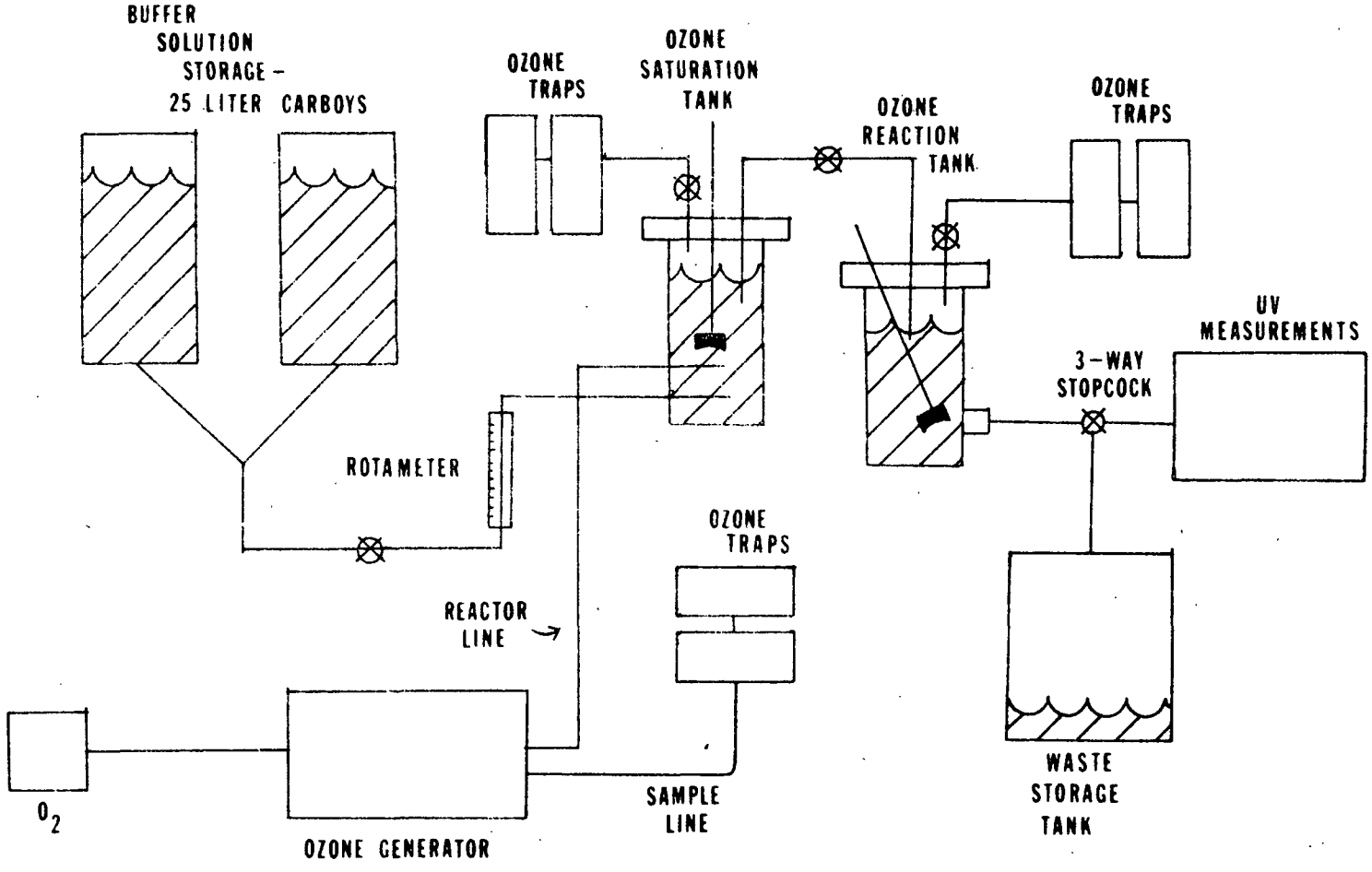

Figure 67. Flow diagram of the reaction apparatus.

were dropped into the reaction tank through the addition port. Ozone concentration was monitored during the reaction by UV measurements (Appendix II). Fiber samples were ozonated for various times ranging from 5-180 minutes. The reaction was stopped by adding a sodium bisulfite solution (0.1 g in 50 mL distilled water) to the ozonated fiber suspension. The fibers were washed several times with distilled water (4 x 100 mL) and filtered. A portion of the fibers were solvent exchanged into ethanol for microscopic analyses (see Analytical Procedures). The remainder of the fibers were dried over phosphorus pentoxide in a vacuum desiccator for chemical analyses.

ANALYTICAL PROCEDURES

PHYSICAL ANALYSES

Holocellulose Isolation

Chlorite liquor was prepared by dissolving technical grade sodium chlorite (5 g) in distilled water (99 g). Glacial acetic acid (1 mL) was added to the solution. Never-dried pulp samples (1 g o.d.) were placed in 70-mL culture tubes and chlorite liquor (20 mL) added. The culture tubes were tightly sealed and placed in a water bath at 30°C for 24 hours. The spent liquor was decanted, replaced with freshly prepared chlorite liquor (20 mL) and placed back in the water bath for 24 hours. For each ozonation time, the above procedure was repeated until the holocellulose was prepared: 0-10 minutes (6X), 30-90 minutes (5X), 120-180 minutes (4X). The samples were washed thoroughly with 3 L distilled water and freeze-dried.

Tricarbanilation

Tricarbanilate derivatives were prepared from isolated holocellulose samples. Samples (62.5 mg o.d.) were weighed into 30-mL hypovials and dried over phosphorus pentoxide, *in vacuo*. Anhydrous distilled pyridine (25 mL) and

phenyl isocyanate (1.5 mL) were added to the samples and the vials sealed with Teflon-silicone septa using aluminum crimp caps. The hypovials were placed in stainless steel bombs and heated in an oil bath at 80°C for 48 hours.

The resulting carbanilate solutions were cooled and methanol (0.7 mL) slowly injected into the hypovials via syringe. Carbanilate solutions were diluted with p-dioxane (25 mL) and filtered through glass fiber filter pads (1.2 μm poresize). The gelatinous material which collected on the filter pad was rederivatized and analyzed separately.

The solution filtrate was added dropwise to a stirred solution of methanol (200 mL) and acetic acid (1.25 mL). The precipitated carbanilate was washed with methanol (200 mL) containing acetic acid (1.25 mL), distilled water (200 mL) containing acetic acid (1.25 mL), distilled water (2 x 200 mL) and then freeze-dried.

Degree of polymerization of carbanilate derivatives were determined by gel permeation chromatography (88) using the calibration procedure described by Ring, et al. (92).

Viscosity

Cupriethylenediamine viscosities of holocellulose samples were determined using TAPPI T230 SU-66 (pipet method) modified according to TAPPI 37:273(1954) (0.5% in CED).

CHEMICAL ANALYSES

Carbohydrate Content

Carbohydrate contents of fiber samples were determined by TAPPI Standard Method T 249.

Klason Lignin

Klason lignin was determined as the weight of the precipitate acquired after hydrolysis of fiber samples during the carbohydrate treatment (103).

Acid Soluble Lignin

Acid soluble lignin was determined according to TAPPI useful Method 250.

MICROSCOPIC ANALYSES

Light Microscopy

Never-dried control and ozonated fiber samples were Graff C-stained and examined under polarized light using an Olympus Vanox microscope.

Transmission Electron Microscopy

Ultrathin cross sections of stained, embedded fiber samples were prepared with the following procedures for TEM analyses. Never-dried fibers (~ 100 mg) were stained according to the following procedure prior to embedding (100):

1% periodic acid (HIO_3) at 25°C; overnight.

1% thiocarbohydrazide at 50°C; 2 hr.

1% osmium tetraoxide at 50°C; 6 hr.

The fibers were washed carefully between every step with distilled water (~ 5 mL) at 50°C. The periodic acid treatment was conducted in the dark.

To ensure proper curing of the embedding medium, all water was removed from the fiber samples. Therefore, the fiber samples (~ 100 mg) were dehydrated in acetone (~ 10 mL) according to the sequence shown in Table XIII.

TABLE XIII

DEHYDRATION OF FIBER SAMPLE FOR TEM ANALYSES

Acetone Solution, %	Time, hr
30	24
50	24
70	24
90	24
100	24
100	24

After dehydration, fibers were embedded in an epoxy resin according to Spurr (93). Ultrathin cross sections of fibers were cut about 600-800 μm in thickness with a diamond knife on a Sovall MT2-B ultramicrotome. The sections were mounted on 200-mesh copper grids and examined with a JEOL JEM-100CX II STEM at 80 kv.

Scanning Electron Microscopy

Fiber samples (~ 100 mg) were dehydrated in ethanol (~ 10 mL) according to the sequence shown in Table XIV. The samples were then critical point dried, mounted on brass stubs and coated with gold-palladium using a Hummer V sputter coater. The coated samples were examined with a JEOL-35C SEM at 15 kv.

TABLE XIV

DEHYDRATION OF FIBER SAMPLES FOR SEM ANALYSIS

Ethanol Solution, %	Time, hr
5	24
10	24
25	24
50	24
70	24
90	24
100	24
100	24
100	24

CONCLUSIONS

The purpose of this study was to investigate the mode and selectivity of ozone attack on wood fibers. Chemical analyses showed lignin and hemicellulose were removed during ozonation. In contrast, cellulose removal was negligible during ozonation even though large drops in viscosity and degree of polymerization values showed that it was degraded. Therefore, ozone does not demonstrate a wood component selectivity in that both lignin and polysaccharides were degraded. However, there was preferential removal of the wood components in the order of lignin > hemicellulose >> cellulose. It was not possible to determine whether preferential removal of wood components was due to chemical reactivity or topochemical restraint.

Light and TEM microscopies showed lignin removal started at the outer surfaces of the fibers and proceeded through the cell wall toward the lumen. TEM micrographs further showed fiber cell wall degradation through change in apparent microfibrillar orientation, fragmentation and separation between the S1, S2, and S3 layers. SEM micrographs showed loss of fiber rigidity as ozonated fibers appeared collapsed and twisted. Pitting, erosion, and cell wall debris were also observed on the external surfaces of the fibers through SEM analysis. Thus, ozonation resulted in degradation of the cell wall structure at both the internal and external surfaces of the fibers.

Kinetic analysis showed the rate of delignification for both LW and EW fibers was more dependent on lignin content than on ozone concentration. The rate constants for LW and EW delignification reactions were 7.59×10^{-4} $\underline{mM}^{-0.24}$ sec^{-1} ($5.68 \times 10^{-4} \longrightarrow 10.2 \times 10^{-4}$ $\underline{mM}^{-0.24}$ sec^{-1}) and 5.30×10^{-4} $\underline{mM}^{-0.11}$ sec^{-1} ($4.17 \times 10^{-4} \longrightarrow 6.74 \times 10^{-4}$ $\underline{mM}^{-0.11}$ sec^{-1}), respectively. Therefore, the rates of delignification for LW and EW fibers were not statistically different.

Chemical, physical, microscopic and kinetic analyses of LW and EW fibers were in agreement at comparable ozonation times. Thus, ozone reacts with wood components of LW fibers at essentially the same rate as EW fibers (i.e., does not exhibit tissue selectivity).

SUGGESTIONS FOR FUTURE RESEARCH

The objective of the present investigation was to elucidate the mode and selectivity of ozone attack on wood fibers. Although results from this study have advanced the understanding of ozone attack on wood fibers, additional research may be carried out which would further this knowledge.

In the present investigation the pattern of lignin removal from the fibers was found to start at the outer cell wall and proceed toward the cell lumen. The relationship between molecular weight distribution of dissolved lignin fragments and pore size distribution of the fiber cell wall could be investigated with respect to ozonation time. This could aid in understanding the mechanisms of lignin removal (e.g., gel degradation, pore sieve) from the fibers during ozonation.

Finally, an ozonation study similar to this thesis could be carried out on fibers from different wood species to determine the effect of ozonation on hardwoods relative to softwoods. Also, a study could be carried out on fibers having primarily a carbohydrate external surface to investigate the effect of ozonation on chemical pulps.

ACKNOWLEDGMENTS

The author expresses her sincere appreciation to the members of her thesis advisory committee: Drs. John D. Litvay, chairman of the committee, Earl W. Malcolm and Norman S. Thompson, for their assistance, guidance and many helpful discussions throughout the course of this work.

The contributions and helpfulness of the Institute faculty and staff are gratefully acknowledged. Although it is impossible to acknowledge everyone individually, special recognition is given to Hilkka Kaustinen and Mary Block for the electron microscopy work; Walter Rantanen and Ellen Foxgrover for the light microscopy work; Art Webb for carbohydrate and lignin analyses; Bruce Andrews for design of the reactors; and Marvin Filz and Paul Van Rossum for construction of the reactors.

The financial support of The Institute of Paper Chemistry and member companies is appreciated for giving me this educational opportunity.

To my parents, relatives and personal friends, I am deeply indebted for their encouragement, confidence and friendship.

Above everyone else, I would like to thank my loving husband, Mark, whose patience, understanding and support were instrumental in making this goal a reality.

LITERATURE CITED

1. Bailey, P. S., Ozonation in Organic Chemistry, Volume I, Academic Press, New York, 1978.

2. Eckert, R. and Singh, R., Ozone Reactions in Relation to the Aromatic Structure of Lignin: A Review of Selected Topics in Ozone Chemistry, presented at the International Symposium on Delignification with Oxygen, Ozones and Peroxides, Raleigh, NC, May, 1975.

3. Weiss, J., Trans. Far. Soc. 31:668(1935).

4. Alder, M. G. and Hill, G. R., J. Am. Chem. Soc. 72:1884(1950).

5. Kilpatrick, M. L., Herrick, C. C., and Kilpatrick, M., J. Am. Chem. Soc. 78:1784(1956).

6. Hewes, G. G. and Davidson, R. R., AIChE Symposium 17(1):141(1971).

7. Gorbenko-Germanov, D. S. and Kozlova, I. V., Russian J. of Phys. Chem. 48(8):1179(1974).

8. Staehelln, J. and Hoigne, J., Environ. Sci. Technol. 16(10):676(1982).

9. Forni, L., Bahnemann, D. and Hart, E. J., J. Phys. Chem., 86(2):255(1982).

10. Hoigne, J. and Bader, H., Water Res. 10:377(1976).

11. Forcheimer, O. L. and Taube, H., J. Am. Chem. Soc. 76:2099(1954).

12. Greenwood, F. L., J. Org. Chem. 10:414(1945).

13. Mc Grath, W. D. and Norrish, R. G. W., Nature (London), 182:235(1958).

14. Walter, R. H. and Sherman, R. M., J. Food Sci. 41:993(1976).

15. Gurol, M. D. and Singer, P. C., Environ. Sci. Technol. 16(7):377(1982).

16. Sullivan, D. E. Self-Decomposition and Solubility of Ozone in Aqueous Solutions. Ph.D. Dissertation, Vanderbilt University, 1979.

17. Kuo, C. H., Li, K. Y., Wen, C. P., and Weeks, J. L., AIChE Symposium 73(166):250(1976).

18. Hoigne, J. and Bader, H., Ozone: Sci. Eng. 1:73(1979).

19. Pan, G., Chen, C. L., Chang, H. M., and Gratzl, J. S. Model Experiments on the Splitting of Glycosidic Bond Linkages by Ozone. International Symposium on Wood and Pulping Chemistry, Vol. 2, Stockholm, Sweden, June, 1981.

20. Hoigne, J. and Bader, H. Ozone and Hydroxyl Radical Initiated Oxidation of Organic and Organometallic Trace Impurities in Water. ACS Symposium Series 18:292(1978).

21. Hill, G. R., J. Am. Chem. Soc. 71:2434(1949).

22. Hill, G. R., J. Am. Chem. Soc. 70:1306(1948).

23. Walling, C. and EL-Taliawi, G. M., J. Am. Chem. Soc. 95(3):3844(1973).

24. Balousek, P. J. The Effects of Ozone upon a Lignin-Related Model Compound Containing a β-Aryl Ether Linkage. Ph.D. Dissertation, Appleton, WI, The Institute of Paper Chemistry, 1979.

25. Kratzl, K., Claus, P., and Reichel, G., Tappi 59(11):86(1976).

26. Kojima, Y., Miura, K., and Kayama, T., Res. Bull. Expt. Forests, Hokkaido University, Japan, 31(1):165(1978).

27. Kaneko, H., Hosoya, S., and Nakano, J., Mokuzai Gakkaishi 27(9):678 (1981).

28. Nakano, J., Ishizu, A., Hosoya, S., Kaneko, H., and Matsumoto, Y. Proceedings of the TAPPI Pulping Conference, Toronto, Canada, Oct., 1982. pp. 61.

29. Hatakeyama, H., Tonooka, T., Nakano, J., and Migita, N., Kogyo Kagaku Zasshi 71(8):1214(1968).

30. Kaneko, H., Hosoya, S., and Nakano, J., Mokuzai Gakkaishi 26(11):752 (1980).

31. Matsumoto, Y., Ishizu, A., and Nakano, J., Mokuzai Gakkaishi 27(10):750 (1981).

32. Katuscak, S., Hrivik, A., and Macak, K., Paperi Puu 54(4a):201(1972).

33. Katuscak, S., Hrivik, A., and Mahdalik, M., Paperi Puu 53(9):519(1971).

34. Katuscak, S., Rybarik, I., Paulinyova, E. and Madalik, M., Paperi Puu 53(11):665(1971).

35. Criegee, R., Angew. Chem. 14(11):745(1975).

36. Bailey, P. S. Reactivity of Ozone with Various Organic Functional Groups Important to Water Purification. First International Ozone Institute Meeting, Austin, TX, 1973.

37. Eckert, R. C. and Singh, R. P. Chemistry of Delignification with Oxygen, Ozone, and Peroxides, Unipublishers Co., Ltd., Tokyo, Japan, p. 229-242 (1980).

38. Murray, R. W., Lumma, W. C., and Lin, J. W. P., J. Am. Chem. Soc. 92:3205(1970).

39. Katai, A. A. and Schuerch, C., J. Polymer Sci. 4(10):2683(1966).

40. Deslongchamps, P., Atlani, P., Frehel, D., and Malava, A., Can. J. Chem. 50:3405(1972).

41. Deslongchamps, P., Moreal, C., Frehel, D. and Atlani, P., Can. J. Chem. 50:3402 (1972).

42. Deslongchamps, P., Atlani, P., Frehel, D., and Malarial, A., Can. J. Chem. 52:3651(1974).

43. Rothenberg, S., Robinson, D. H., and Johnsonbaugh, D. K., Tappi 58(8):182(1975).

44. Singh, R. P., Tappi 65(2):45(1982).

45. Allison, R. W., Appita 36(1):42(1982).

46. Liebergott, N., Pulp Paper Mag. Can. 73(9):70(1972).

47. Liebergott, N. and Van Lierop, B., Tappi 64(6):95(1981).

48. Brabender, G. J. and Ward, J. W., U.S. pat. 2,466,633(1949).

49. Kamishima, H., Fujii, T., and Akamatsu, I., Japan Tappi 30(7):39(1974).

50. Kamishima, H., Fujii, T., and Akamatsu, I., Japan Tappi 30(7):381(1976).

51. Kamishima, H., Fujii, T., and Akamatsu, I., Japan Tappi 31(9):664(1977).

52. Kamishima, H., Fujii, T., and Akamatsu, I., Japan Tappi 31(10):699(1977).

53. Miura, K., Res. Bull. Coll. Expt. Forests 32(1):63(1975).

54. Osawa, Z., Erby, W. A., Sarkanen, K. V., Carpenter, E., and Schuerch, C., Tappi 46(2):84(1963).

55. Soteland, N., Pulp Paper Mag. Can. 75(4):T153(1974).

56. Soteland, N. and Kringstad, K., Norsk. Skogind. 22(2):46(1968).

57. Soteland, N. and Loras, V., Norsk. Skogind. 28(6):165(1974).

58. Soteland, N., Norsk. Skogind. 27(10):274(1973).

59. Soteland, N., Norsk. Skogind. 32(9):199(1978).

60. Soteland, N., Pulp Paper Mag. Can. 78(7):45(1977).

61. Lyse, T. E. A Study on Ozone Modification of Lignin in Alkali-Fiberized Wood. Ph.D. Dissertation, The Institute of Paper Chemistry, Appleton, WI, 1979.

62. Procter, A. R., Pulp Paper Mag. Can. 75(6):58(1974).

63. Allison, R. W., Appita 32(4):279(1979).

64. Kibblewhite, R. P., Brooks, D., and Allison, R. W., Tappi 63(4):133(1980).

65. Secrist, R. B. and Singh, R. P., Tappi 54(4):581(1971).

66. Lantican, D. M., Cote, W. A., and Skaar, C., I. and E.C., Prod. Res. Devt. 4(2):66(1965).

67. Moore, W. E., Effland, M., Sinha, B., Burdick, M. P., and Schuerch, C., Tappi 49(5):206(1966).

68. John, B. and Krueger, W., Unpublished Work, Appleton, WI, The Institute of Paper Chemistry, 1978.

69. Osawa, Z. and Schuerch, C., Tappi 46(2)79(1963).

70. Kassebi, A., Gratzl, J. S., and Chen, C. L., and Singh, R. P., Proceedings of the TAPPI Pulping Conf., Toronto, Canada, October 25-27, 1982. p. 327.

71. Mbachu, R. A. D. and Manley, R. S. J., J. Poly. Sci. Chem. Ed. 19(8):2053 (1981).

72. Mbachu, R. A. D. and Manley, R. S. J., J. Poly. Sci. Chem. Ed. 19(8):2065 (1981).

73. Mbachu, R. A. D. and Manley, R. S. J., J. Poly. Sci. Chem. Ed. 19(8):2079 (1981).

74. Lindholm, C. A., Paperi Puu 59(1):17(1977).

75. Lindholm, C. A., Paperi Puu 59(2):47(1977).

76. Lindholm, C. A., Paperi Puu 59(4a):217(1977).

77. Lindholm, C. A. and Gummers, M., Paperi Puu 60(11):653(1978).

78. White, C. Ozonation of Kraft Pulp at Various pH Levels: Strength Improvements by Post-Borax Treatment. Special Studies, Appleton, WI, The Institute of Paper Chemistry, 1981.

79. Soteland, N., Norsk. Skogind. 25(3):61(1971).

80. Hornof, V. and Hopmans, J. J., Cell. Chem. Technol. 13:363(1979).

81. Sjostrom, E. Wood Chemistry: Fundamentals and Applications. Academic Press, New York, NY, 1981.

82. Fergus, B. J., Procter, A. R., Scott, J. A. N. and Goring, D. A. I., Wood Sci. Technol. 3:117(1969).

83. Goring, D. A. I., Pulp Paper Mag. Can. 64(12):T517(1963).

84. Koran, Z., Wood Fiber 2(3):(1970).

85. Kerr, A. J. and Goring, D. A. I., Tappi 59(10):116(1976).

86. Atack, D., Svensk Papperstid. 75(3):89(1972).

87. Wise, L. E. and Ratliff, E. K., Anal. Chem. 19:59(1947).

88. Schroeder, L. R. and Haigh, F. C., Tappi 62(10):103(1979).

89. Schroeder, L. R. and Wabers, B., Unpublished Work, Appleton, WI, The Institute of Paper Chemistry, 1980.

90. Ott, E. and Spurlin, H. M., Cellulose and Cellulose Derivatives, Part I, Interscience Publishers, Inc., New York, NY, 1954.

91. TAPPI Standard Method T 233 sm-53.

92. Ring, G. J. F., Stratton, R. A., and Schroeder, L. R., J. Liq. Chromatogr., 6(3):401(1983).

93. Spurr, A. R., J. Ultrastruct. Res. 26:31(1969).

94. Rizzuti, L., Augugliaro, V., and Marrucci, G., Chem. Eng. Sci. 31:877(1976).

95. Ostle, B. and Mensing, R. W., Statistics in Resesarch, Third Edition, The Iowa State University Press, Ames, IA, 1979.

96. Moore, W. J., Physical Chemistry, Prentice-Hall, Inc., Englewood Cliffs, NJ, 1972.

97. Yocum, F. Conference Proceedings Ozone/Chlorine Dioxide Oxidation Products of Organic Material. Cincinnati, OH, 1978.

98. Purcell, E. J., Calculus, Meredith Corporation, New York, NY, 1972.

99. Borchardt, L. G. and Piper, C. V., Tappi 53(2):257(1970).

100. Seligman, A. M., Hanker, J. S., Wasserkrug, H., Dmochowski, H., and Katzoff, L., J. Histochem. Cytochem. 13(8):629(1965).

101. Timell, T. E., Advances in Carbohydrate Chemistry, Vol. 20, Academic Press, New York, 1965. p. 409.

102. Kreyzig, E., Advanced Engineering Mathematics, Fourth Edition, John Wiley & Sons, New York. 1979.

103. Effland, M. J., Tappi 60(10):143(1977).

APPENDIX I

CALIBRATION OF OZONE GENERATOR

Ozone for the experiments was produced by passing oxygen (ED grade, Matheson Gas Products) through a Welsbach model T-816 laboratory ozone generator. The generator was set at the following conditions: oxygen pressure, 8 psig; corona discharge power, 75 watts; reactor line flow rate, 2.0 L/min; sample line flow rate, 0.5 L/min.

Ozone traps were constructed from two gas washing bottles connected in series both containing a solution 0.8N potassium iodide (150 mL) and 1N sodium hydroxide (150 mL, Fig. 68). The reactor line was connected to one set of bottles and to an ozone "killer" solution via a three-way stopcock. The same arrangement was used for the sample line. The "killer" solution was prepared by dissolving potassium iodide (10 g) and sodium thiosulfate (250 g) in distilled water (4 L) and acidified to pH 4.0 with concentrated sulfuric acid.

Prior to the run, the ozone generator was purged with oxygen for 30 minutes. The oxygen stream was directed to the ozone "killer" solution and the generator turned on and allowed to equilibrate for 30 minutes. The ozone streams were then directed to the gas washing bottles for specified lengths of time. After the run, the ozone streams were diverted back to the "killer" solution and the generator turned off. The generator was purged with oxygen for 30 minutes.

Ozone concentration in the ozone traps was determined by iodometric titration (Appendix III). Ozone production for the Welsbach generator at the given conditions was found to be 43.9 ± 0.6 mg/L-gas (~ 2% by volume).

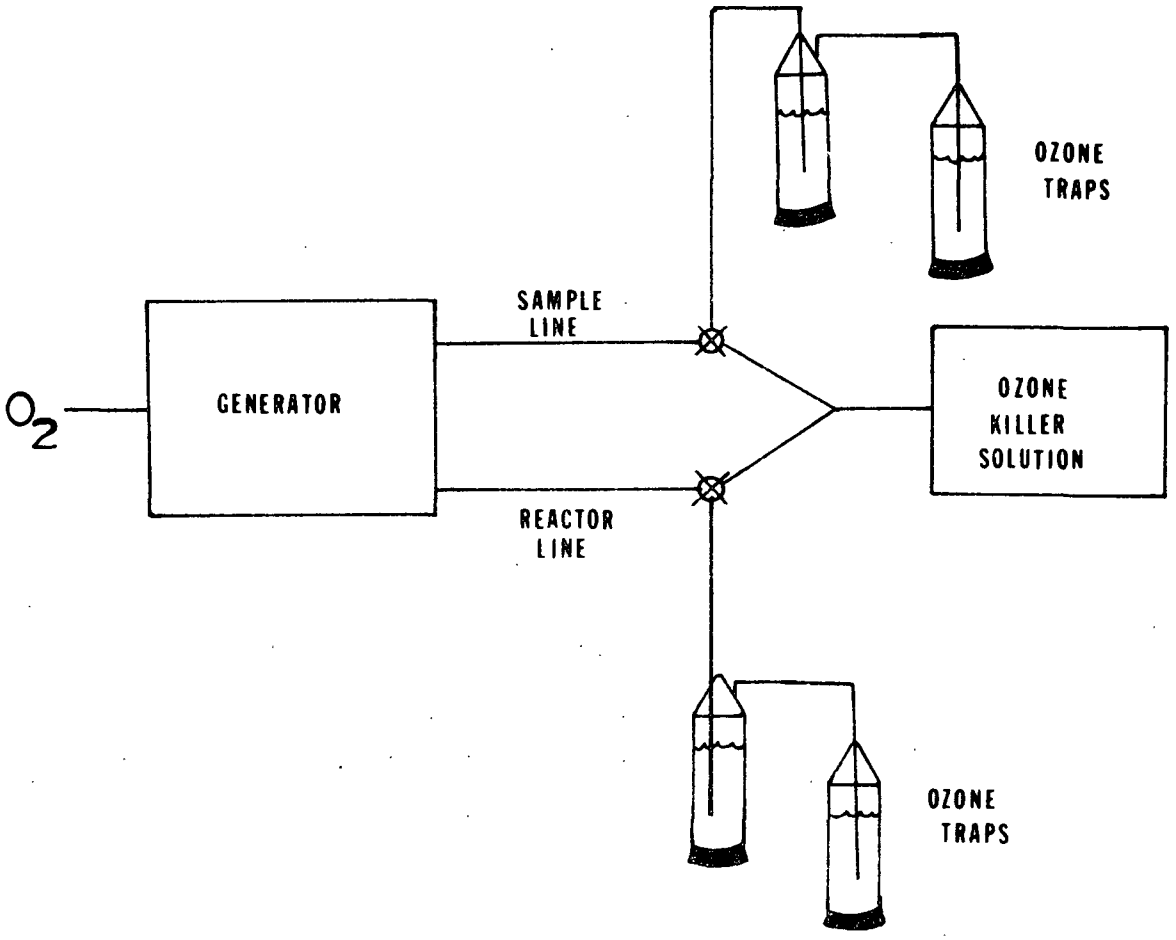

Figure 68. Flow diagram of apparatus used for calibration of ozone generator.

APPENDIX II

UV ABSORBANCE MEASUREMENTS

The concentration of dissolved ozone in buffer solution was determined by UV absorbance measurements. Ozone gas was bubbled 30 min through an acetic acid (HAc)/sodium acetate (NaAc) buffer solution (2 L, 25°C) in a round bottom flask fitted with a top from a gas washing bottle having a gas sparger. This ozonated stock solution was pipetted (100 mL) into an Erlenmeyer flask containing 0.8N potassium iodide (50 mL) and 1N sodium hydroxide. As simultaneously as possible, a sample aliquot of stock solution was also pipetted into a cuvette and the UV absorbance (λ = 260 nm) recorded. The stock solution in the round bottom flask was diluted with nonozonated buffer solution (10-100 mL) and the above procedure repeated. Dissolved ozone concentrations for the samples in the Erlenmeyer flasks were determined by iodometric titration (Appendix III).

A straight line calibration curve was obtained from the plot of UV absorbance versus ozone concentration determined by iodometric titration (Fig. 69). A least squares linear regression analysis (95) performed on the data points gave the equation for the line:

$$Y = 0.0656X + 0.003 \qquad (18)$$

where Y = UV absorbance and X = ozone concentration.
Dissolved ozone concentrations were calculated from Eq. (15) using UV absorbance measurements recorded during ozonation experiments.

A molar absorptivity coefficient for dissolved ozone (25°C) was found to be ε = 3125 L mol^{-1} cm^{-1} at λ = 260 nm. This value is in agreement with molar

absorptivity coefficients determined by other researchers for ozone dissolved in acetic acid solutions (4,5,10).

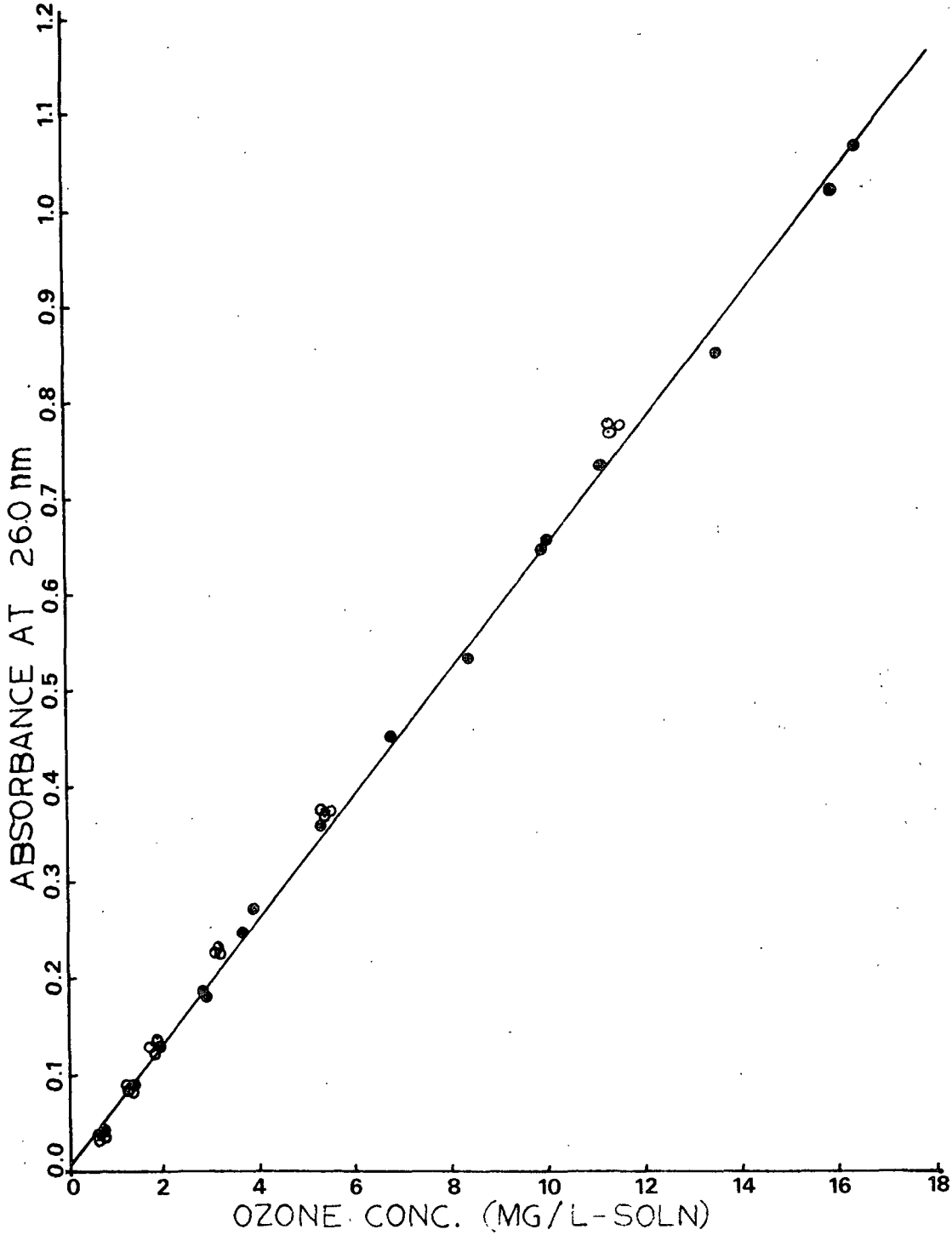

Figure 69. The relationship between UV absorbance and ozone concentration in buffer solution (r^2 = 0.99).

APPENDIX III

IODOMETRIC TITRATION

Ozone concentration was determined by iodometric titration for calibration of the ozone generator and for establishing the UV absorbance versus ozone concentration calibration curve. The procedure used was similar to that described by Rizzuti, et al. (94) in which ozone is absorbed by an alkaline potassium iodide solution (KI). Sample aliquots (25-100 mL) of the ozonated KI solution were acidified with 4N sulfuric acid solution (20 mL) and titrated with a standard sodium thiosulfate solution until a 4% starch solution (5 mL) as the indicator gave a colorless endpoint.

Ozone concentration was calculated from Eq. (19):

$$C = 24\ V_T C_T / V_S \qquad (19)$$

where C = ozone concentration, mg/L

V_T = volume of sodium thiosulfate solution, L

C_T = concentration of sodium thiosulfate solution, mmol/L

V_S = volume of sample aliquot, L

For calibration of the ozone generator, the amount of ozone produced was determined by iodometric titration. The KI solutions (300 mL) were taken from the ozone traps (Appendix I) and each diluted to 500 mL with distilled water. Aliquots of these solutions were acidified with sulfuric acid and titrated with 0.1N sodium thiosulfate.

For establishing the UV absorbance versus ozone concentration calibration curve (Appendix II), the KI solution was acidified with sulfuric acid and titrated with 0.005N sodium thiosulfate solution.

APPENDIX IV

CONSTRUCTION OF REACTION TANKS

The basic reaction system was designed to continuously supply solubilized ozone to the reactor during ozonation. A detailed description of the construction of the reaction tanks is given below.

Ozone Saturation Tank

The ozone saturation tank was constructed from an 11-inch long Lucite cylinder (4-inch ID) to which a flanged Lucite disk was solvent sealed to one end (Fig. 70). A buffer solution inlet was placed 1/2-inch from the tank bottom. A 9-mm OD glass tube was inserted through the inlet to the center of the cylinder. An ozone gas inlet was placed 1/2-inch directly above the buffer solution inlet. A sintered glass dispersion tube (12 C) was placed through the inlet to the center of the cylinder. The glass tubing inserted through each inlet was held in place by Teflon packing glands. The snugness of the fit between the glass tubing, packing gland and Lucite tank prevented solution and gas leaks around the inlets.

To eliminate gaseous ozone from being carried over to the reaction tank, a small Lucite cylinder was added to the saturation tank. The cylinder (5-inch x 1-inch ID) was closed at one end by solvent sealing a flanged Lucite disk to it. A 28 mesh polypropylene screen was cut to fit flush with the outer wall of the small cylinder. The screen was placed over the cylinder and held in place with a Lucite ring. The small cylinder was fastened to the side of the ozone saturation tank with a Lucite pin.

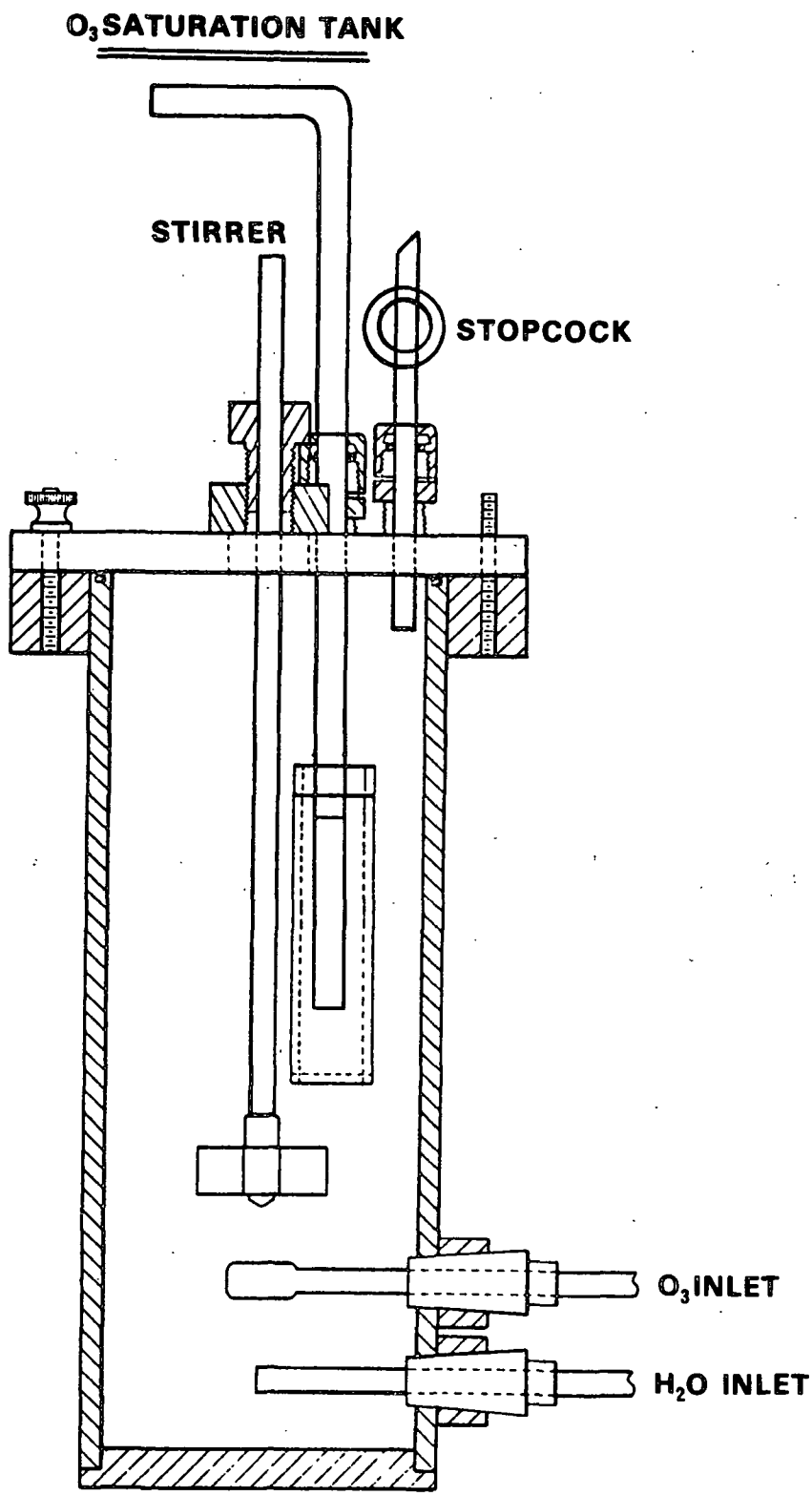

Figure 70. Ozone saturation tank.

The saturation tank cover had three ports fitted with Teflon packing glands. A polypropylene stirrer extended through the center port to approximately 1/2-inch above the gas dispersion tube. To prevent gas leakage, the rod was covered with a stainless steel sleeve long enough to extend only through the packing gland.

The second port in the cover acted as an ozone exhaust gas outlet. A 9-mm OD glass tube extended through the packing gland so that it did not come in contact with the solution in the tank. The glass tube was connected to gas traps containing a potassium iodide-sodium hydroxide solution.

A 9-mm glass tube extended through the packing gland of the remaining port. The glass tubing went through the screen on the small cylinder and came approximately 1/2-inch from the bottom of the small cylinder. Ozonated buffer solution passed through this tube to the reaction tank.

The cover was bolted to the saturation tank prior to the reaction. Gas leakage between the cover and tank body was prevented by a rubber O-ring which was seated in a groove in the lip of the tank body.

Ozone Reaction Tank

The reaction tank (Fig. 71) was constructed of the same materials and dimensions as the ozone saturation tank.

A solution outlet was placed 1/2-inch from the bottom of the reaction tank. The outlet was constructed from a 4-inch x 1-inch ID Lucite cylinder (Fig. 72). The cylinder was closed by solvent sealing a Lucite flanged disk to each end. Tightly spaced, 1/8-inch diameter holes were drilled through one end

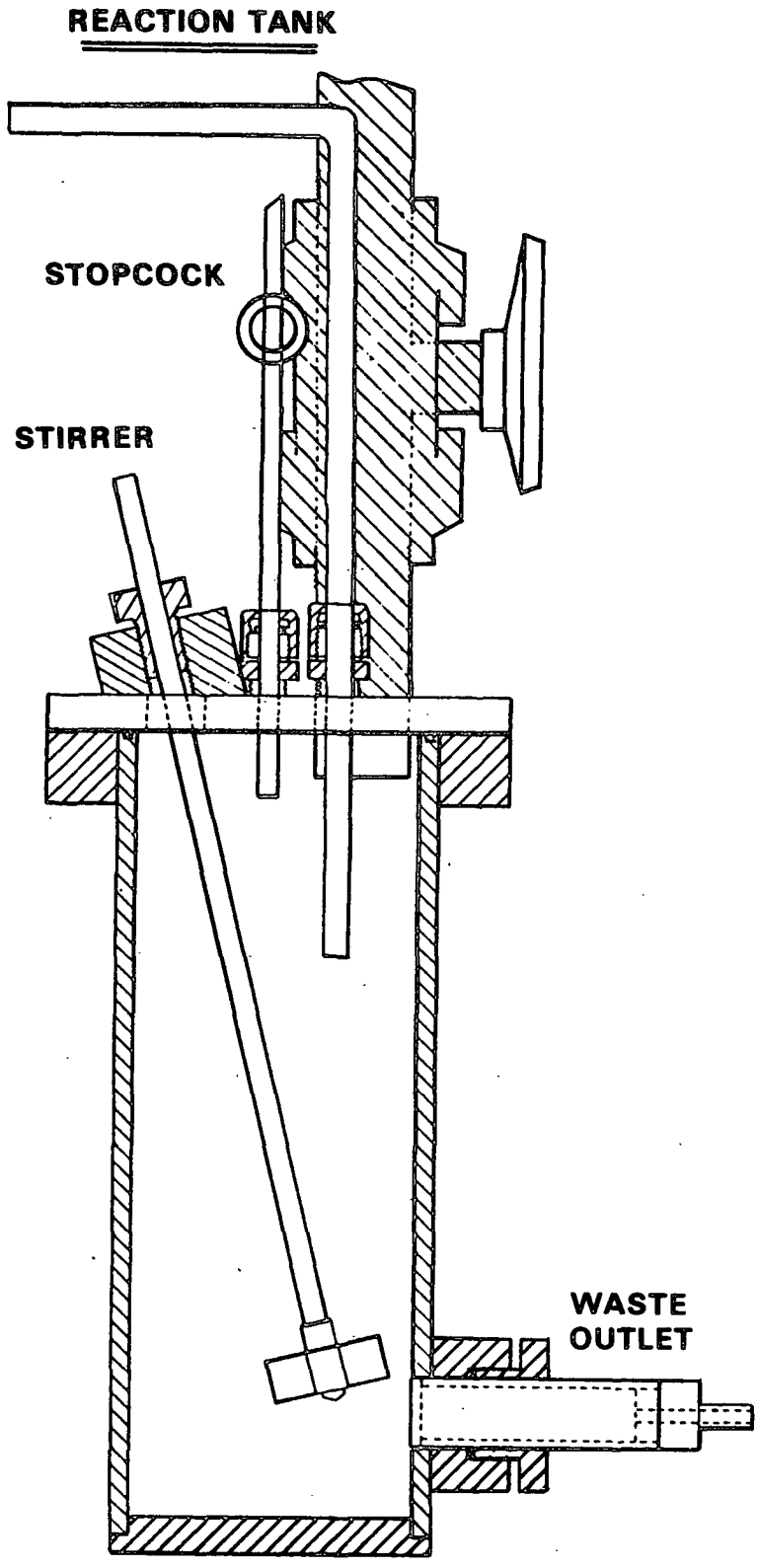

Figure 71. Ozone reaction tank.

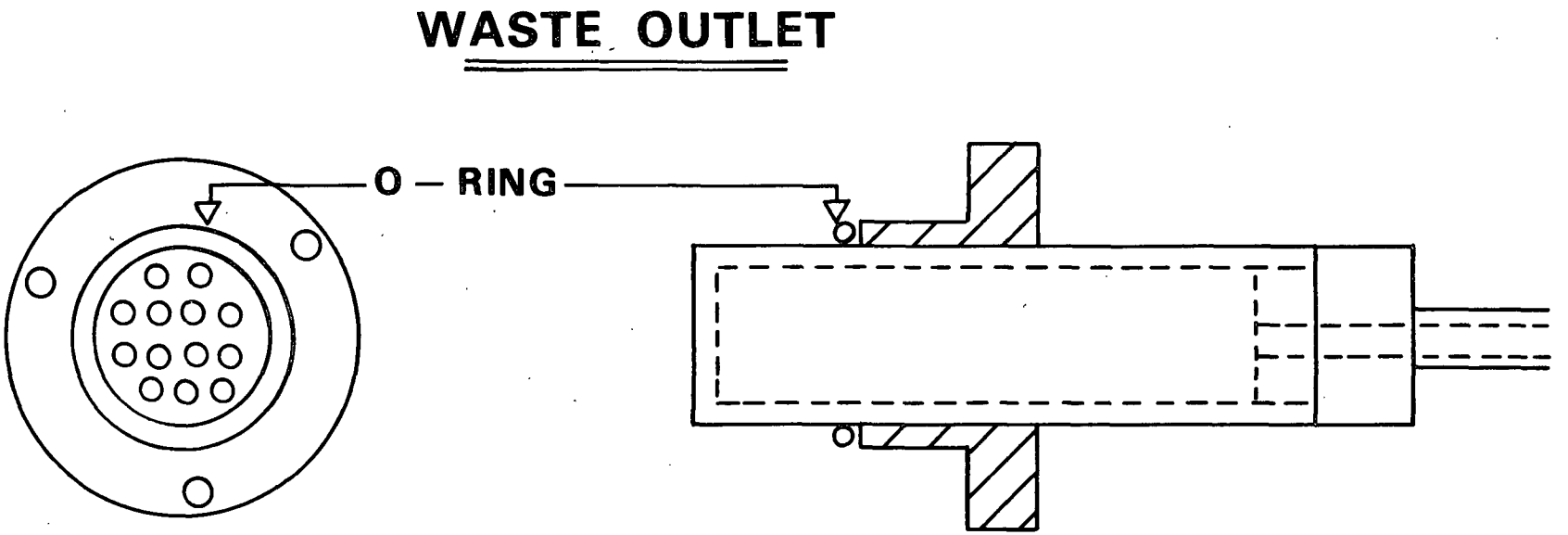

Figure 72. Waste outlet on ozone reaction tank.

of the outlet cylinder. A polypropylene screen (56 mesh) was placed over the holes and secured with a Lucite ring. The outlet screen was positioned flush with the inside wall of the reaction tank body. A rubber O-ring was placed around the outlet cylinder to prevent solution from leaking between the reaction tank and cylinder. The outlet cylinder was held in place by a flanged Lucite ring. The ring was fastened to the reactor with three screws.

The other end of the cylinder had a 9-mm diameter hole drilled through the center to which a 9-mm OD Lucite tube was solvent sealed. Tygon tubing was used to connect the outlet to a solution waste tank.

The reactor cover had four ports. Three of the ports were fitted with Teflon packing glands. One port consisted of an L-shaped, 9-mm OD glass tube which extended through the packing gland to approximately one-fourth of the way into the reaction tank. Ozonated solution from the saturation tank was fed into the reaction tank through this tube.

The second port acted as an ozone gas exhaust outlet. A 9-mm OD glass tube extended through the packing gland into the reactor so that it did not contact the solution. The other end of the glass tube was connected to gas traps containing a potassium iodide-sodium hydroxide solution.

A two bladed, polypropylene stirrer fitted with a stainless steel sleeve was placed at a sixty degree angle through the packing gland of the third port. The stirrer was placed at an angle to sweep fibers from the screen of the solution outlet during reaction.

The remaining port in the cover allowed for pulp addition to the reaction tank. The addition port was constructed from two polyvinyl chloride (PVC)

pipes (3-inch x 1-inch OD) joined by a 1-inch PVC ball valve. One end of the pipe was threaded and screwed into the reactor cover.

The cover was bolted to the reactor prior to the start of the reaction. Gas leakage between the cover and tank body was prevented by a rubber O-ring which was seated in a groove in the lip of the tank body.

APPENDIX V

REACTOR VARIABLES

To achieve reproducible and controlled ozonations, reactor variables such as concentration of buffer solution, buffer solution flow rate, ozone gas flow rate and mixing speed were investigated first using the ozone saturation tank and then extended to the reaction tank.

Prior to the start of the experimental runs, the ozone generator was allowed to come to equilibrium (Appendix I). The saturation tank was filled with buffer solution (1800 mL, pH 3). A continuous flow of buffer solution into and out of the saturation tank was maintained at 4 mL/sec. The buffer solution in the tank was not stirred during ozonation. Ozone gas was directed into the tank at the start of the run. Aliquots of ozonated solution were taken at specified times and the ozone concentration determined iodometrically (Appendix III).

Effect of buffer solution concentration and ozone gas flow rate on ozone solubility is shown in Fig. 73. By decreasing buffer solution concentration from 1M HAc/0.018M NaAc (curve 1) to 0.14M HAc/0.0072M NaAc (curve 2), ozone solubility increased. This effect has been observed previously for solubility of gases in aqueous media containing salts (96). Unexpectedly, increasing ozone gas flow rate into the saturation tank from 2 to 4 L/min, reduced soluble ozone concentration (Fig. 73, curves 2 and 3, respectively). It was thought that by increasing the gas flow rate without increasing the generator wattage lowered the partial pressure of ozone in the gas stream. This resulted in the reduced ozone equilibrium concentration. Therefore, the more dilute buffer solution (0.14M HAc/0.0072M NaAc) and lower gas flow rate (2 L/min) was used in further experiments.

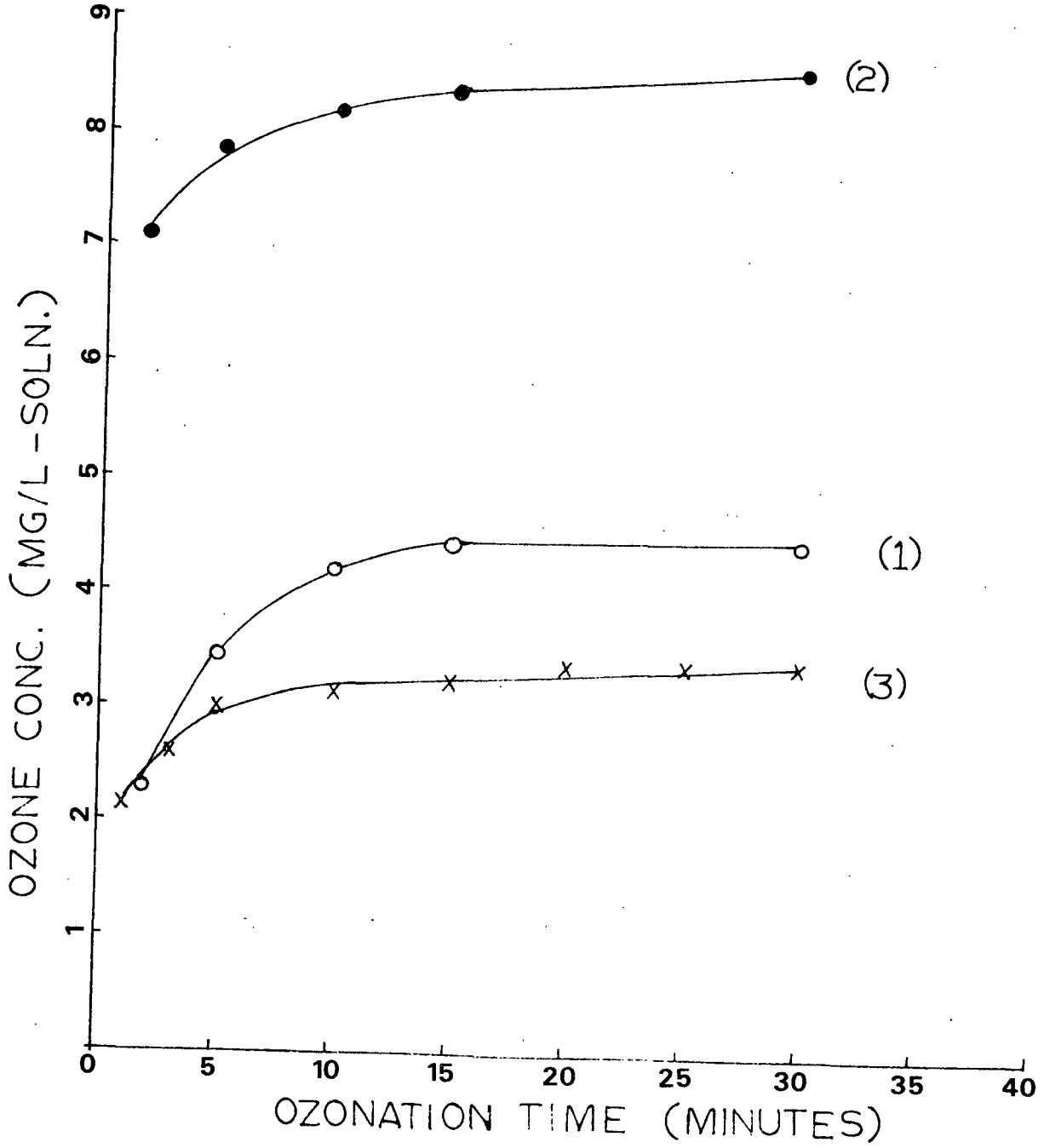

Figure 73. Ozone solubility in acetic acid buffer solution, no mixing, (1) 1M HAc/0.18M NaAc, 2 L/min-gas; (2) 0.14M HAc/0.0072M NaAc, 2 L/min-gas; (3) 0.14M HAc/0.0072M NaAc, 4 L/min-gas.

Effect of mixing on ozone solubility was investigated using the experimental procedure and conditions described above except ozone concentration was determined from UV measurements (Appendix II). Ozone solubility with respect to time is shown in Fig. 74 for various levels of mixing. Dissolved ozone concentration increased as mixing increased from 0-750 rpm; at 1000 rpm solubility decreased. Yocum (97) observed a similar trend for ozone absorption in aqueous solutions for various levels of mixing in a semibatch reactor. Ozonation experiments were carried out using a solution mixing rate of 500 rpm. This level of mixing was chosen because it was easier to maintain over prolonged periods of time.

Buffer solution flow rate was varied to determine the maximum solution flow rate that could be put through the reaction system. The reaction tank was connected to the ozone saturation tank. Once an ozone equilibrium concentration was reached in the saturation tank (15 minutes), the ozonated buffer solution was allowed to flow to the reaction tank at a rate of 4 cc/sec until it contained 1800 mL of solution. Mixing in this tank was also 500 rpm. At this point, the three way stopcock was opened to allow solution to flow from the reaction tank to the waste tank at 4 cc/sec. Sample aliquots were withdrawn at various times and the ozone concentration measured by UV absorbance. A plot of ozone concentration versus time at flow rates of 4 and 5 cc/sec are shown in Fig. 75. Higher flow rates were not obtainable due to limitation of reactor design. An ozone equilibrium concentration of ~9.0 mg/L-soln was reached in approximately ten minutes at both flow rates. This concentration is 10% lower than the equilibrium concentration achieved in the saturation tank. Hoigne and Bader (10) have also reported a 10% loss in ozone concentration during transfer of ozonated solution from one vessel to another.

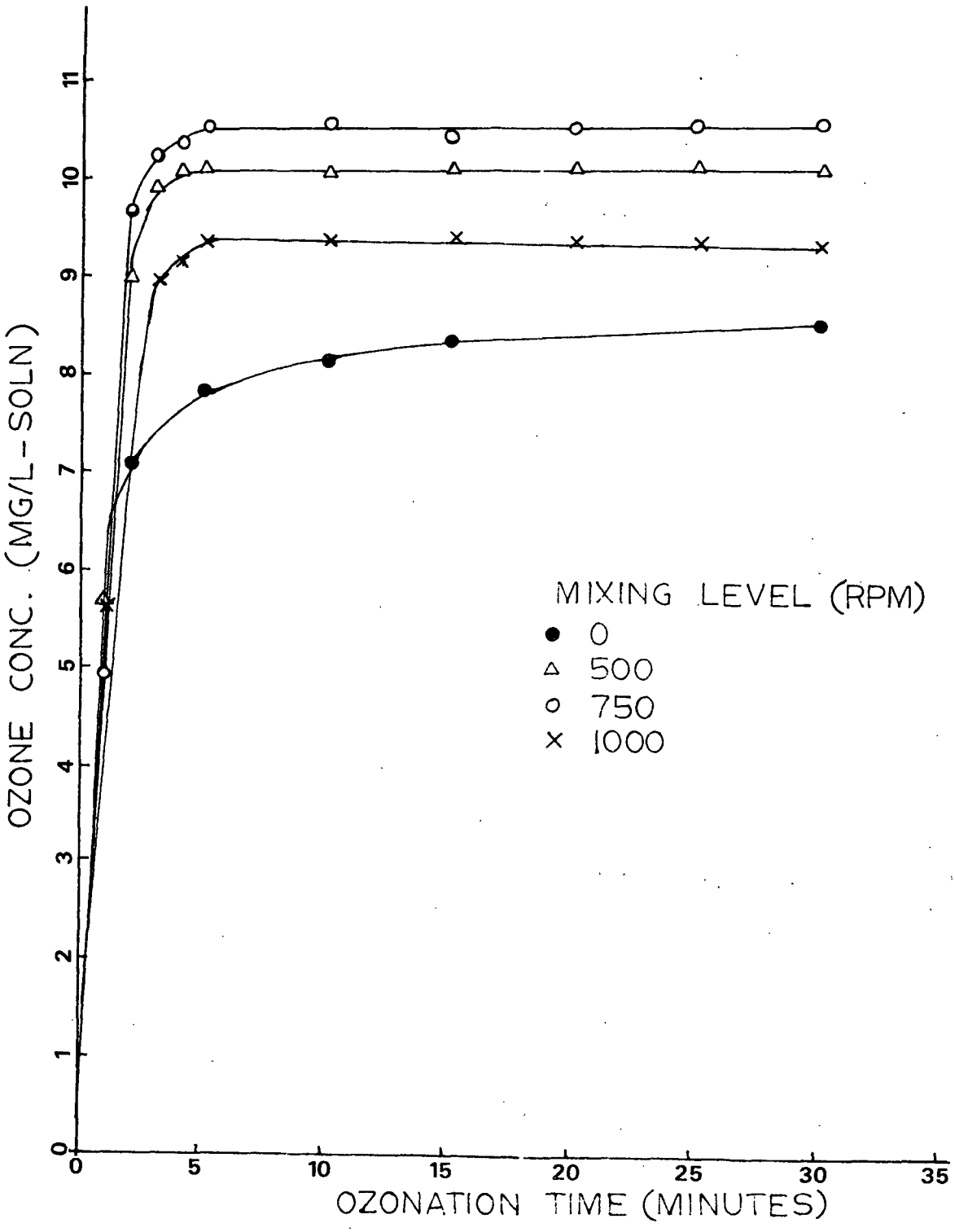

Figure 74. Ozone solubility versus time for various mixing levels.

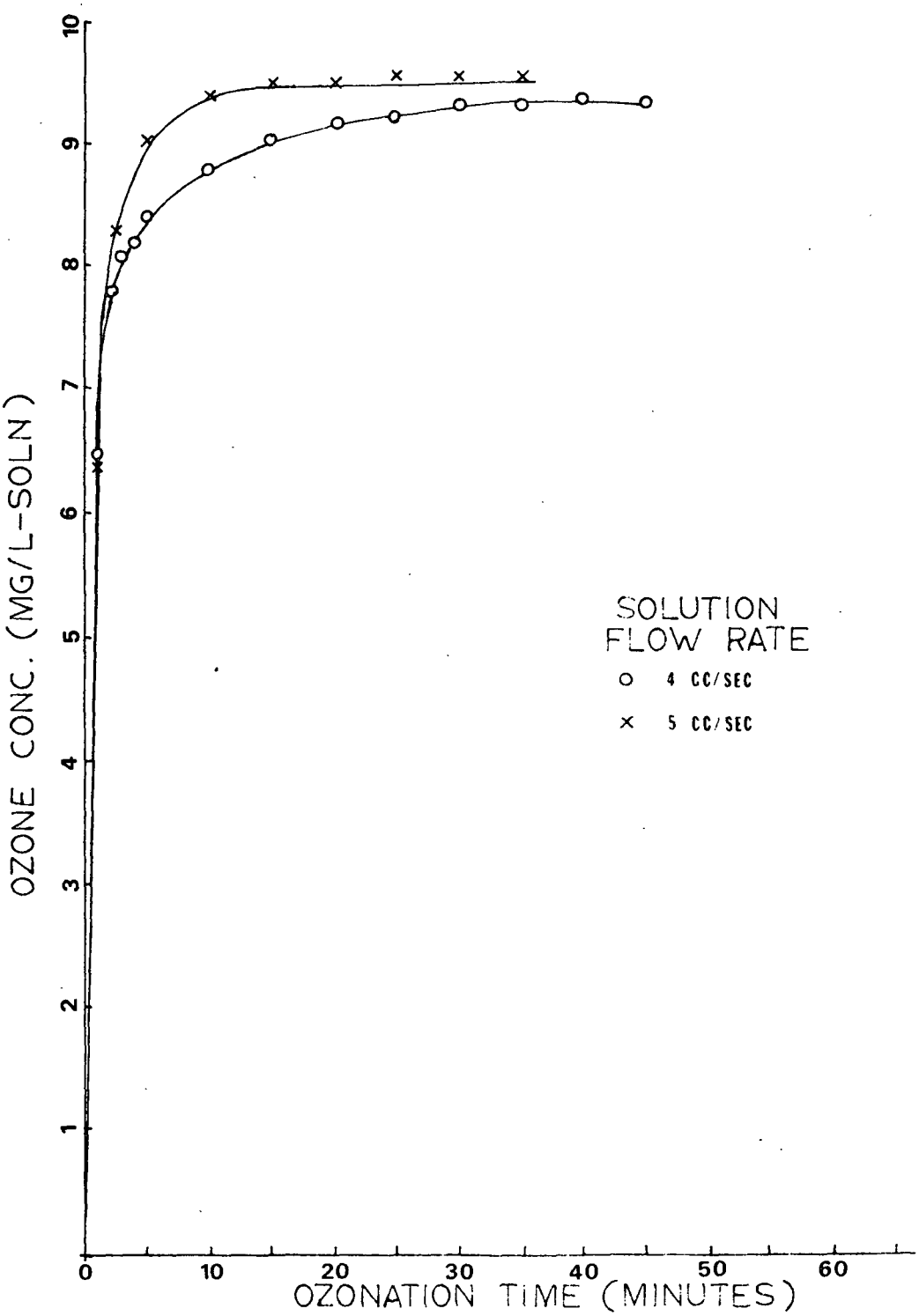

Figure 75. Ozone solubility versus time for various buffer solution flow rates.

Based on results from the above mentioned preliminary experiments, the operating conditions used in this study were as follows:

Temperature: 25°C
pH: 3
Buffer Solution Concentration: 0.4M HAc/0.0072M NaAc
Buffer Solution Flow Rate: 0.3 L-soln/min
Ozone Gas Flow Rate: 2 L-gas/min
Mixing Rate: 500 rpm

These conditions were easy to maintain and gave reproducible and controllable ozonation experiments.

APPENDIX VI

FIBER CONSISTENCY

Using the previously given reaction conditions (Appendix V), it was desirable to maintain a steady state ozone concentration in solution during ozonation of fibers. Soluble ozone concentration would be affected by the amount of fibers ozonated during the experiments. Therefore, the effect of fiber consistency on soluble ozone concentration was investigated.

The reaction apparatus was allowed to come to equilibrium as described in the Experimental section. Fibers dispersed in 50 mL of buffer solution were added to the reactor and ozonated for various lengths of time. Sample aliquots of buffer solution were withdrawn during the reaction and ozone concentration calculated from UV absorbance measurements. A plot of ozone concentration with respect to reaction time for ozonation runs utilizing various consistencies of fibers is shown in Fig. 76. As fiber consistency decreased, ozone consumption decreased. Even at very low consistencies (e.g., 0.006%), a constant dissolved ozone concentration was not maintained. A 0.05% consistency was used in further experiments. Under these conditions, excess ozone was maintained during the entire experimental run while obtaining the largest quantity of ozonated material possible.

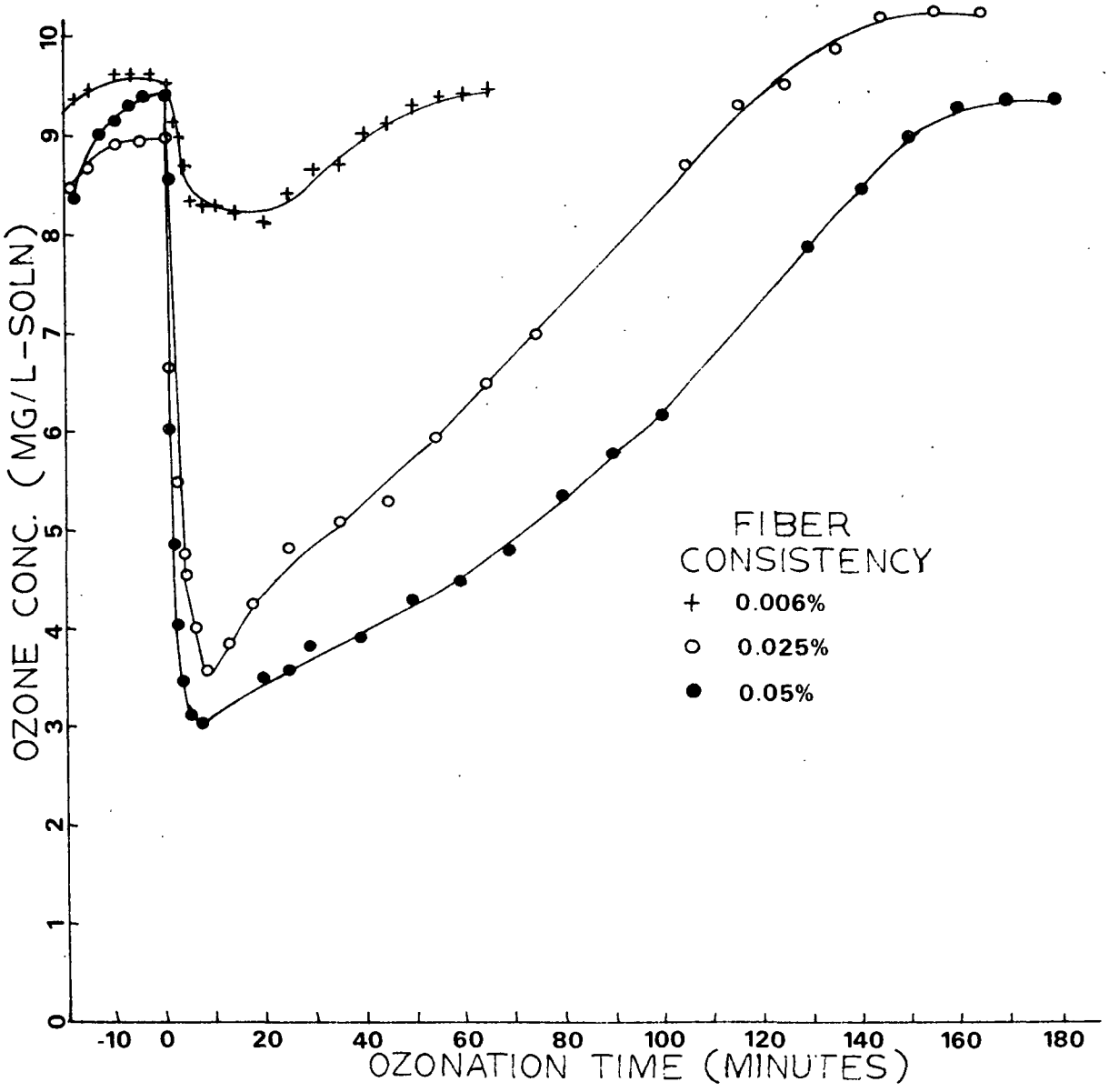

Figure 76. Ozone concentration versus reaction time at various fiber consistencies.

APPENDIX VII

OZONATION OF FIBERS

Fibers were ozonated for specified lengths of time ranging from 5-180 minutes. Several ozonation runs had to be carried out at a specified time to collect enough sample for chemical, physical and microscopic analyses. Mean values, standard deviations and per cent coefficient of variations for a specified ozonation run are shown in Table XV (LW fibers) and Table XVI (EW fibers). Plots of ozone concentration mean values (± standard deviations) *versus* reaction time are shown in Fig. 77-83 for LW fibers and Fig. 84-90 for EW fibers.

TABLE XV

OZONE CONCENTRATION SUMMARY FOR LATEWOOD FIBER EXPERIMENTS

Time, min	Mean Value	Std. Dev.	Coefficient of Variation, %	Time, min	Mean Value	Std. Dev.	Coefficient of Variation, %
-15	9.577	0.133	1.385	-15	9.447	0.215	2.276
-10	9.605	0.094	0.979	-10	9.568	0.134	1.401
-5	9.598	0.072	0.750	-5	9.600	0.141	1.469
0	9.619	0.073	0.759	0	9.611	0.144	1.498
1	8.521	0.268	3.145	2	4.735	0.313	6.610
2	6.841	0.615	8.990	4	3.323	0.203	6.109
3	5.431	0.395	7.273	6	2.915	0.156	5.352
4	4.764	0.299	6.276	8	2.879	0.106	3.682
5	4.369	0.273	6.249	10	2.940	0.136	4.626

Time, min	Mean Value	Std. Dev.	Coefficient of Variation, %	Time, min	Mean Value	Std. Dev.	Coefficient of Variation, %
-15	9.708	0.207	2.132	-15	9.517	0.150	1.576
-10	9.733	0.202	2.075	-10	9.573	0.161	1.682
-5	9.760	0.160	1.639	-5	9.710	0.093	0.958
0	9.758	0.149	1.527	0	9.792	0.084	0.858
5	3.375	0.164	4.859	5	3.582	0.076	2.122
10	3.037	0.044	1.449	10	3.552	0.125	3.519
15	3.173	0.114	3.593	15	3.623	0.137	3.781
20	3.375	0.087	2.578	20	3.796	0.110	2.898
25	3.573	0.072	2.015	25	3.867	0.122	3.155
30	3.691	0.064	1.734	30	4.024	0.076	1.889
				40	4.319	0.062	1.436
				50	4.527	0.115	2.540
				60	4.797	0.104	2.168

TABLE XV (Continued)

OZONE CONCENTRATION SUMMARY FOR LATEWOOD FIBER EXPERIMENTS

Time, min	Mean Value	Std. Dev.	Coefficient of Variation, %	Time, min	Mean Value	Std. Dev.	Coefficient of Variation, %
-15	9.743	0.131	1.345	-15	9.131	0.185	2.026
-10	9.767	0.143	1.464	-10	9.294	0.303	3.260
-5	9.788	0.147	1.502	-5	9.299	0.161	1.731
0	9.781	0.153	1.564	0	9.436	0.337	3.571
5	3.494	0.275	7.871	5	3.313	0.072	2.173
10	3.182	0.242	7.605	10	3.166	0.084	2.693
15	3.281	0.258	7.863	15	3.283	0.058	1.767
20	3.464	0.282	8.141	20	3.440	0.069	2.006
25	3.614	0.275	7.609	25	3.511	0.084	2.392
30	3.737	0.268	7.172	30	3.664	0.072	1.965
40	3.978	0.294	7.391	40	4.050	0.101	2.494
50	4.229	0.303	7.165	50	4.273	0.072	1.683
60	4.566	0.345	7.556	60	4.614	0.089	1.929
70	4.865	0.403	8.284	70	4.964	0.130	2.619
80	5.230	0.392	7.495	80	5.274	0.079	1.498
90	5.577	0.397	7.119	90	5.625	0.137	2.436
				100	6.011	0.213	3.627
				110	6.555	0.137	2.090
				120	6.921	0.079	1.141

Time, min	Mean Value	Std. Dev.	Coefficient of Variation, %
-15	9.644	0.149	1.545
-10	9.665	0.126	1.304
-5	9.684	0.125	1.291
0	9.681	0.137	1.415
5	3.623	0.134	3.699
10	3.284	0.164	4.994
15	3.394	0.185	5.451
20	3.524	0.184	5.221
25	3.679	0.188	5.110
30	3.800	0.191	5.026
40	4.084	0.268	6.594
50	4.340	0.268	6.175
60	4.613	0.302	6.540
70	4.938	0.309	6.258
80	5.320	0.315	5.921
90	5.712	0.351	6.145
100	6.124	0.367	5.993
110	6.584	0.378	5.741
120	7.070	0.393	5.559
130	7.617	0.418	5.488
140	8.074	0.405	5.016
150	8.503	0.394	4.634
160	8.854	0.388	4.382
170	9.144	0.410	4.484
180	9.337	0.389	4.166

TABLE XVI

OZONE CONCENTRATION SUMMARY FOR EARLYWOOD FIBER EXPERIMENTS

Time, min	Mean Value	Std. Dev.	Coefficient of Variation, %	Time, min	Mean Value	Std. Dev.	Coefficient of Variation, %
-15	9.489	0.011	0.116	-15	9.306	0.011	0.118
-10	9.566	0.011	0.115	-10	9.367	0.054	0.576
-5	9.527	0.022	0.231	-5	9.390	0.022	0.234
0	9.535	0.054	0.566	0	9.413	0.032	0.340
1	4.024	0.043	1.069	2	3.613	0.280	7.750
2	3.049	0.151	4.952	4	2.172	0.075	3.453
3	2.515	0.129	5.129	6	2.005	0.032	1.596
4	2.477	0.011	0.444	8	2.111	0.054	2.558
5	2.454	0.065	2.649	10	2.218	0.097	4.373

Time, min	Mean Value	Std. Dev.	Coefficient of Variation, %	Time, min	Mean Value	Std. Dev.	Coefficient of Variation, %
-15	9.308	0.202	2.170	-15	9.456	0.127	1.343
-10	9.360	0.224	2.393	-10	9.466	0.183	1.933
-5	9.373	0.230	2.454	-5	9.507	0.223	2.346
0	9.356	0.223	2.383	0	9.517	0.175	1.839
5	2.536	0.320	12.618	5	2.510	0.328	13.068
10	2.584	0.320	12.384	10	2.622	0.213	8.124
15	2.746	0.347	12.637	15	2.825	0.182	6.442
20	2.925	0.332	11.350	20	3.013	0.167	5.543
25	3.064	0.333	10.868	25	3.135	0.177	5.846
30	3.148	0.324	10.292	30	3.283	0.196	5.970
				40	3.425	0.241	7.036
				50	3.699	0.311	8.408
				60	4.055	0.344	8.483

TABLE XVI (Continued)

OZONE CONCENTRATION SUMMARY FOR EARLYWOOD FIBER EXPERIMENTS

Time, min	Mean Value	Std. Dev.	Coefficient of Variation, %	Time, min	Mean Value	Std. Dev.	Coefficient of Variation, %
-15	9.522	0.241	2.531	-15	9.436	0.349	3.699
-10	9.472	0.124	1.309	-10	9.558	0.279	2.919
-5	9.416	0.118	1.253	-5	9.568	0.202	2.174
0	9.441	0.087	0.922	0	9.624	0.194	2.016
5	2.637	0.066	2.503	5	2.571	0.062	2.412
10	2.647	0.146	5.516	10	2.688	0.087	3.237
15	2.759	0.225	8.155	15	2.886	0.098	3.396
20	2.888	0.277	9.598	20	3.059	0.088	2.877
25	2.998	0.269	8.973	25	3.310	0.137	4.377
30	3.135	0.308	9.825	30	3.242	0.114	3.516
40	3.389	0.282	7.731	40	3.450	0.163	4.725
50	3.628	0.205	5.650	50	3.557	0.093	2.615
60	3.963	0.053	1.388	60	3.897	0.101	2.592
70	4.304	0.275	6.389	70	4.436	0.081	1.826
80	4.883	0.476	9.748	80	5.107	0.015	0.294
90	5.488	0.686	12.500	90	6.067	0.155	2.555
				100	6.921	0.121	1.748
				110	7.591	0.230	3.030
				120	8.293	0.385	4.642

Time, min	Mean Value	Std. Dev.	Coefficient of Variation, %
-15	9.568	0.163	1.704
-10	9.624	0.183	1.901
-5	9.639	0.163	1.891
0	9.726	0.132	1.357
5	2.556	0.338	13.224
10	2.490	0.308	12.369
15	2.785	0.266	9.551
20	2.927	0.268	9.156
25	3.110	0.275	8.842
30	3.242	0.271	5.359
40	3.436	0.372	10.830
50	3.638	0.383	10.526
60	4.035	0.432	10.706
70	4.456	0.257	5.768
80	5.158	0.163	3.141
90	6.133	0.171	2.766
100	6.870	0.058	0.844
110	7.536	0.093	1.234
120	8.191	0.089	1.087
130	8.694	0.323	3.715
140	0.096	0.415	4.562
150	9.309	0.455	4.886
160	9.436	0.447	4.737
170	9.614	0.444	4.618
180	9.700	0.353	3.639

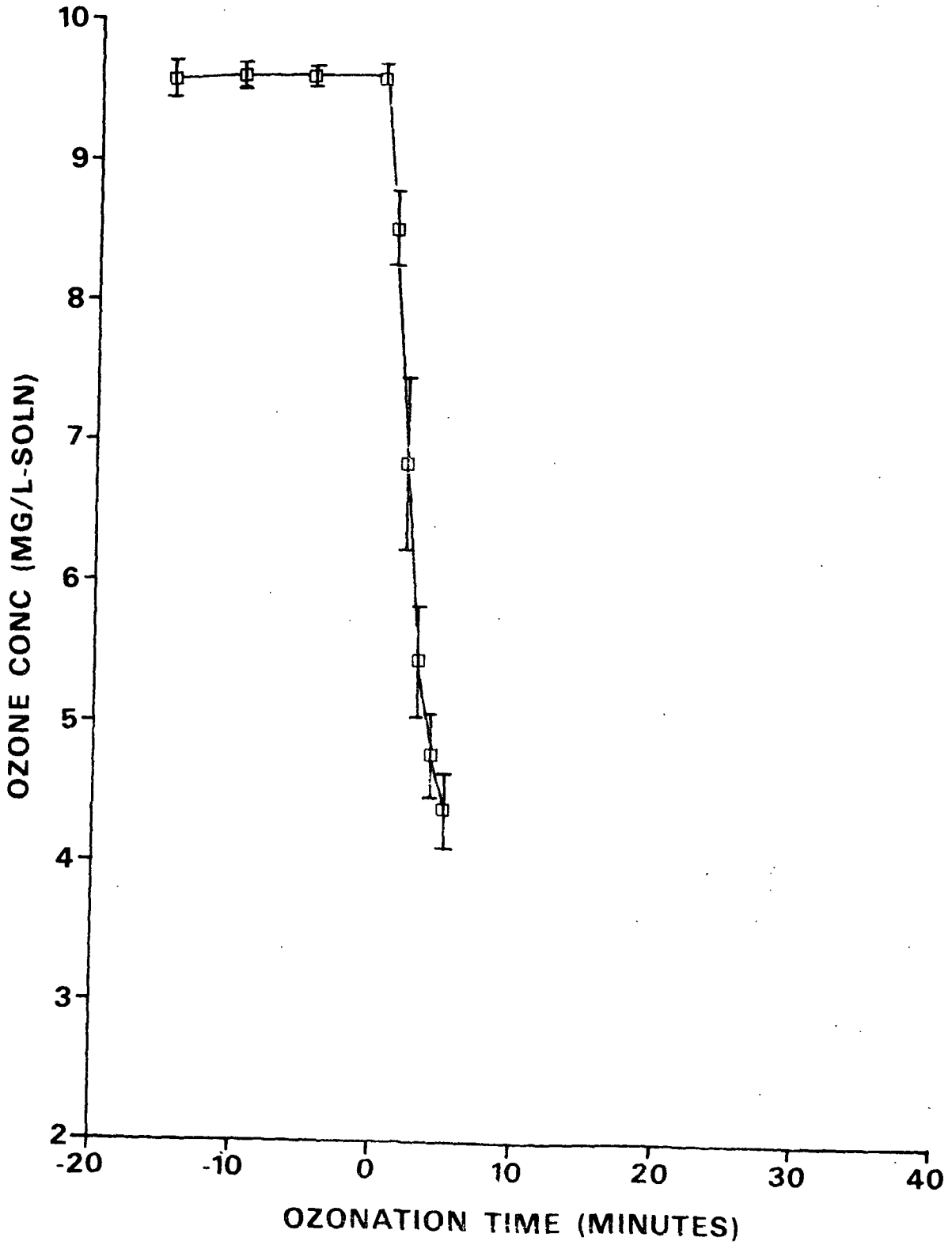

Figure 77. Ozonation of LW fibers (0.9 g o.d.) for 5 minutes in acetic acid buffer solution (1800 mL).

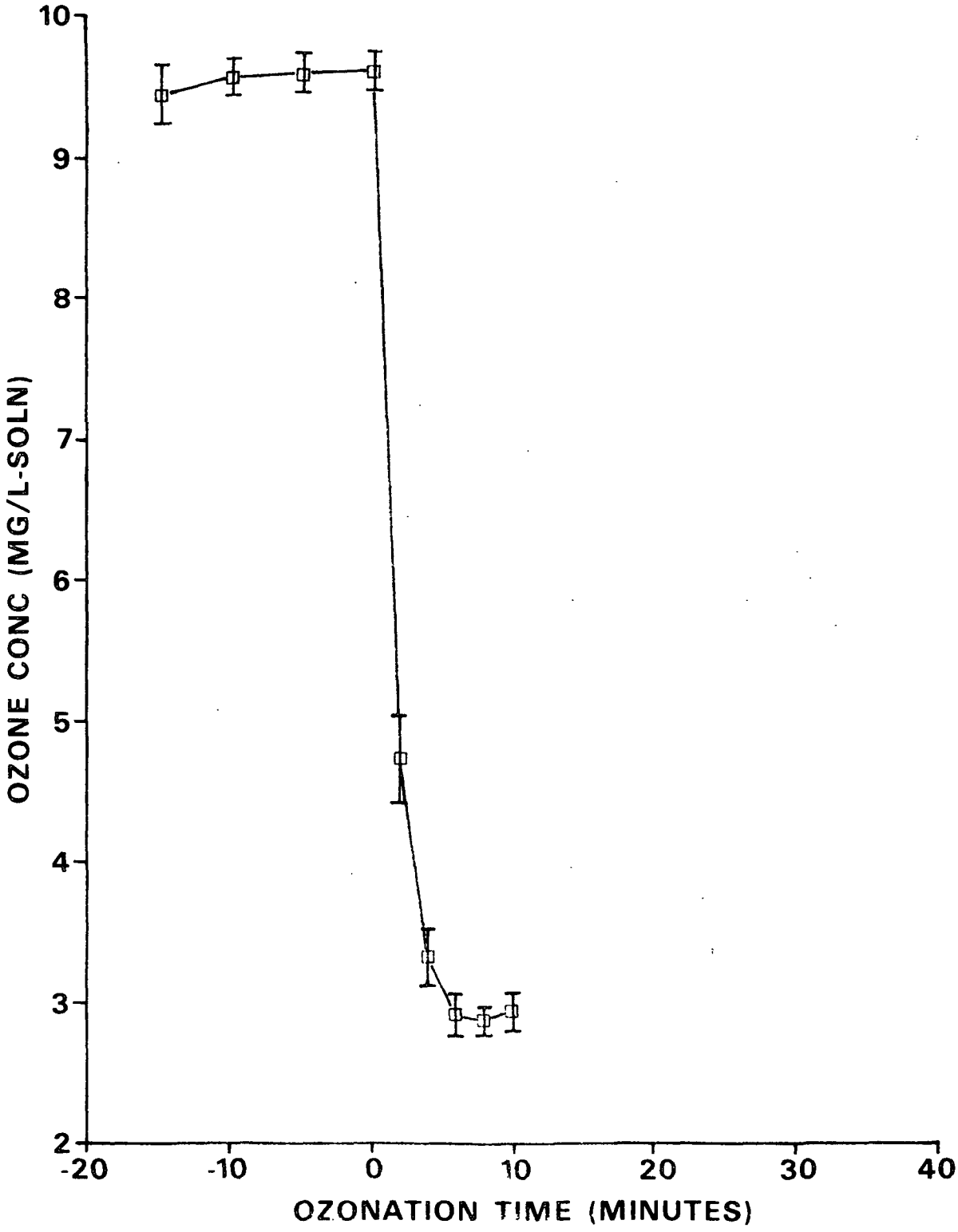

Figure 78. Ozonation of LW fibers (0.9 g o.d.) for 10 minutes in acetic acid buffer solution (1800 mL).

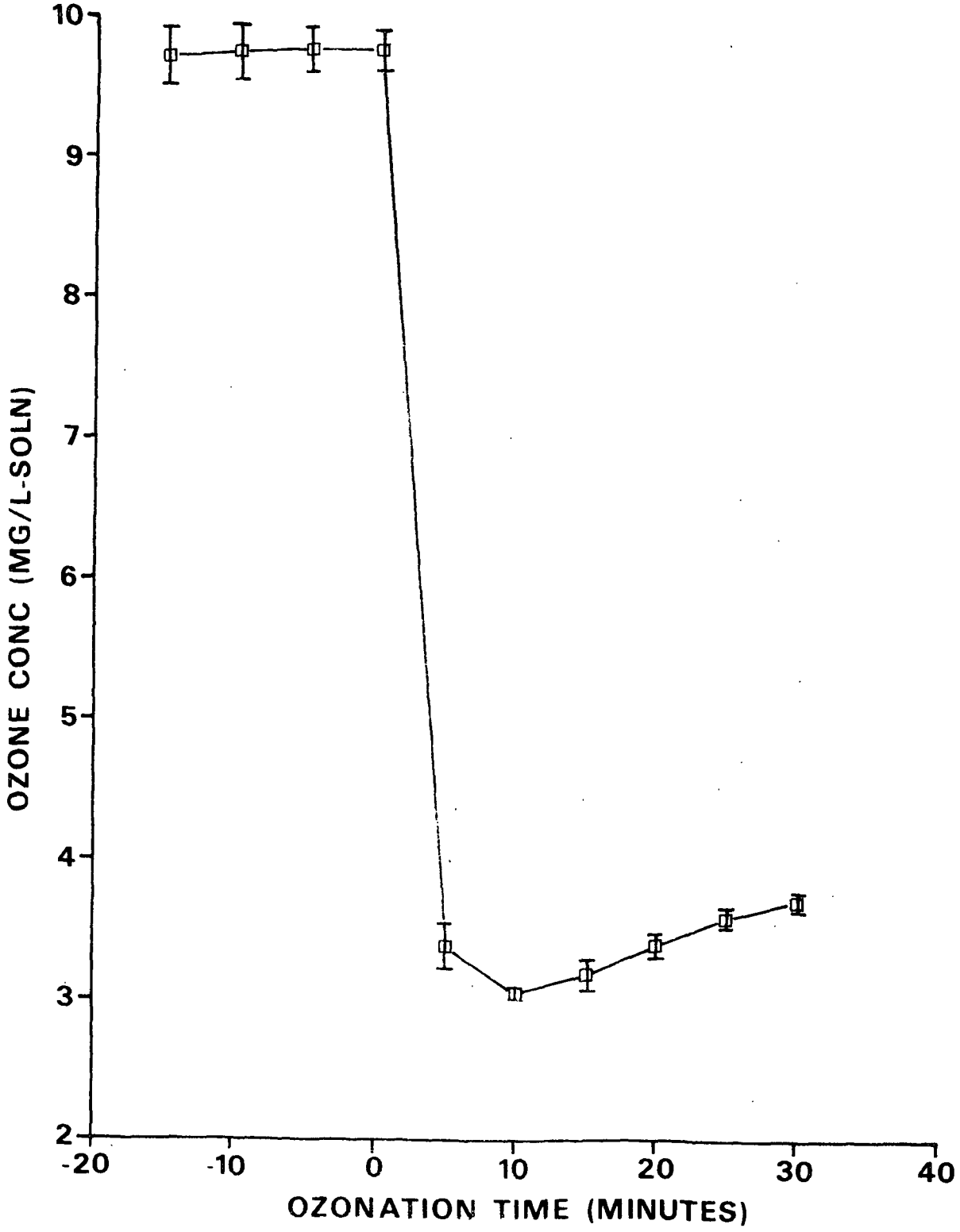

Figure 79. Ozonation of LW fibers (0.9 g o.d.) for 30 minutes in acetic acid buffer solution (1800 mL).

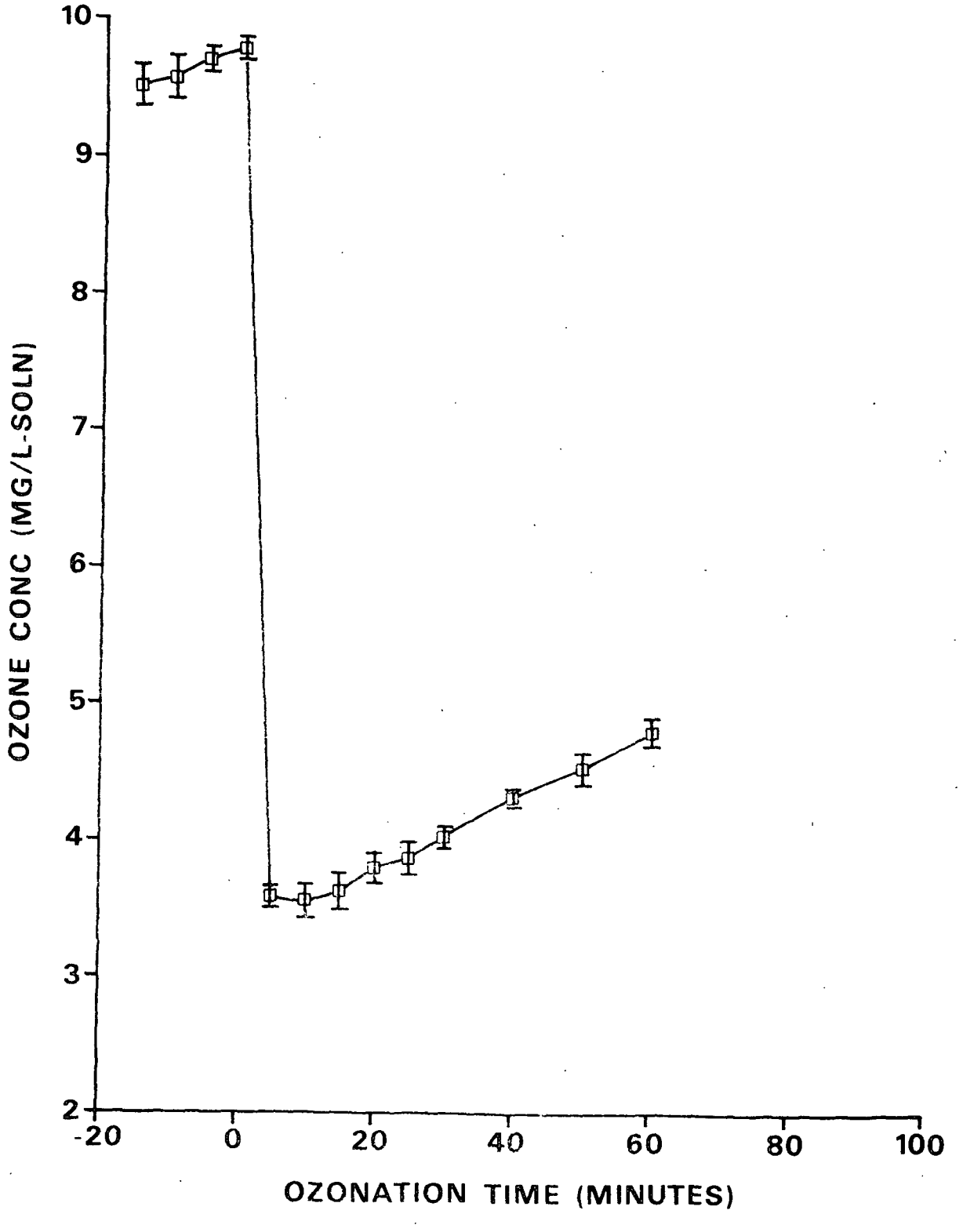

Figure 80. Ozonation of LW fibers (0.9 g o.d.) for 60 minutes in acetic acid buffer solution (1800 mL).

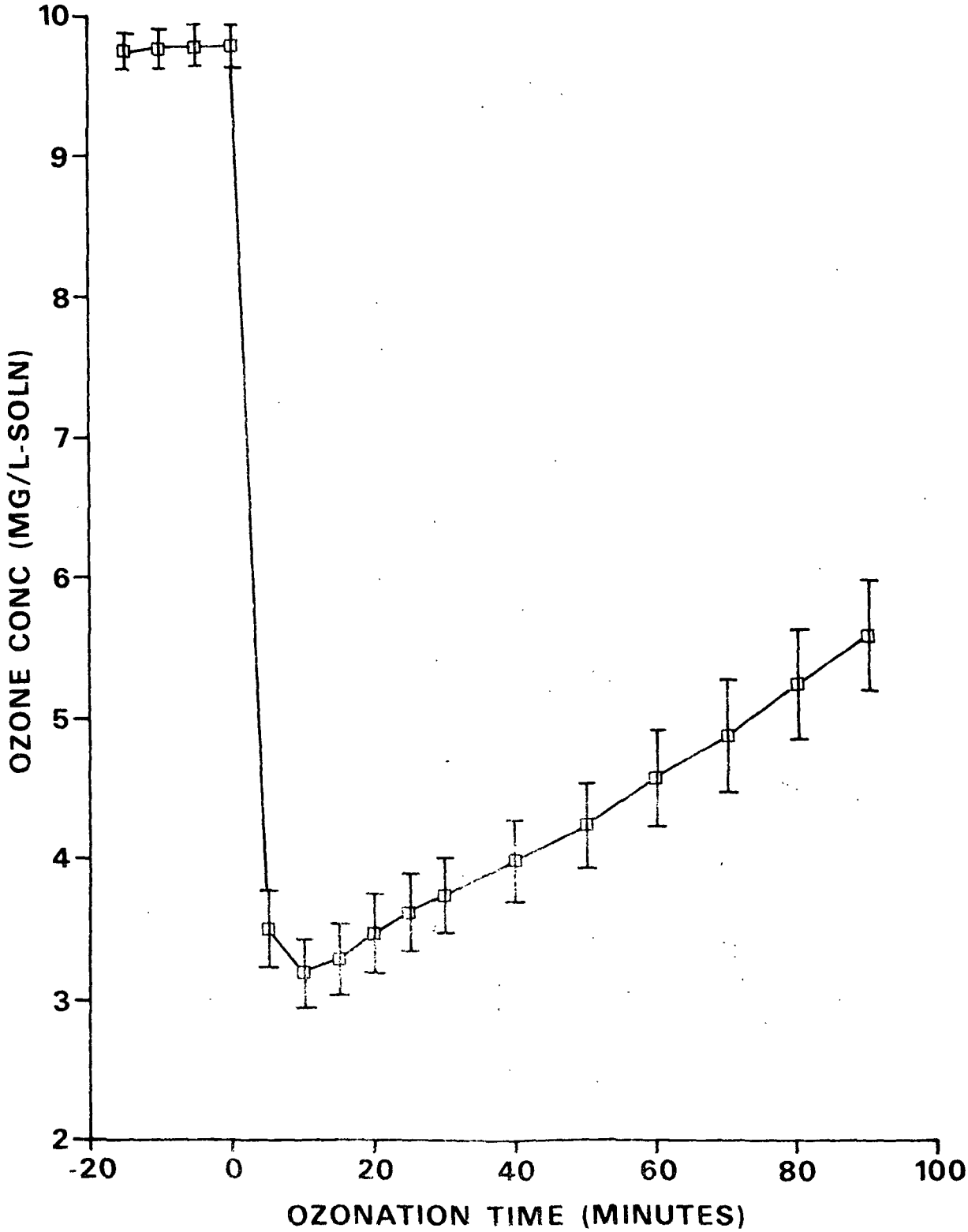

Figure 81. Ozonation of LW fibers (0.9 g o.d.) for 90 minutes in acetic acid buffer solution (1800 mL).

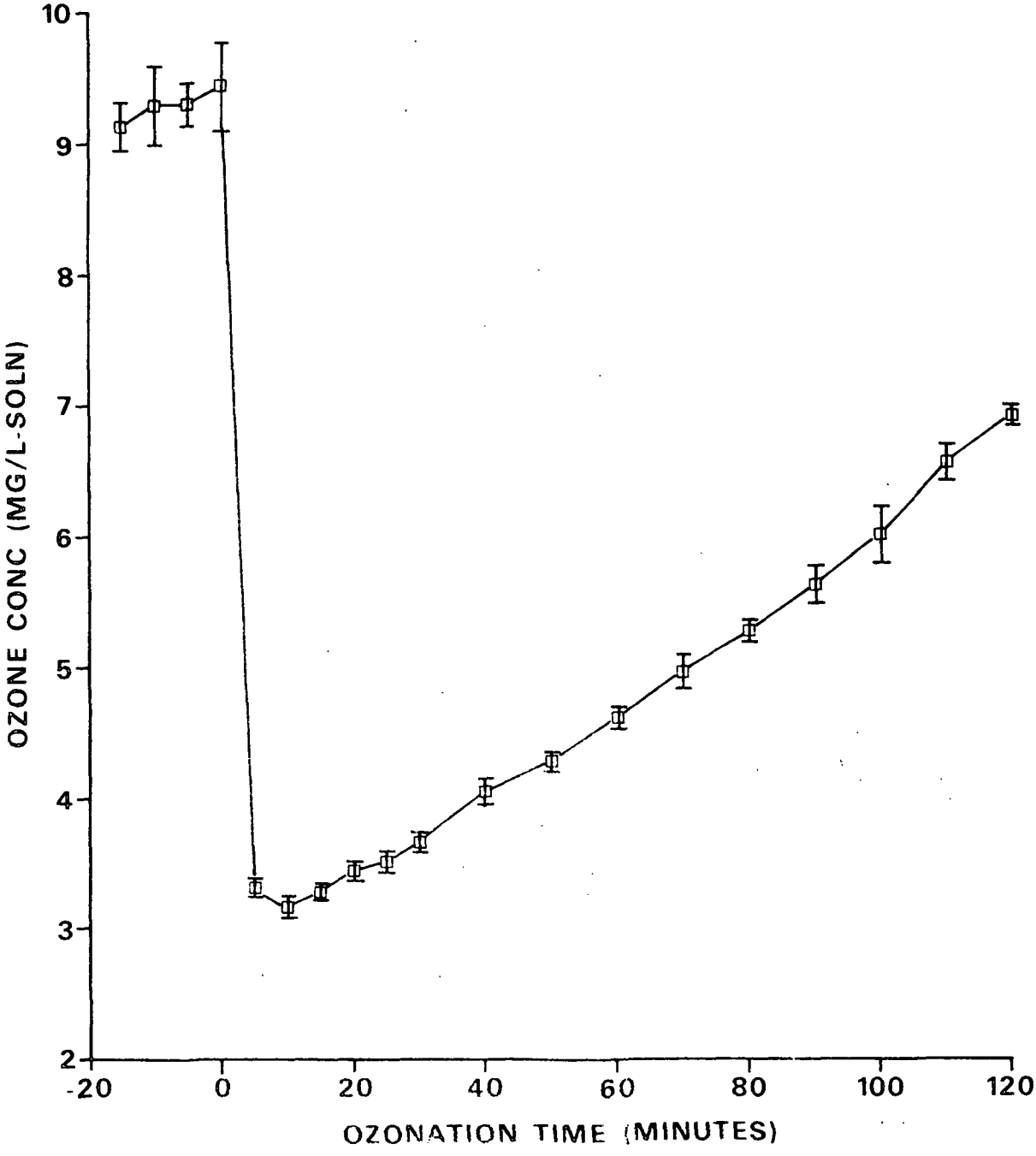

Figure 82. Ozonation of LW fibers (0.9 g o.d.) for 120 minutes in acetic acid buffer solution (1800 mL).

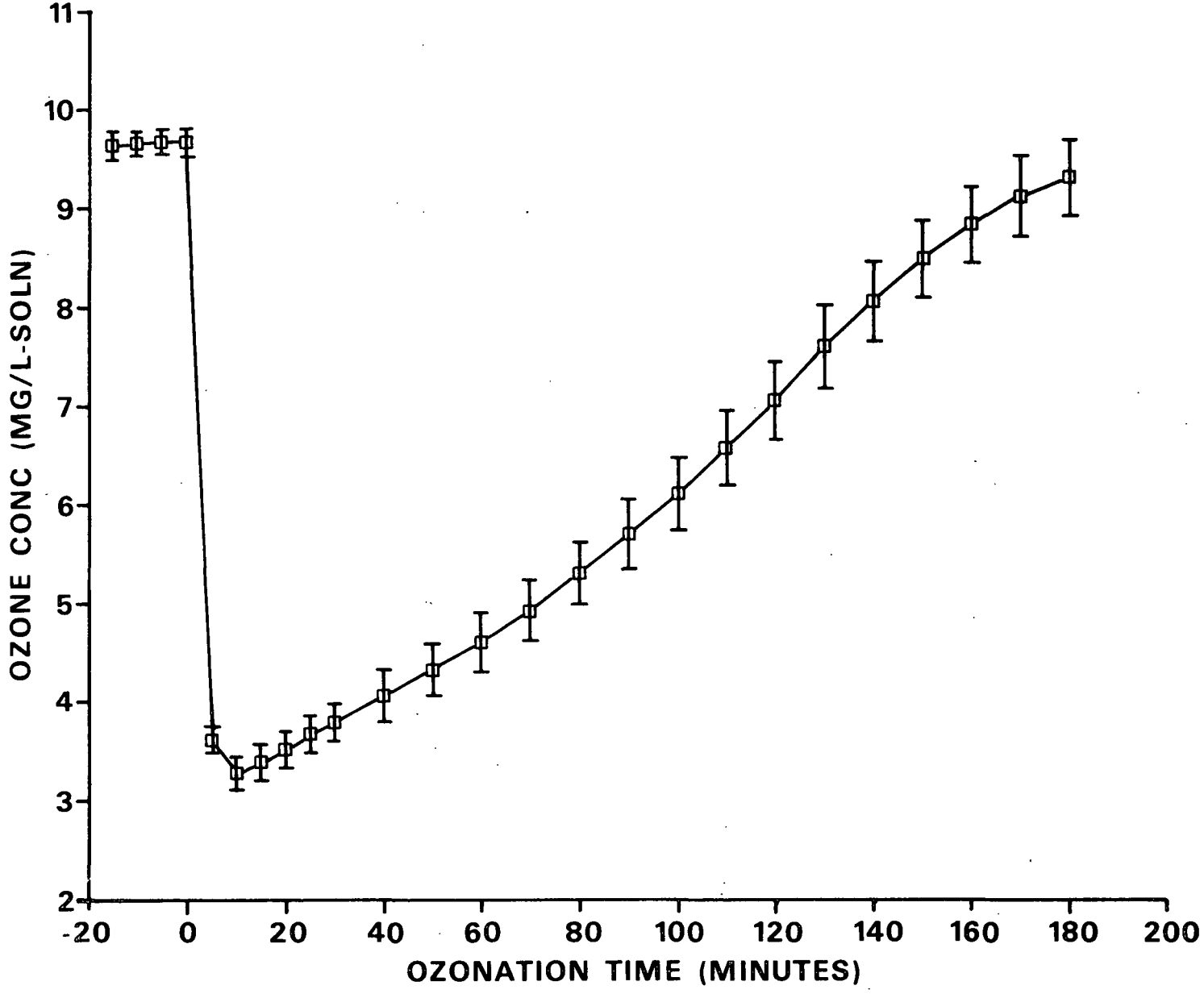

Figure 83. Ozonation of LW fibers (0.9 g o.d.) for 180 minutes in acetic acid buffer solution (1800 mL).

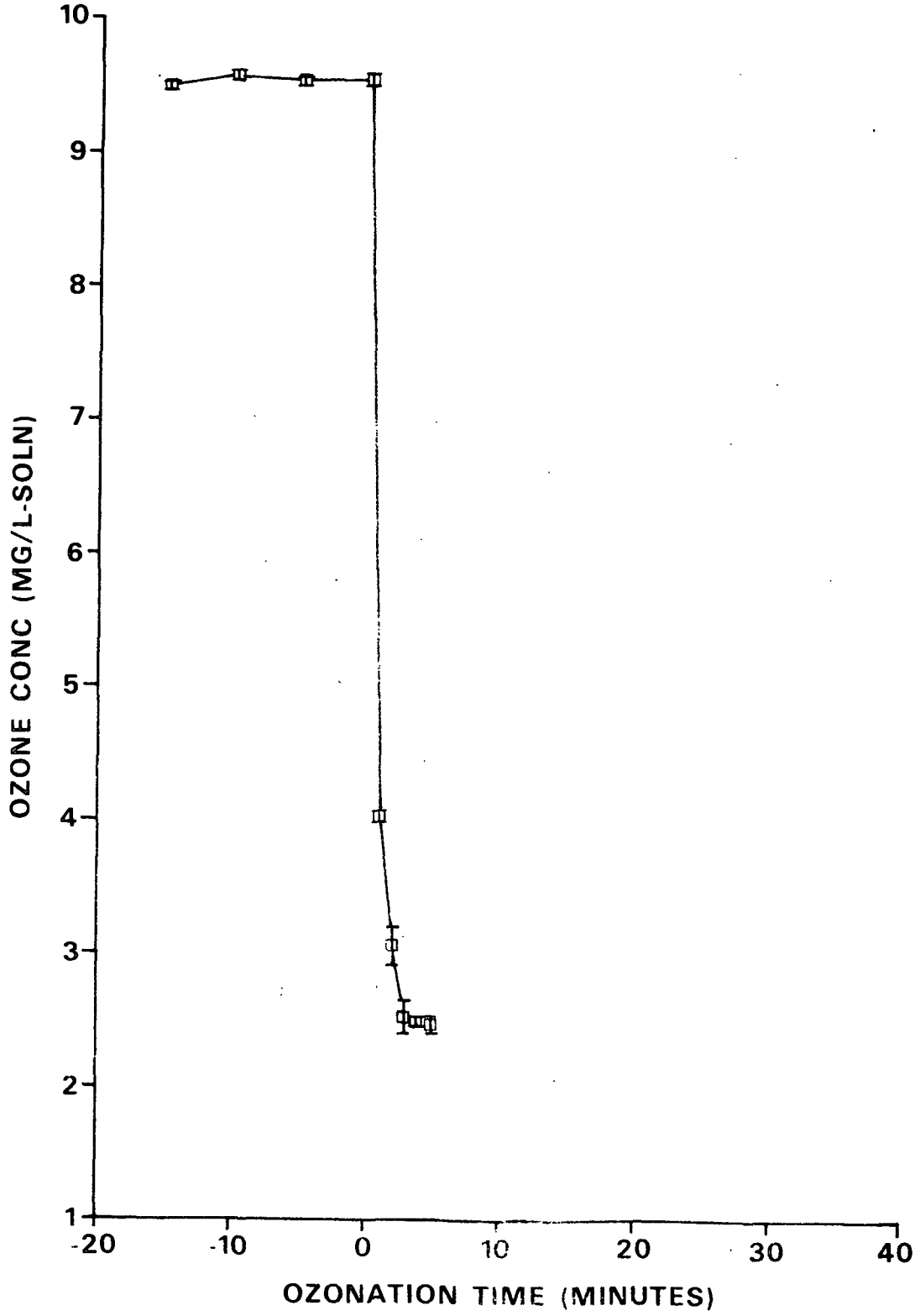

Figure 84. Ozonation of EW fibers (0.9 g o.d.) for 5 minutes in acetic acid buffer solution (1800 mL).

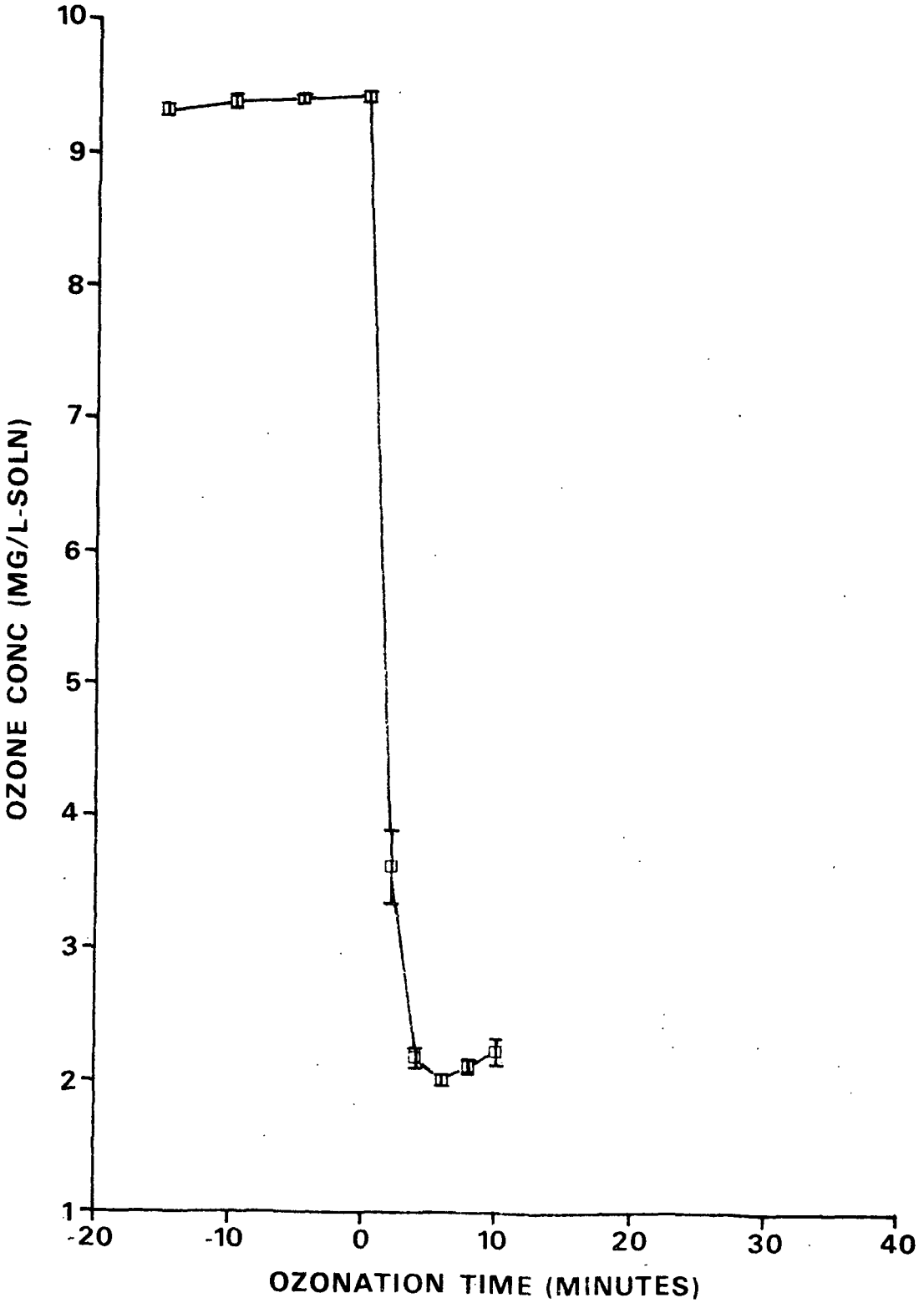

Figure 85. Ozonation of EW fibers (0.9 g o.d.) for 10 minutes in acetic acid buffer solution (1800 mL).

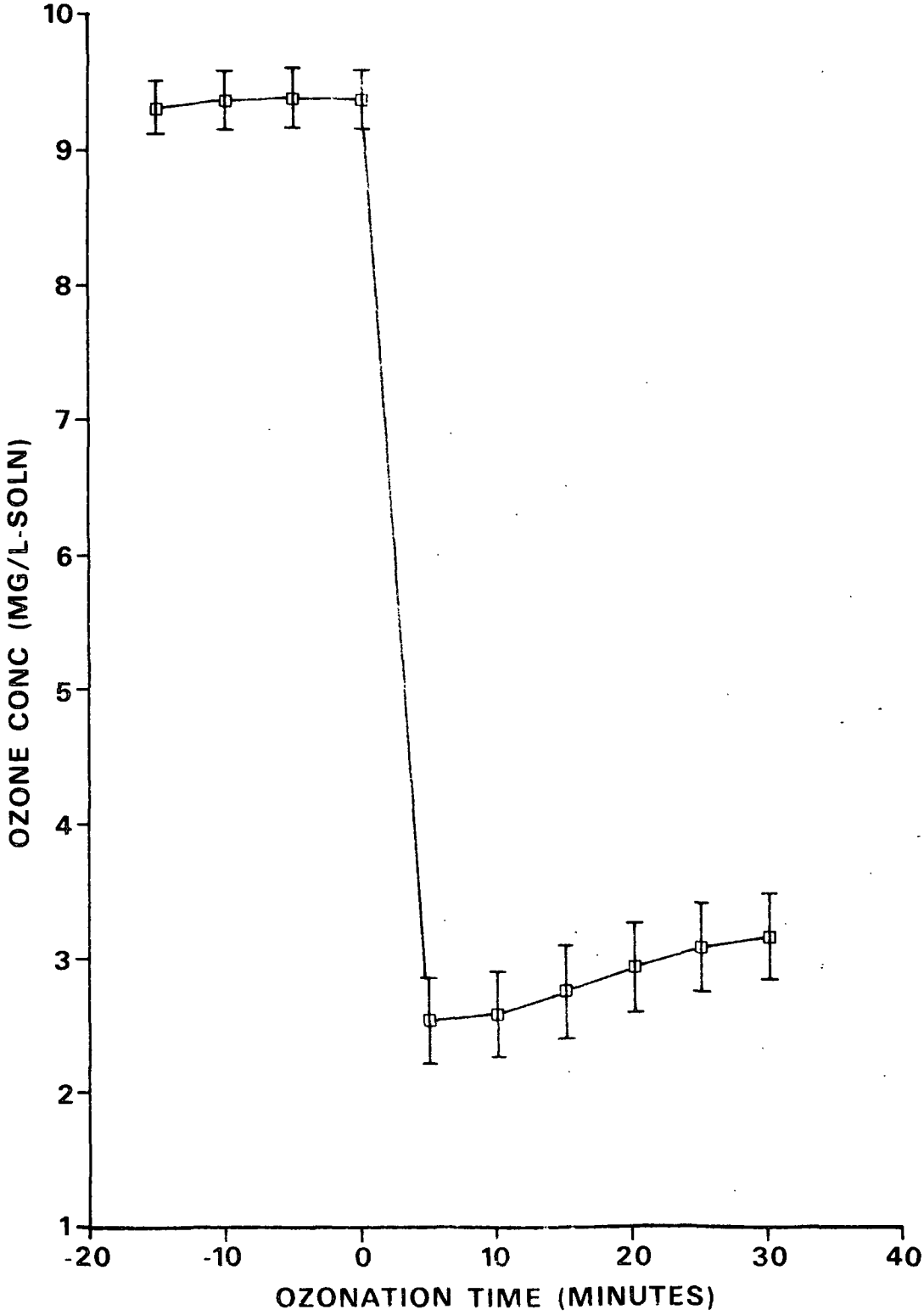

Figure 86. Ozonation of EW fibers (0.9 g o.d.) for 30 minutes in acetic acid buffer solution (1800 mL).

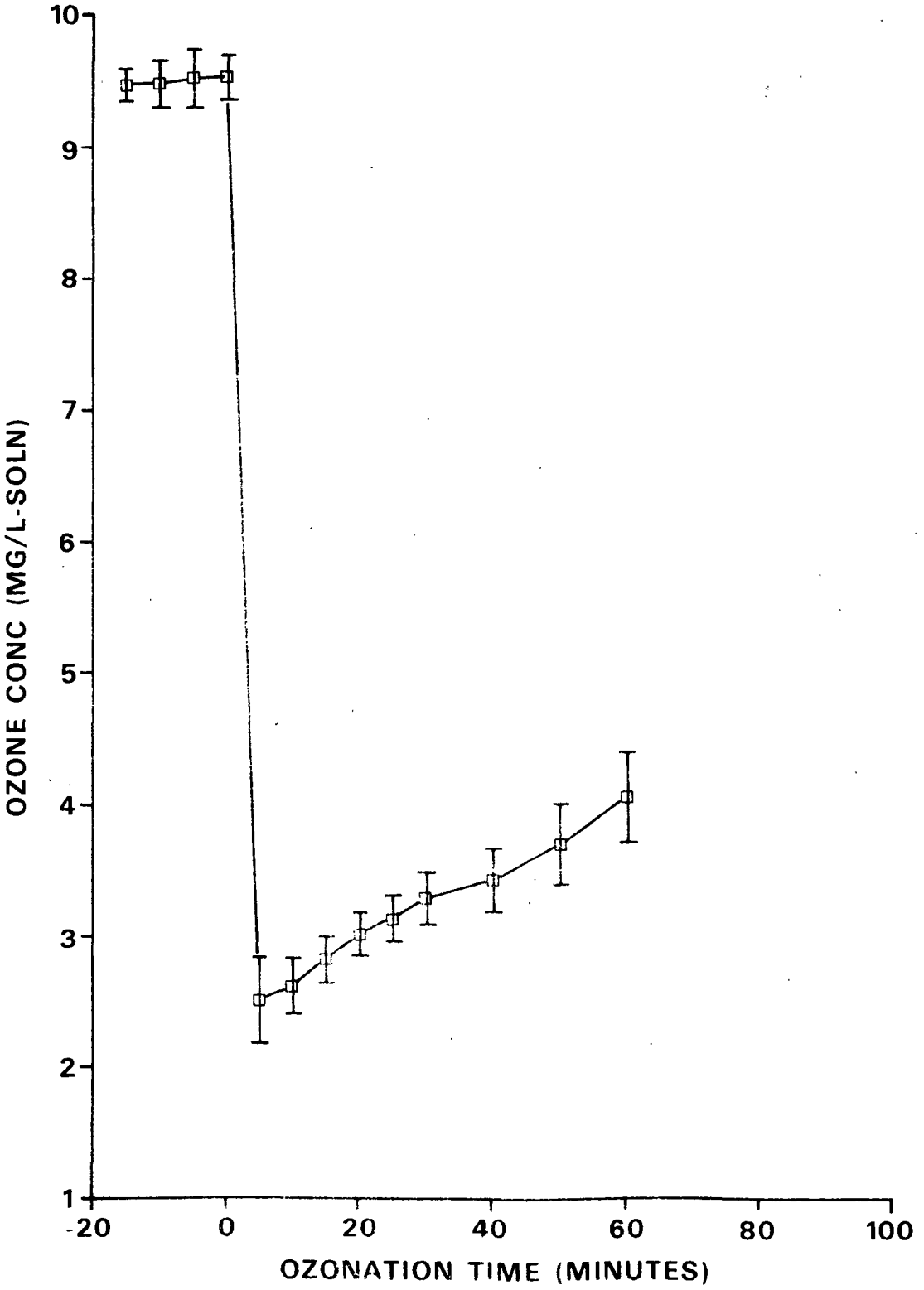

Figure 87. Ozonation of EW fibers (0.9 g o.d.) for 60 minutes in acetic acid buffer solution (1800 mL).

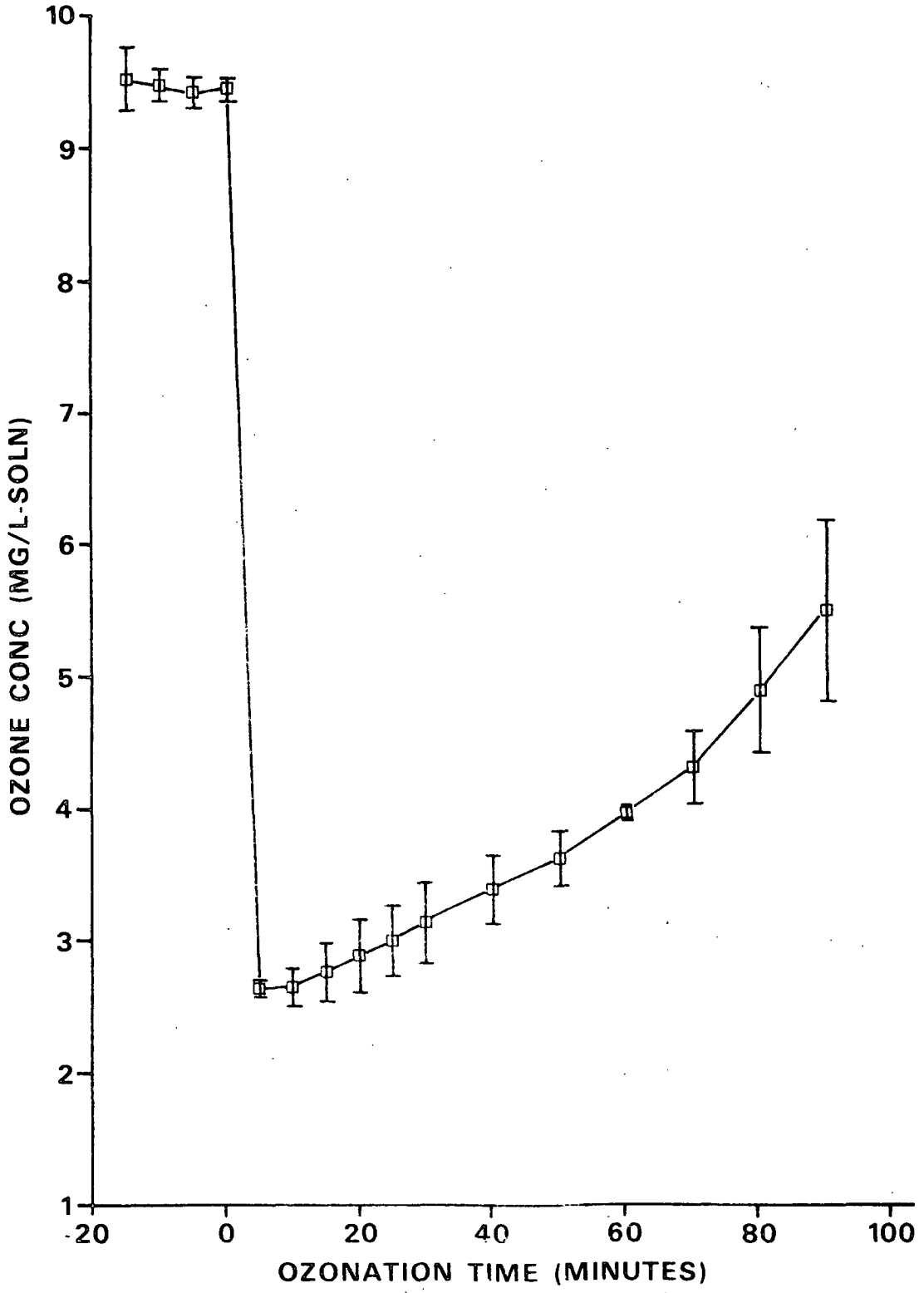

Figure 88. Ozonation of EW fibers (0.9 g o.d.) for 90 minutes in acetic acid buffer solution (1800 mL).

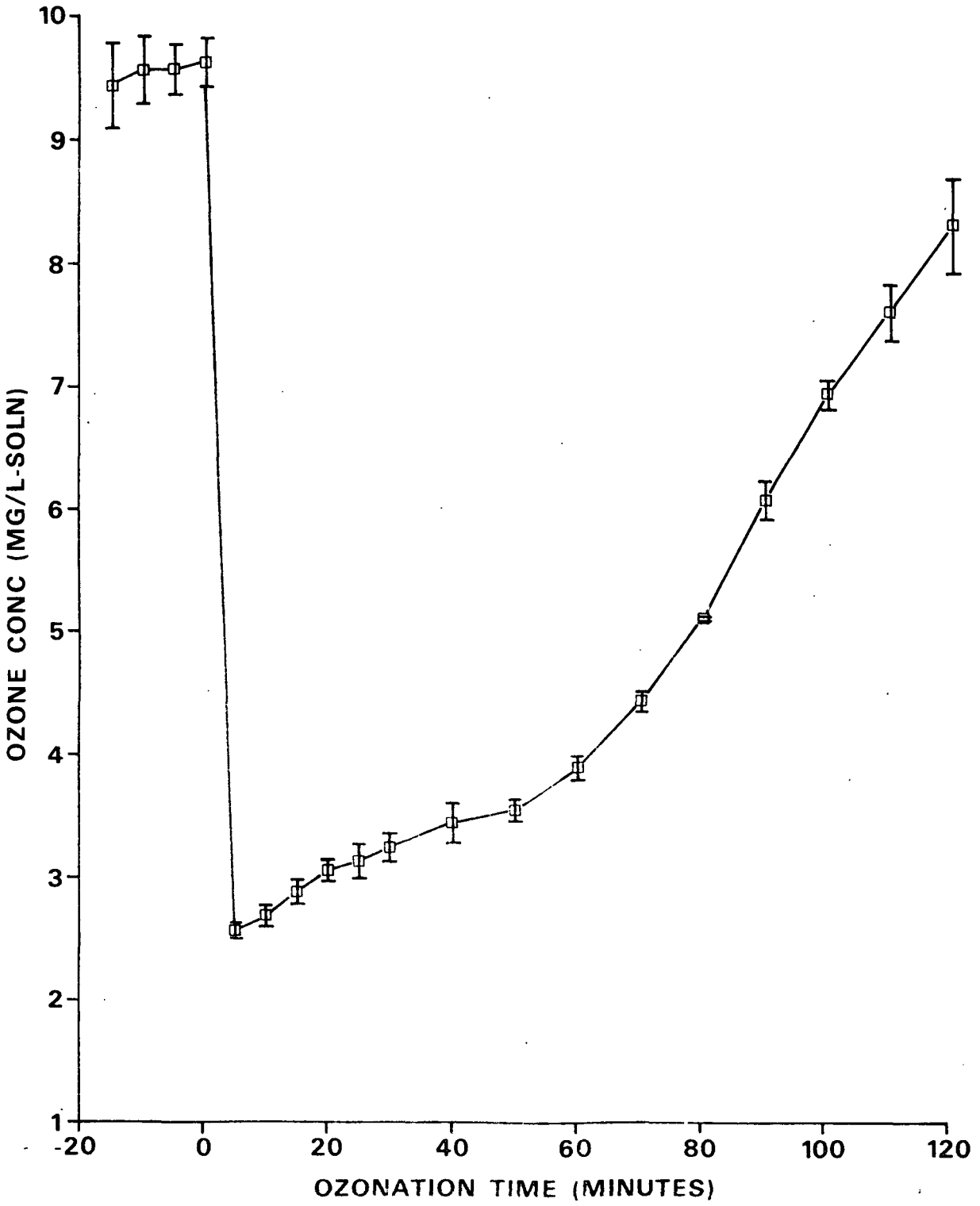

Figure 89. Ozonation of EW fibers (0.9 g o.d.) for 120 minutes in acetic acid buffer solution (1800 mL).

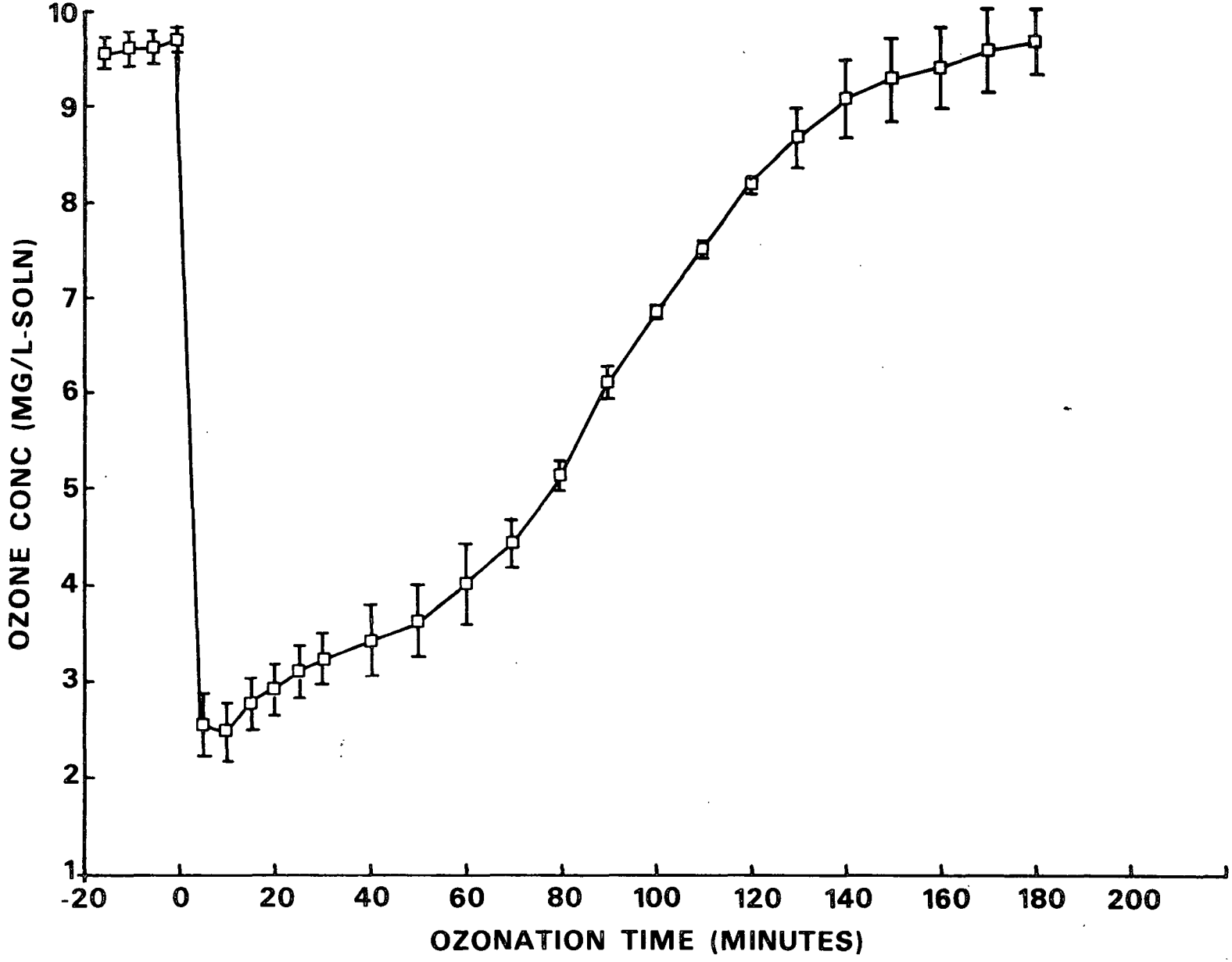

Figure 90. Ozonation of EW fibers (0.9 g o.d.) for 180 minutes in acetic acid buffer solution (1800 mL).

APPENDIX VIII

OZONE CONSUMPTION DUE TO BY-PRODUCT DEGRADATION AND SELF-DECOMPOSITION

Latewood fiber samples (0.9 g.o.d.) were ozonated for 180 minutes. Sample aliquots of fiber-free reaction solution were taken at various ozonation times. The aliquots were transferred to a cuvette and the UV absorbances measured at 5 minute intervals. A plot of ozone concentration with respect to time is shown in Fig. 91.

About 5% ozone decomposition occurred in 30 minutes for buffer solution alone (zero minutes) which was considered to be ozone self decomposition. The ozone decomposition curve for an aliquot taken at 170 minutes is almost identical to the buffer solution curve. This would indicate ozone decomposition due to by-product degradation was negligible after 170 minutes ozonation and was probably primarily due to ozone self decomposition. Ozone self decomposition rates for both 0 and 170 minutes were determined to be 0.04 mg/L-soln.

Ozone decomposition curves for aliquots taken at 5-120 minutes have similar shapes. Ozone decomposition rates for these times were calculated to be 0.14 ± 0.02 mg/L-min. Increased ozone decomposition rates for 5-120 minutes compared to 0 and 170 minutes were attributed to increased ozone consumption due to by-product degradation.

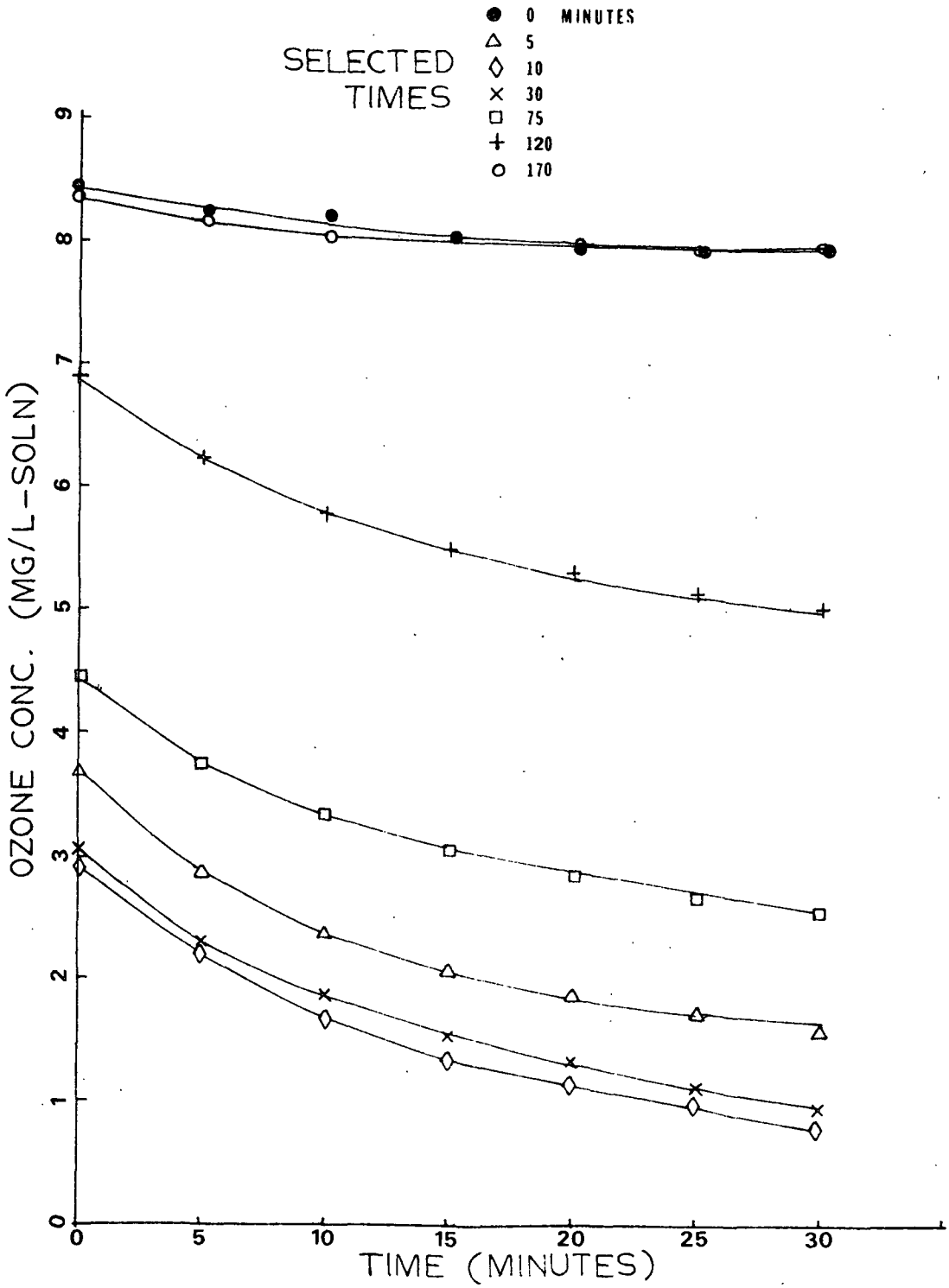

Figure 91. Ozone decomposition due to by-product degradation and ozone self-decomposition versus time.

APPENDIX IX

OZONE CONSUMPTION DUE TO FIBERS

The amount of ozone consumed by the fibers was calculated from the following equation:

Total Ozone Consumed	=	Ozone Offered to Tank	+	Ozone in Tank at T=0	-	Ozone Leaving Tank	-	Ozone in Tank After Reaction

Written in terms of measurable quantities, Equation (20) becomes:

$$C_T = C_i v_i t + C_p V - C_o v_o t - C_n V \qquad (21)$$

where C_T = total ozone consumed, mmole/L
C_i = input ozone concentration, mmole/L
C_p = ozone concentration at T=0, mmole/L
C_o = output ozone concentration, mmole/L
C_n = ozone not consumed during reaction, mmole/L
v_i = input volumetric flow rate, L/min
v_o = output volumetric flow rate, L/min
t = time, minutes
V = volume of reaction tank, L

Ozone consumption by LW fibers for a given reaction time is shown in Table XVII. The total amount of ozone consumed by the fibers was the sum of ozone consumed in the tank and that consumed during the specified reaction time. The amount of ozone consumed in the tank was the difference between the ozone in the tank at T=0 and ozone in the tank after the specified reaction time. The amount of ozone consumed during the reaction was the difference between the amount of ozone offered to the reaction tank and the amount of ozone leaving the tank over the specified reaction time. The amount of ozone not consumed during a specific reaction time was calculated by finding the area under the curves for the plots of ozone concentration versus reaction time (Fig. 77-90) and multiplying by the volumetric flow rate (0.3 L-soln/min). Areas under the curves were calculated by using the trapezoidal rule (98).

TABLE XVII

OZONE CONSUMPTION BY LATEWOOD FIBERS

Ozonation Time, min	Ozone Consumed Reaction, mM	Ozone Consumed in Tank, mM	Total Ozone Consumed, mM	Ozone Consumed By-products[a], mM	Total Ozone Consumed Corrected, mM
0	0.0	0.0	0.0	0.0	0.0
5	0.14	0.23	0.37	0.03	0.34
10	0.35	0.24	0.59	0.05	0.54
30	1.06	0.22	1.28	0.16	1.12
60	2.08	0.19	2.27	0.32	1.95
90	2.94	0.15	3.09	0.47	2.62
120	3.56	0.10	3.66	0.63	3.03
180	4.18	0.01	4.19	0.94	3.24

[a]Ozone consumption due to by-product degradation and self-decomposition.

Corrected values for the total amount of ozone consumed (Table XVII) were determined as the difference between the total amount of ozone consumed and the amount of ozone consumption due to byproduct degradation and ozone self-decomposition. The amount of ozone consumed as a result of by-product and self-decomposition was calculated from the decomposition rate, 0.14 mg/L-min (Appendix VIII). The corrected ozone values were used in calculating the stoichiometric ratios presented in Tables VII and X.

The above procedure was used for calculating the amount of ozone consumed by EW fibers. The amount of ozone consumed as a result of by-product and self-decomposition was calculated using the decomposition rate found for LW fibers (Appendix VIII). Ozone consumption by EW fibers is shown in Table XVIII.

TABLE XVIII

OZONE CONSUMPTION BY EARLYWOOD FIBERS

Ozonation Time, min	Ozone Consumed Reaction, mM	Ozone Consumed in Tank, mM	Total Ozone Consumed, mM	Ozone Consumed By-products[a], mM	Total Ozone Consumed Corrected, mM
0	0.0	0.0	0.0	0.0	0.0
5	0.18	0.26	0.44	0.03	0.41
10	0.39	0.27	0.66	0.05	0.61
30	1.17	0.24	1.41	0.16	1.25
60	2.25	0.20	2.45	0.32	2.13
90	3.07	0.15	3.22	0.47	2.75
120	3.64	0.04	3.68	0.63	3.05
180	3.92	0.01	3.93	0.94	2.99

[a]Ozone consumption due to by-product degradation and self-decomposition.

APPENDIX X

LIGNIN CONTENTS OF FIBERS

TABLE XIX

LIGNIN CONTENT FOR OZONATED LATEWOOD FIBERS[a]

Ozonation Time, min	Klason Lignin, %	Acid-Soluble Lignin, %	Total Lignin, %
0	27.4	0.32	27.7
5	23.4	1.10	24.5
10	22.0	0.56	22.6
30	16.8	0.87	17.7
60	10.5	0.48	11.0
90	5.3	0.35	5.6
120	1.3	1.20	2.5
180	0.2	0.94	1.1

[a]Percent o.d. wood basis.

TABLE XX

LIGNIN CONTENT FOR OZONATED EARLYWOOD FIBERS[a]

Ozonation Time, min	Klason Lignin, %	Acid-Soluble Lignin, %	Total Lignin, %
0	29.4	0.96	30.4
5	25.2	1.06	26.3
10	23.1	1.48	24.6
30	15.9	0.36	16.3
60	6.4	1.37	7.8
90	3.5	0.91	4.4
120	1.2	0.62	1.8
180	0.5	0.49	0.9

[a]Percent o.d. wood basis.

APPENDIX XI

CALCULATION OF HEMICELLULOSE AND CELLULOSE CONTENT

Carbohydrate contents of control and ozonated loblolly pine fibers were determined experimentally using the procedure by Piper and Borchardt (99). Individual carbohydrate contents for LW and EW fibers are shown in Tables XXI and XXII, respectively. Hemicellulose and cellulose contents for for LW and EW fibers are shown in Table XXIII and XXIV, respectively. Total hemicellulose content was calculated from the sum of galactoglucomannan, arabinoxylan and arabinogalactan contents which are the principle hemicelluloses in softwood (81). These hemicelluloses were determined from the individual carbohydrate contents using the ratios of mannan:glucan:galactan = 19:7:1 and xylan:araban = 9:1 for softwoods (101).

Cellulose content was calculated as the difference between glucan content and the fraction of glucan considered to make-up the galactoglucomannan.

TABLE XXI

CARBOHYDRATE CONTENT OF OZONATED LATEWOOD FIBERS[a]

Ozonation Time, min	Araban, %	Xylan, %	Mannan, %	Galactan, %	Glucan, %
0	1.0	6.1	10.7	3.1	44.8
5	0.9	6.3	10.8	2.9	44.8
10	0.8	6.3	10.6	3.1	44.7
30	0.7	5.5	9.8	2.4	44.0
60	0.8	5.9	9.6	2.1	43.3
90	0.6	5.4	9.3	2.0	45.0
120	0.7	5.2	9.4	1.5	43.1
180	0.5	4.5	8.4	1.1	43.5

[a]Percent o.d. wood basis.

TABLE XXII

CARBOHYDRATE CONTENT OF OZONATED EARLYWOOD FIBERS[a]

Ozonation Time, min	Araban, %	Xylan, %	Mannan, %	Galactan, %	Glucan, %
0	1.2	6.7	10.8	2.9	46.4
5	1.2	6.3	10.8	2.5	45.7
10	1.0	6.3	10.8	2.6	46.0
30	1.0	6.0	10.0	2.4	46.0
60	0.8	5.9	10.4	2.0	46.6
90	0.7	5.5	10.1	1.7	46.6
120	0.7	4.5	9.5	1.4	43.3
180	0.6	4.6	8.8	1.2	43.1

[a]Percent o.d. wood basis.

TABLE XXIII

HEMICELLULOSE AND CELLULOSE CONTENT FOR OZONATED LATEWOOD FIBERS[a]

Ozonation Time, min	Arabino-xylan	Galacto-gluco-mannan	Arabino-galactan	Total Hemi-cellulose	Total cellulose
0	6.8	15.2	2.9	24.9	40.8
5	7.0	15.3	2.5	24.8	40.8
10	7.0	15.1	2.7	24.8	40.8
30	6.2	13.9	2.0	22.1	40.3
60	6.6	13.7	1.6	21.9	39.8
90	6.0	13.3	1.7	20.8	41.5
120	5.8	13.3	1.1	20.2	39.6
180	4.9	11.9	0.8	17.6	40.4

[a]Percent on o.d. wood.

TABLE XXIV

HEMICELLULOSE AND CELLULOSE CONTENT FOR OZONATED EARLYWOOD FIBERS[a]

Ozonation Time, min	Arabino-xylan	Galacto-gluco-mannan	Arabino-galactan	Total Hemi-cellulose	Total Cellulose
0	7.4	15.4	2.7	25.5	42.4
5	7.0	15.3	2.4	24.7	41.7
10	7.0	15.3	2.4	24.7	42.0
30	6.6	14.3	2.3	23.2	42.3
60	6.6	14.8	1.5	22.9	42.8
90	6.1	14.3	1.2	21.6	42.9
120	5.0	13.5	1.1	19.6	39.8
180	5.2	12.4	0.9	18.5	39.9

[a]Percent on o.d. wood.

APPENDIX XII

KINETIC ANALYSIS OF CHEMICAL DATA

Experimentally determined lignin and ozone concentrations were plotted against time and a spline function (102) was used to generate a curve that best fit the data. Lignin content and ozone concentration curves are shown in Fig. 92 and 93, respectively, for ozonation of LW fibers and Fig. 94 and 95, respectively, for EW fibers.

Rates of delignification at given times were calculated by taking the first derivative of the spline function for the established lignin curves. Values for the rates of delignification, lignin content and ozone concentration were calculated at one-minute intervals using the spline functions and analyzed by multiple linear regression to determine reaction orders and rate constants. The data was evaluated over a range from 0-120 minutes and the results shown in Table XXV and XXVI for LW and EW, respectively.

The computer program used to generate the spline curves is shown in Program 1 which incorporated IMSL Routine Package ICSSCU "Smoothing by Cubic Splines" and CALCOMP/1012 for plotting. The computer program used for statistical analysis of data is shown in Program 2 which uses IMSL Routine Package RLMUL, "Multiple Linear Regression."

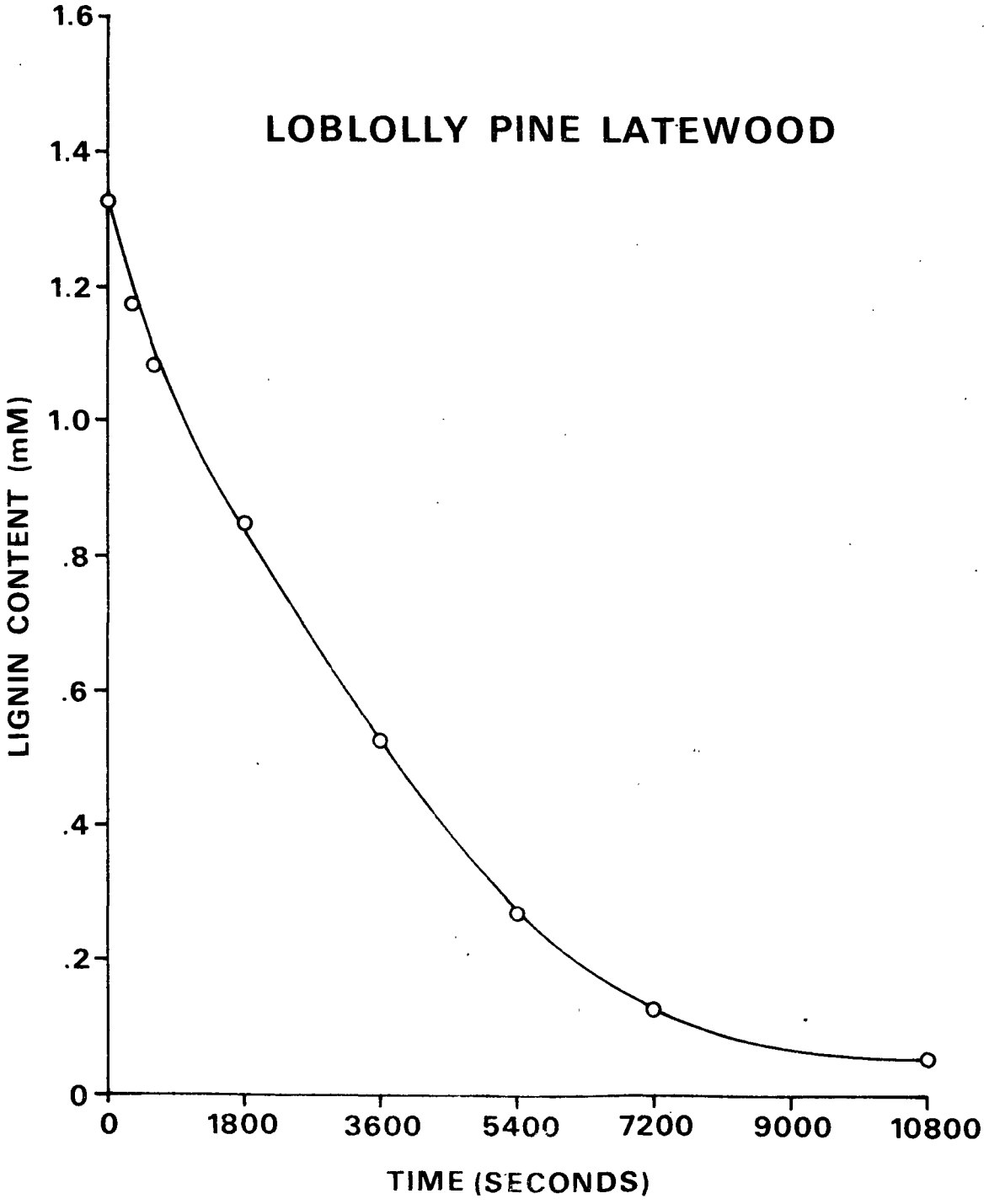

Figure 92. Spline function curve of lignin content versus time for LW fibers.

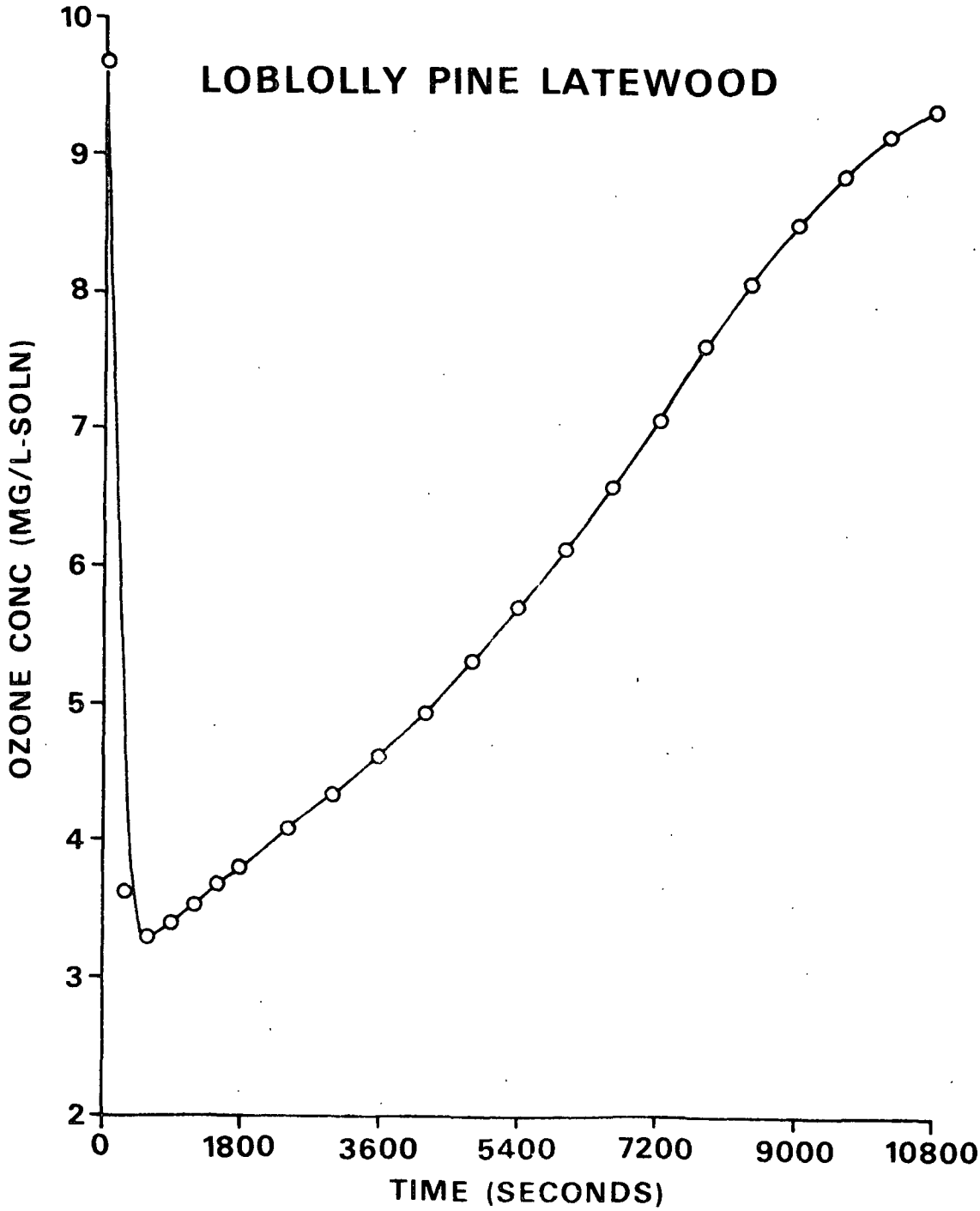

Figure 93. Spline function curve of ozone concentration versus time for LW fibers.

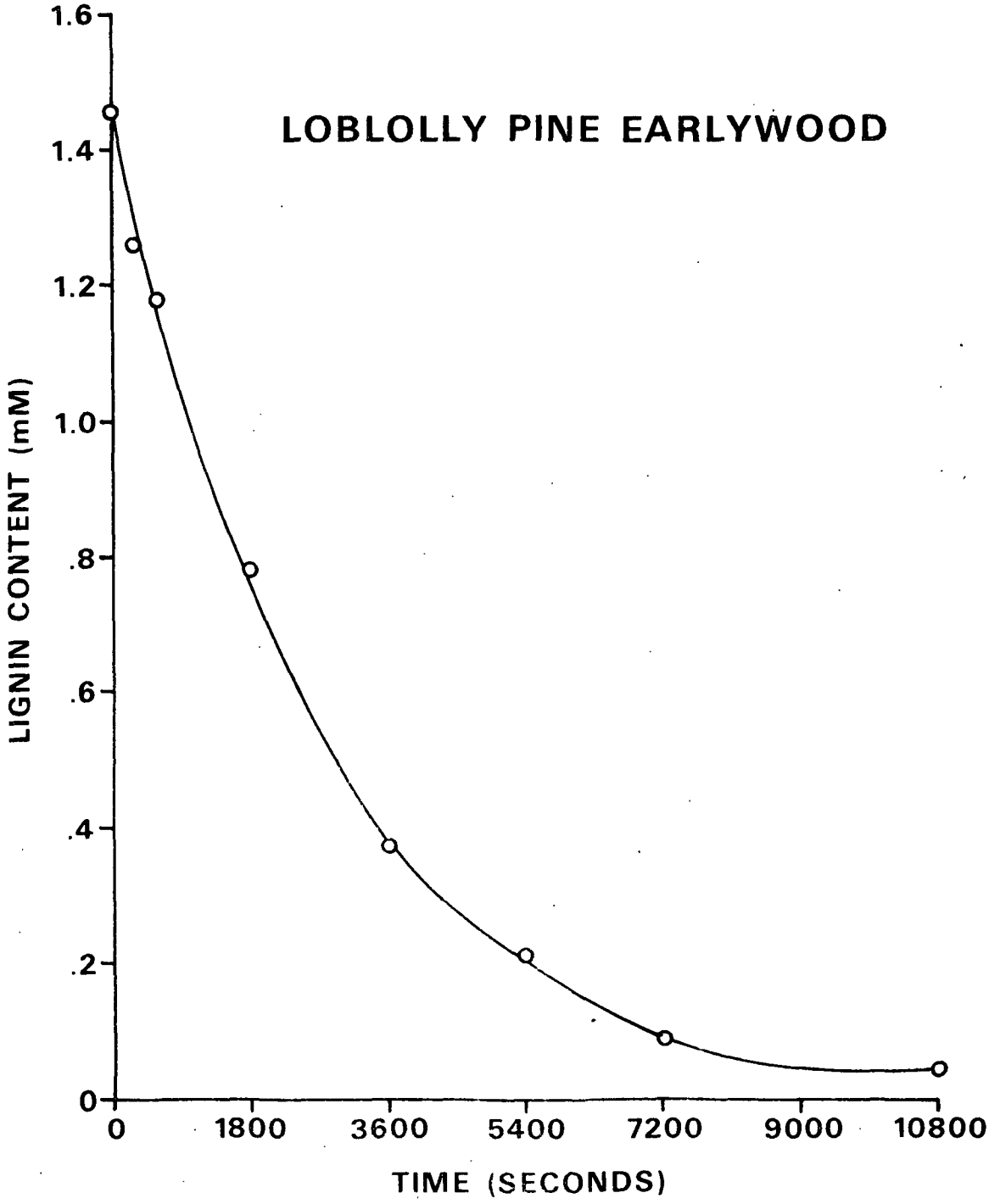

Figure 94. Spline function curve of lignin content versus time for EW fibers.

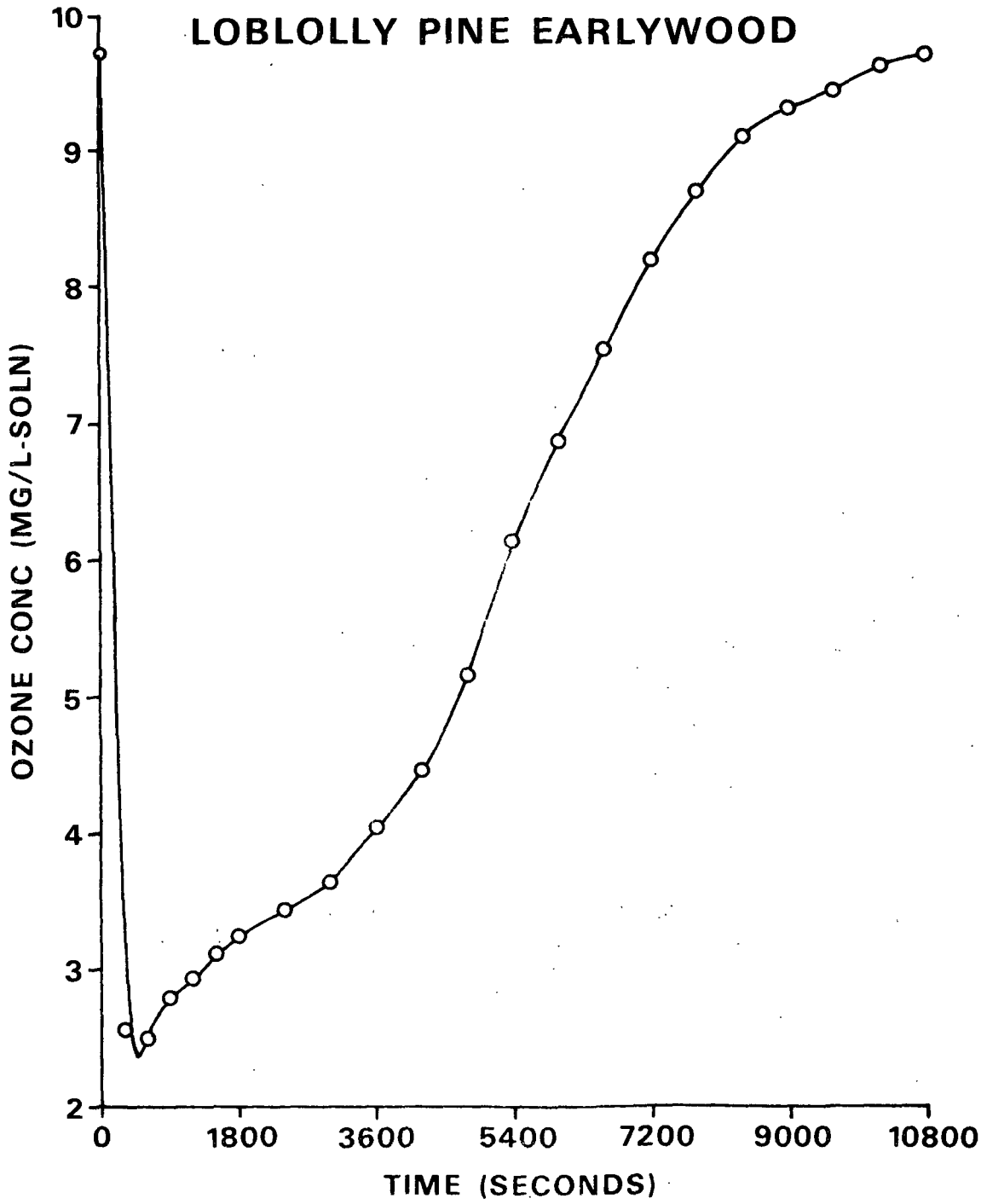

Figure 95. Spline function curve of ozone concentration versus time for EW fibers.

TABLE XXV

ANALYSES OF VARIANCE OF KINETIC DATA
FOR LATEWOOD FIBERS

Source of Variation	Degrees of Freedom	Sums of Squares	Mean Squares	F-test**	Correlation Coefficient
Regression	2	25.98	12.99	1314	0.96
Residual	118	1.17	0.01		
Total	120	27.15			

TABLE XXVI

ANALYSES OF VARIANCE OF KINETIC DATA
FOR EARLYWOOD FIBERS

Source of Variation	Degrees of Freedom	Sums of Squares	Mean Squares	F-test**	Correlation Coefficient
Regression	2	61.15	30.58	3041	0.98
Residual	118	1.19	0.01		
Total	120	62.34			

```
C-                                                                      00000100
C-                    PROGRAM 1                                         00000200
C-                                                                      00000300
C- A PROGRAM TO PERFORM CUBIC SPLINE FUNCTION PLOTS                     00000400
C-                                                                      00000500
$RESET FREE                                                             00000600
FILE  6(KIND=PRINTER)                                                   00000700
FILE  5(KIND=DISK,TITLE="SPLINE/DATA",FILETYPE=7)                       00000800
FILE  7(KIND=REMOTE,MYUSE=IO)                                           00000900
FILE  8(KIND=DISK,TITLE="WOOKE",FILETYPE=8,PROTECTION=SAVE,             00001000
    *MAXRECSIZE=1,BLOCKSIZE=420,AREASIZE=120)                           00001100
C-                                                                      00001200
C- READ IMSL PROGRAM PACKAGE INSTRUCTIONS (PI) FOR EXPLANATIONS         00001300
C- OF VARIABLES AND DETERMINING DIMENSIONS OF ARRAYS                    00001400
C-                                                                      00001500
C- INCLUDE PACKAGED SUBROUTINE PROGRAMS                                 00001600
C-                                                                      00001700
$INCLUDE "*CALCOMP/1012"                                                00001800
$INCLUDE "*IMSL/ICSSCU"                                                 00001900
$INCLUDE "*IMSL/UERTST"                                                 00002000
$INCLUDE "*IMSL/UGETIO"                                                 00002100
$INCLUDE "*IMSL/USPKD"                                                  00002200
C-                                                                      00002300
C- DIMENSION VARIABLE ARRAYS                                            00002400
C-                                                                      00002500
     DIMENSION X(10),F(10),Y(10),WK(84),C(83,3),DF(10)                  00002600
     REAL S(300),T(300),INCREM, INCRE,DT(300)                           00002700
C-                                                                      00002800
C- INPUT NUMBER OF DATA POINTS, SMOOTHING FACTORS (READ                 00002900
C- IMSL PI), AND PLOTTING VARIABLE (NO=0, YES=1)                        00003000
C- INPUT VARIABLES IN X-Y PAIRS WITH THEIR RESPECTIVE                   00003100
C- WEIGHTING FACTORS (READ IMSL PI)                                     00003200
C- IC=ROW DIMENSION MATRIX (READ ISML PI),INCREM AND INCRE              00003300
C- IS THE INCREMENT AT WHICH  DATA POINTS ARE CALCULATED                00003400
C-                                                                      00003500
     READ (5,/) NX,SM,NG                                                00003600
     READ(5,/) (X(I),F(I),DF(I), I=1,NX)                                00003700
     IC=83.                                                             00003800
     INCREM=60.                                                         00003900
    INCRE=60.                                                           00004000
C-                                                                      00004100
C- CALL SPLINE FUNCTION SUBROUTINE                                      00004200
C- CALL SUBROUTINE TO DETERMINE POINTS TO PLOTTED                       00004300
C- CALL PLOTTING SUBROUTINE                                             00004400
C-                                                                      00004500
     CALL ICSSCU(X,F,DF,NX,SM,Y,C,IC,WK,IER)                            00004600
C-                                                                      00004700
     S(1)=X(1)                                                          00004800
     CALL POINTS(X,Y,C,NX,INCREM,S,T,NVAL)                              00004900
     IF (NG.EQ.0) GO TO 13                                              00005000
     CALL PLOTS(0,0,999)                                                00005100
     CALL GRAF(S,T,X,F,NVAL,NX)                                         00005200
```

```
C-                                                                      00005300
C- CALL SUBROUTINE TO TAKE FIRST DERIVATIVE OF                          00005400
C- SPLINE FUNCTION AND WRITE VALUES ON DISK                             00005500
C-                                                                      00005600
13    CALL DIFF(X,Y,C,NX,INCRE,S,DT,NSAL)                               00005700
      WRITE(8,200) NSAL                                                 00005800
      WRITE (8,100)  (T(I),DT(I), I=1,NSAL)                             00005900
100   FORMAT(1PE12.3,2X,12X,2X,1PE12.3)                                 00006000
200   FORMAT(I3)                                                        00006100
      STOP                                                              00006200
      END                                                               00006300
C-                                                                      00006400
C- SUBROUTINE TO DETERMINE POINTS TO BE PLOTTED                         00006500
C-                                                                      00006600
      SUBROUTINE POINTS(X,Y,C,N,INCREM,S,T,NVAL)                        00006700
      DIMENSION X(10),Y(10),C(83,3),S(300),T(300)                       00006800
C-                                                                      00006900
      DO 10 NVAL=1,999                                                  00007000
      DO 20 I=1,N                                                       00007100
      IF (S(NVAL)-X(I+1)) 30,30,33                                      00007200
30    IF (X(I+1)) 32,33,32                                              00007300
32    D=S(NVAL)-X(I)                                                    00007400
      T(NVAL)=((C(I,3)*D+C(I,2))*D+C(I,1))*D +Y(I)                      00007500
      S(NVAL+1)=S(NVAL)+INCREM                                          00007600
      GO TO 10                                                          00007700
33    IF (I-N) 20,40,40                                                 00007800
20    CONTINUE                                                          00007900
10    CONTINUE                                                          00008000
40    NVAL=NVAL-1                                                       00008100
      RETURN                                                            00008200
      END                                                               00008300
C-                                                                      00008400
C- PLOTTING SUBROUTINE                                                  00008500
C-                                                                      00008600
      SUBROUTINE GRAF(S,T,X,F,NVAL,N)                                   00008700
      REAL S(300),T(300), X(10),F(10)                                   00008800
C-                                                                      00008900
      CALL PLOT (1.5,1.5,-3)                                            00009000
      T(NVAL+1)=0.0                                                     00009100
      T(NVAL+2)=0.20                                                    00009200
      S(NVAL+1)=0.0                                                     00009300
      S(NVAL+2)=1800.                                                   00009400
      F(N+1)=T(NVAL+1)                                                  00009500
      F(N+2)=T(NVAL+2)                                                  00009600
      X(N+1)=S(NVAL+1)                                                  00009700
      X(N+2)=S(NVAL+2)                                                  00009800
C-                                                                      00009900
C- INPUT X-Y AXES LABELS                                                00010000
```

```
C-                                                                      00010100
      CALL AXIS(0.,0.,14HTIME (SECONDS),-14,6.0,0.0,                    00010200
     -S(NVAL+1),S(NVAL+2))                                              00010300
      CALL AXIS(0.0,0.0,3HLIG,3,8.0,90,                                 00010400
     -T(NVAL+1),T(NVAL+2))                                              00010500
      CALL LINE(S,T,NVAL,1,0,0)                                         00010600
      CALL LINE(X,F,N,1,-1,1)                                           00010700
      CALL PLOT (7.0,-1.5,999)                                          00010800
      RETURN                                                            00010900
      END                                                               00011000
C-                                                                      00011100
C- PROGRAM TO TAKE FIRST DERIVATIVE OF SPLINE FUNCTION                  00011200
C- AND STORE CALCULATE VALUE IN AN ARRAY                                00011300
C-                                                                      00011400
      SUBROUTINE DIFF(X,Y,C,N,INCRE,S,DT,NSAL)                          00011500
      DIMENSION X(10),Y(10),C(83,3),S(300),DT(300)                      00011600
C-                                                                      00011700
      DO 10 NSAL=1,999                                                  00011800
      DO 20 I=1,N                                                       00011900
     IF (S(NSAL)-X(I+1)) 30,30,33                                       00012000
30    IF (X(I+1)) 32,33,32                                              00012100
32    D=S(NSAL)-X(I)                                                    00012200
      DT(NSAL)=(3*C(I,3)*D+2*C(I,2))*D+C(I,1)                           00012300
      S(NSAL+1)=S(NSAL)+INCRE                                           00012400
      GO TO 10                                                          00012500
33    IF (I-N) 20,40,40                                                 00012600
20    CONTINUE                                                          00012700
10    CONTINUE                                                          00012800
40    NSAL=NSAL-1                                                       00012900
      RETURN                                                            00013000
      END                                                               00013100
```

```
C-                                                                      000001
C-                                                                      000002
C-                        PROGRAM 2                                     00000300
C-                                                                      00000350
C- A PROGRAM TO PERFORM MULTIPLE LINEAR REGRESSION                      00000355
C-                                                                      00000400
$RESET FREE                                                             00000500
FILE  6(KIND=PRINTER)                                                   00000600
FILE  5(KIND=DISK,TITLE="STAT/DATA",FILETYPE=7)                         00000700
C-                                                                      00000800
C- READ IMSL PROGRAM PACKAGE INSTRUCTIONS (PI) FOR EXPLANATION          00000900
C- OF VARIABLES AND DETERMINING DIMENSIONS OF ARRAYS                    00001000
C-                                                                      00001100
C- INCLUDE PACKAGED SUBROUTINE PROGRAMS                                 00001200
C-                                                                      00001300
$INCLUDE "*IMSL/RLMUL"                                                  00001400
$INCLUDE "*IMSL/LUELMP"                                                 00001500
$INCLUDE "*IMSL/MDBETA"                                                 00001600
$INCLUDE "*IMSL/MDBETI"                                                 00001700
$INCLUDE "*IMSL/UERTST"                                                 00001800
$INCLUDE "*IMSL/UGETIO"                                                 00001900
$INCLUDE "*IMSL/VMULFS"                                                 00002000
$INCLUDE "*IMSL/BECOVM"                                                 00002100
$INCLUDE "*IMSL/USPKD"                                                  00002200
C-                                                                      00002300
C- DIMENSION VARIABLE ARRAYS                                            00002400
C-                                                                      00002500
      INTEGER N,M,IER,NBR(6),IX                                         00002600
      REAL XY(121,3),TEMP(3),XYBAR(3),A(6),ANOVA(14),B(3,7),VARB(3)     00002700
      REAL ALFA,X(121,3)                                                00002800
C-                                                                      00002900
C- INPUT NUMBER OF INITIAL DATA RECORD, NUMBER OF DATA                  00003000
C- POINTS, INPUT NUMBER OF INDEPENDENT VARIABLES, INPUT ROW             00003100
C- DIMENSION (READ IMSL PI)                                             00003200
C-SEE IMSL PI FOR INPUT VARIABLES NBR(1)-NBR(6)                         00003300
C-                                                                      00003400
      READ(5,/)IN,N,M,IX                                                00003500
      READ(5,/) NBR(1),NBR(2),NBR(3),NBR(4),NBR(5),NBR(6)               00003600
      ALFA = 0.05                                                       00003700
      IB=3                                                              00003800
      LN=N+IN-1                                                         00003900
      IF (IN.LE.1) GO TO 13                                             00004000
      KN=IN-1                                                           00004100
      DO 10 K=1,KN                                                      00004200
C-                                                                      00004300
C- SKIP DATA INPUT YOU DO NOT WANT READ                                 00004400
C- THESE VALUES ARE READ IN BY THE COMPUTER                             00004500
C-                                                                      00004600
  10  READ (5,300)DUM1,DUM2,DUM3                                       00004700
  13  DO 20 J = IN,LN                                                   00004800
      I=J-IN+1                                                          00004900
```

```
C-                                                                      00005000
C- INPUT DATA, TAKE NATURAL LOGS AND STORE IN NEW ARRAY                 00005100
C-                                                                      00005200
      READ(5,300) X(I,1),X(I,2),X(I,3)                                  00005300
  600 FORMAT(1X,2I5,3(1PE14.3))                                         00005400
      WRITE (6,600) I+IN-1,I+IN-2, X(I,1), X(I,2), X(I,3)               00005500
  300 FORMAT(1PE12.3,2X,1PE12.3,2X,1PE11.3)                             00005600
      XY(I,1)=ALOG(X(I,1))                                              00005700
      XY(I,2)=ALOG(X(I,2))                                              00005800
   20 XY(I,3)=ALOG(X(I,3))                                              00005900
C-                                                                      00006000
C- CALL MEAN, VARIANCE AND CO-VARIANCE MATRIX SUBROUTINE                00006100
C- CALL MULTIPLE LINEAR REGRESSION SUBROUTINE                           00006200
      CALL RLMUL(A,XYBAR,N,M,ALFA,ANOVA,B,IB,VARB,IER)                  00006300
      CALL BECOVM(XY,IX,NBR,TEMP,XYBAR,A,IER)                           00006400
C-                                                                      00006500
C- PRINT TABLE HEADINGS AND ANALYZED DATA                               00006600
C-                                                                      00006700
      WRITE(6,997)                                                      00006800
      WRITE(6,998)                                                      00006900
      DO 50 I = 1,M+1                                                   00007000
      WRITE(6,999) XYBAR(I)                                             00007100
   50 WRITE(6,1000) (B(I,J),J=1,6)                                      00007200
      WRITE(6,1001)                                                     00007300
      WRITE(6,1010)                                                     00007400
      WRITE(6,1020)                                                     00007500
      WRITE(6,1006) ANOVA(1),ANOVA(4),ANOVA(7),ANOVA(9)                 00007600
      WRITE(6,1007) ANOVA(2),ANOVA(5),ANOVA(8)                          00007700
      WRITE(6,1008) ANOVA(3),ANOVA(6)                                   00007800
      DO 70 J=1,3                                                       00007900
   70 B(3,J) = EXP(B(3,J))                                              00008000
      WRITE(6,1003) B(3,1)                                              00008100
      WRITE(6,1050) B(3,2)                                              00008200
      WRITE(6,1052) B(3,3)                                              00008300
  998 FORMAT(17X,'COEFFICIENT',6X,'LIMIT',8X,'LIMIT',10X,'ERROR',       00008400
     *9X,'SQUARES',/)                                                   00008500
  997 FORMAT('1',4X,'MEAN',8X,'REGRESSION',7X,'LOWER',8X,'UPPER',9X,    00008600
     *'STANDARD',7X,'SUMS OF',7X,'F-TEST')                              00008700
  999 FORMAT(1PE12.3)                                                   00008800
 1000 FORMAT('+',12X,1PE14.3,1PE14.3,1PE14.3,1PE14.3,1PE14.3,           00008900
     *1PE14.3)                                                          00009000
 1001 FORMAT(/,/)                                                       00009100
 1006 FORMAT(/,2X,'REGRESSION',1PE14.3,1PE15.3,1PE15.3,1PE14.3)         00009200
 1007 FORMAT(2X,'RESIDUAL',1PE16.3,1PE15.3,1PE15.3)                     00009300
 1008 FORMAT(2X,'TOTAL',1PE19.3,1PE15.3)                                00009400
 1002 FORMAT(/,1PE12.3)                                                 00009500
 1003 FORMAT(/,/,1X,'RATE CONSTANT = ',1PE12.3)                         00009600
 1010 FORMAT(/,2X,'SOURCE OF',6X,'DEGREES OF',6X,'SUMS OF',9X,          00009700
     *'MEAN',9X,'F-TEST')                                               00009800
 1020 FORMAT(2X,'VARIATION',6X,'FREEDOM',9X,'SQUARES',8X,'SQUARES')     00009900
 1050 FORMAT(1X,'LOWER LIMIT   = ',1PE12.3)                             00010000
 1052 FORMAT(1X,'UPPER LIMIT   = ',1PE12.3)                             00010100
C-                                                                      00010200
      STOP                                                              00010300
      END                                                               00010400
```

```
C-                                                                      00005000
C- INPUT DATA, TAKE NATURAL LOGS AND STORE IN NEW ARRAY                 00005100
C-                                                                      00005200
      READ(5,300) X(I,1),X(I,2),X(I,3)                                  00005300
  600 FORMAT(1X,2I5,3(1PE14.3))                                         00005400
      WRITE (6,600) I+IN-1,I+IN-2, X(I,1), X(I,2), X(I,3)               00005500
  300 FORMAT(1PE12.3,2X,1PE12.3,2X,1PE11.3)                             00005600
      XY(I,1)=ALOG(X(I,1))                                              00005700
      XY(I,2)=ALOG(X(I,2))                                              00005800
   20 XY(I,3)=ALOG(X(I,3))                                              00005900
C-                                                                      00006000
C- CALL MEAN, VARIANCE AND CO-VARIANCE MATRIX SUBROUTINE                00006100
C- CALL MULTIPLE LINEAR REGRESSION SUBROUTINE                           00006200
      CALL RLMUL(A,XYBAR,N,M,ALFA,ANOVA,B,IB,VARB,IER)                  00006300
      CALL BECOVM(XY,IX,NBR,TEMP,XYBAR,A,IER)                           00006400
C-                                                                      00006500
C- PRINT TABLE HEADINGS AND ANALYZED DATA                               00006600
C-                                                                      00006700
      WRITE(6,997)                                                      00006800
      WRITE(6,998)                                                      00006900
      DO 50 I = 1,M+1                                                   00007000
      WRITE(6,999) XYBAR(I)                                             00007100
   50 WRITE(6,1000) (B(I,J),J=1,6)                                      00007200
      WRITE(6,1001)                                                     00007300
      WRITE(6,1010)                                                     00007400
      WRITE(6,1020)                                                     00007500
      WRITE(6,1006) ANOVA(1),ANOVA(4),ANOVA(7),ANOVA(9)                 00007600
      WRITE(6,1007) ANOVA(2),ANOVA(5),ANOVA(8)                          00007700
      WRITE(6,1008) ANOVA(3),ANOVA(6)                                   00007800
      DO 70 J=1,3                                                       00007900
   70 B(3,J) = EXP(B(3,J))                                              00008000
      WRITE(6,1003) B(3,1)                                              00008100
      WRITE(6,1050) B(3,2)                                              00008200
      WRITE(6,1052) B(3,3)                                              00008300
  998 FORMAT(17X,'COEFFICIENT',6X,'LIMIT',8X,'LIMIT',10X,'ERROR',       00008400
     *9X,'SQUARES',/)                                                   00008500
  997 FORMAT('1',4X,'MEAN',8X,'REGRESSION',7X,'LOWER',8X,'UPPER',9X,    00008600
     *'STANDARD',7X,'SUMS OF',7X,'F-TEST')                              00008700
  999 FORMAT(1PE12.3)                                                   00008800
 1000 FORMAT('+',12X,1PE14.3,1PE14.3,1PE14.3,1PE14.3,1PE14.3,           00008900
     *1PE14.3)                                                          00009000
 1001 FORMAT(/,/)                                                       00009100
 1006 FORMAT(/,2X,'REGRESSION',1PE14.3,1PE15.3,1PE15.3,1PE14.3)         00009200
 1007 FORMAT(2X,'RESIDUAL',1PE16.3,1PE15.3,1PE15.3)                     00009300
 1008 FORMAT(2X,'TOTAL',1PE19.3,1PE15.3)                                00009400
 1002 FORMAT(/,1PE12.3)                                                 00009500
 1003 FORMAT(/,/,1X,'RATE CONSTANT = ',1PE12.3)                         00009600
 1010 FORMAT(/,2X,'SOURCE OF',6X,'DEGREES OF',6X,'SUMS OF',9X,          00009700
     *'MEAN',9X,'F-TEST')                                               00009800
 1020 FORMAT(2X,'VARIATION',6X,'FREEDOM',9X,'SQUARES',8X,'SQUARES')     00009900
 1050 FORMAT(1X,'LOWER LIMIT   = ',1PE12.3)                             00010000
 1052 FORMAT(1X,'UPPER LIMIT   = ',1PE12.3)                             00010100
C-                                                                      00010200
      STOP                                                              00010300
      END                                                               00010400
```